University of South-Eastern Norway

www.usn.no

FMH606 Master's Thesis 2021

Electrical Power Engineering

Modeling the Excitation Control System of a Hydropower Controller in Modelica

Luxshan Manoranjan

Faculty of Technology, Natural sciences and Maritime Sciences
Campus Porsgrunn

University of South-Eastern Norway

www.usn.no

Course: FMH606 Master's Thesis, 2021

Title: Modeling the excitation control system of a hydropower controller in Modelica

Number of pages: 142

Keywords: *Hydropower, Modelica, Excitation control system, Protective limiters, Voltage controllers, Reactive power or power factor controller*

Student: Luxshan Manoranjan

Supervisor: Dietmar Winkler

External partner: Hymatek Controls AS and Skagerak Kraft AS

Summary:

Hydropower technologies are crucial to provide flexibility, reliability, and stability to the grid compared to other renewable energy technologies. Therefore, the number of hydropower plants, mainly the small-scale plants, are still increasing worldwide. In order to build the small-scale power plants, proper planning is essential to minimize the cost and environmental impact. To achieve it, accurate modeling and simulation of the existing plants is necessary to predict the new plant's behavior before beginning the construction process.

The thesis's main objective was to create a digital twin of the real-life hydropower controller HYMAREG 10's excitation control system developed by Hymatek Controls AS. The generated models during the thesis were mainly object-oriented modeled in Modelica modeling language with the help of the standard Modelica library and OpenIPSL in the Dymola software tool.

All the models were simulated individually to examine the behavior of the controllers and the limiters. The simulation results showed reasonable behavior of each model, but still, proper tuning and further development are required to obtain accurate behavior as a real controller. Most importantly, the models need to be compared with an actual plant in the future to verify the model's behavior.

Preface

This thesis is the continuation of the Master Project done by the group MP-07-20 during the autumn semester of 2020 at the University of South-Eastern Norway (USN) [1]. And this Master's thesis is submitted to the Department of Electrical Engineering, IT and Cybernetics at the USN campus Porsgrunn and concludes my Master of Science (MSc) degree in Electrical Power Engineering.

The focus of this Master's thesis is mainly laid on modeling the excitation control system of a hydropower controller. During this thesis, collaboration with external partner Hymatek Controls AS helped immensely to extend and improve the excitation control system model to represent the real hydropower controller HYMAREG 10.

Firstly, I would like to express my most sincere gratitude to my supervisor, Dietmar Winkler, for his investment of time, patience, and effort in my work. His patient guidance, encouragement, and advice that he provided throughout my thesis work were invaluable. I would also like to thank Ruben Buchmann, Asgeir Åsnes, and especially Mathias Gallefoss from Hymatek Controls AS for sharing particulars and data of the HYMAREG 10 controller. Additionally, I would thank Tommy Wibetoe from Skagerak Energi for providing the generator's data and Gunne John Hegglid, Marcelo de Castro Fernandes, and Finn Aakre Haugen for their contribution to this thesis.

In this Master's thesis, an excitation control system has been developed in Modelica modeling language with almost similar characteristics as HYMAREG 10's excitation control system. Ultimately, sub models that represent inherent controllers and limiters in the HYMAREG 10 are fitted into a finished excitation system model.

Porsgrunn, 19.05.2021

Luxshan Manoranjan

Contents

Abbreviations

AC	Alternating Current
AVR	Automatic Voltage Regulator
CAD	Computer-Aided Design
CB	Circuit Breaker
CT	Current Transformer
DC	Direct Current
FCOEL	Field Current Overexcitation Limiter
FCUEL	Field Current Underexcitation Limiter
FMI	Functional Mock-up Interface
GCC	Generator Capability Curve
GHG	Green House Gases
HV	High-Value
HVDC	High Voltage Direct Current
LV	Low-Value
NVE	The Norwegian Water Resources and Energy Directorate
NVF	National Guide for Functional Requirements in the Power System
OCC	Open Circuit Characteristics
OEL	Overexcitation Limiter
PF	Power Factor
PI	Proportional-Integral
PID	Proportional-Integral-Derivative
PMG	Permanent Magnet Generator
PPT	Power Potential Transformer

PSAT	Power System Analysis Toolbox
PSS	Power System Stabilizer
PSS®E	Power System Simulator for Engineering
PT	Potential Transformer
SCC	Short Circuit Characteristics
SCOEL	Stator Current Overexcitation Limiter
SCL	Stator Current Limiter
SCPT	Saturable-Current Potential Transformer
SCR	Silicon-Controlled Rectifier
SCT	Saturable-Current Transformer
SCUEL	Stator Current Underexcitation Limiter
SW	Switch
UEL	Underexcitation Limiter
VAR	Volt-Ampere Reactive
V/Hz	Volts-per-Hertz

Nomenclature

The variables presented here are the most common ones. A list of additional parameters can be found in Appendix B – K.

E_A	Induced voltage	$[V]$
E_{FD}	Generator field voltage	$[pu]$
E_{FE}	Exciter field voltage	$[pu]$
$ECOMP$	The input in the *ST7C* model where the output from the terminal voltage transducer interacts, as V_C	$[-]$
$EFD0$	The input in the *ST7C* model where the initial generator field voltage output from the generator interacts	$[-]$
E_{rr}, I_{err}, V_{err}	Feedback error signal	$[-]$
F_1, F_2	The functions that provide the appropriate adjustments so that the effects of terminal voltage on the SCUEL and FCUEL are properly taken into account	$[-]$
f	Actual frequency	$[Hz]$
f_n	Nominal frequency setpoint	$[Hz]$
f_{sp}	Frequency setpoint	$[Hz]$
f_{vsp}	Variable frequency setpoint	$[Hz]$
H	Inertia constant	$[s]$
I_{act}	Actual feedback signal	$[-]$
I_{bias}	The output signal of the activation logic	$[-]$
$I_{ERRinv1}$	The ramp rate characteristic signal	$[-]$
$I_{ERRinv2}$	The inverse-time characteristic signal	$[-]$
I_{FD}	Generator field current	$[pu]$
$I_{FD}{}'$	Normalized field current signal in FCUEL	$[pu]$

I_{FDF}	Filtered field current	$[pu]$
I_{FDn}	Nominal field current	$[pu]$
I_{FDref}	Reference field current in FCUEL	$[pu]$
I_{FDi}	Defined field current at i points	$[pu]$
I_{FD0}	Field current of the air-gap line at stator voltage 1.0 pu	$[A]$
I_{FD1}	Field current of the OCC at stator voltage 1.0 pu	$[A]$
I_{FD2}	Field current of the air-gap line at stator voltage 1.2 pu	$[A]$
I_{FD3}	Field current of the OCC at stator voltage 1.2 pu	$[A]$
I_P	Generator terminal active current	$[pu]$
I_{Pn}	Nominal generator terminal active current	$[pu]$
I_{Psp}	Generator terminal active current setpoint	$[pu]$
I_{Pvsp}	Variable generator terminal active current setpoint input	$[pu]$
I_{pu}	Filtered actual field current	$[-]$
I_Q	Generator terminal reactive current	$[pu]$
$I_Q{}'$	Normalized reactive current signal in SCUEL	$[pu]$
I_{QF}	Filtered reactive current	$[pu]$
I_{Qi}	Defined reactive current at i points	$[pu]$
I_{Qn}	Nominal generator terminal reactive current	$[pu]$
I_{Qref}	Reference reactive current	$[pu]$
I_{Qsp}	Generator terminal reactive current setpoint	$[pu]$
I_{Qvsp}	Variable generator terminal reactive current setpoint input	$[pu]$
I_{ref}	Reference field current in FCOEL	$[pu]$
I_T	Generator terminal current	$[pu]$

J	Moment of inertia	$[kg \cdot m^2]$
K	Generator's construction constant	$[-]$
K_{adj}	Automatic adjustable gain reduction	$[pu]$
K_D	Derivative/differential gain	$[pu]$
K_I	Integral gain	$[pu/s]$
K_P	Proportional gain	$[pu]$
$K(s)$	The output of the PID controller	$[pu]$
M_b	Machine base power	$[MVA]$
m	Mass of rotating part	$[kg]$
P'	Normalized active power signal in SCUEL and FCUEL	$[pu]$
P_i	Defined active power at i points	$[pu]$
P_T	Generator active power output	$[pu]$
P_{TF}	Filtered generator active power	$[pu]$
PF_{active}	Boolean variable to activate the PF controller	$[-]$
PF_{norm}	Power factor input normalizer	$[-]$
$PF_{REFnorm}$	Power factor setpoint/reference normalizer	$[-]$
PF_{sp}	Generator power factor setpoint	[°]
PF_{vsp}	Variable generator power factor setpoint input	[°]
P_0	Initial active power	$[pu]$
Q_T	Generator reactive power output	$[pu]$
Q_0	Initial reactive power	$[Mvar]$
R	Resistance	$[pu]$
R_a	Armature resistance	$[pu]$

r	Distance between axis and rotation mass	$[m]$
$S_{1.0}$	Saturation factor at 1.0 pu	$[pu]$
$S_{1.2}$	Saturation factor at 1.2 pu	$[pu]$
SW_{OEX}	Boolean signal to the switch at the output of the overexcitation region in the SCL to change the position	$[-]$
SW_{PF}	Boolean signal to the switch at the output of the PF controller to change the position	$[-]$
SW_{UEX}	Boolean signal to the switch at the output of the underexcitation region in the SCL to change the position	$[-]$
SW_{VAR}	Boolean signal to the switch at the output of the VAR controller to change the position	$[-]$
T_D	Derivative/differential time constant	$[s]$
T_i	Integral time	$[s]$
V_b	Base voltage	$[kV]$
V_C	Compensated voltage, the output of the voltage transducer and current compensation model, and input to the excitation system models	$[pu]$
V_{CORR}	The output signal of the voltage droop/compensation controller model	$[-]$
V_{FB}	The signal from the *ST7C* that can only be used as an input only for the UEL type *UEL2C* model	$[-]$
V_{FCOEL}	The output signal of the field current overexcitation limiter (FCOEL) model and interacts with the excitation system model inputs V_{OEL}	$[-]$
V_{FCUEL}	The output signal of the field current underexcitation limiter (FCUEL) model and interacts with the excitation system model inputs V_{UEL}	$[-]$

V_F, V_{FE}	Signal proportional to exciter field current (DC rotating exciter or AC rotating exciter)	$[-]$
V_{OEL}	The output signal of the overexcitation limiter (OEL) models and input to the excitation system model	$[-]$
V_{REF}	Voltage reference setpoint	$[pu]$
V_S	Combined power system stabilizer model output and possibly discontinuous excitation control output after any limits or switching and input to the excitation system models	$[-]$
V_{SCL}	The output signal of the stator current limiter (SCL) model	$[-]$
V_{SCOEL}	The output signal of the stator current overexcitation limiter (SCOEL) model and interacts with the excitation system model inputs V_{OEL}	$[-]$
V_{SCUEL}	The output signal of the stator current underexcitation limiter (SCUEL) model and interacts with the excitation system model inputs V_{UEL}	$[-]$
V_{SI}	Power system stabilizer model input variable	$[-]$
V_{ST}	Power system stabilizer model output	$[-]$
V_T	Generator terminal voltage	$[pu]$
V_{TF}	Filtered generator terminal voltage	$[pu]$
V_{Tsp}	Generator terminal voltage setpoint input	$[pu]$
V_{UEL}	The output signal of the underexcitation limiter models and input to the excitation system model	$[-]$
V_{VARPF}	The output signal of the VAR/PF controller model	$[-]$
V_{VHz}	The output signal of the V/Hz limiter model	$[-]$
VAR_{active}	Boolean variable to activate the VAR controller	$[-]$
VAR_{sp}	Generator reactive power setpoint	$[pu]$
VAR_{vsp}	Variable generator reactive power setpoint input	$[pu]$

VOTHSG	The input in the *ST7C* model in OpenIPSL, where the output from the PSS or discontinuous excitation control interacts, as V_S	$[-]$
X	The reactance of the transmission line	$[pu]$
$XADIFD$	The input in the *ST7C* model where the generator field current (I_{FD}) interacts	$[pu]$
Z_b	Base impedance	$[\Omega]$
ΔV_{Tsp}	Change in generator terminal voltage setpoint	$[pu]$
ϕ	Magnetic flux	$[T]$
ω	Rotational speed	$[rad/s]$
ω_r	Rated rotational speed	$[rad/s]$

1 Introduction

During the last decades, the focus on renewable energy technologies has increased significantly due to the world's transition towards a more environment-friendly and sustainable energy future. However, renewable energies such as wind and solar power productions are relatively unpredictable, non-controllable, and have intermittent power production in nature. These could lead to fluctuations in the power supply and cause challenges to the grid. Therefore it is crucial to have a technology that is more flexible, reliable, and can provide stability to the grid. One such old and still greatest technology is hydropower.

Hydropower technology is the lowest emission of Green House Gases (GHG) above all the other power generation technologies. The total produced electricity from hydropower accounts for about 17 % of the world's total power generation, whereas 99 % of the total produced electricity in Norway comes from hydropower technology. Moreover, Norwegian hydropower is also called Europe's largest renewable energy battery due to storage facilities in Norway's reservoirs in about 50 % of all the reservoir capacity in Europe.[2]

Since Norway is one of the leading hydropower nations globally, it is important to develop and strengthen hydropower technology to keep the position as a leading hydropower nation. Therefore the development of existing and new hydropower stations is still increasing. The development of existing and new hydropower plants are not only larger but also small-scale hydropower plants. According to The Norwegian Water Resources and Energy Directorate (NVE), there are 762 small-scale hydropower stations in Norway and produce approximately 10.6 TWh yearly [3].

Small-scale hydropower stations are defined as power production capacity between 1 – 10 MW [4]. Since the construction of large-scale hydropower plants involves technical, environmental and, economic issues, future development of hydropower plants is focused on small-scale hydropower plants [5]. According to Rotilio *et al.* [5], "Small hydropower is a mature technology that is economically implementable and, if properly planned, has minimal impact on the environment." In order to execute a properly planned small-scale power station, accurate modeling and simulations play an important role.

A hydropower plant model can be a mathematical representation of a real plant, which should behave similarly to the real system. In comparison, the simulations allow doing experiments on the model to examine and predict the real plant's behavior during the different operation conditions. There are plenty of varieties of software that are used for modeling and simulations of hydropower plants, such as Alab, CASiMiR, etc. However, there are still some spaces for improvements in this field, especially with respect to accurate modeling and simulations of modern real hydropower components. These improvements will help students and engineers in the future to design properly a power plant closed to reality before the construction begins, and thus money and time can be saved.

Concerning the modeling, a small-scale hydropower plant can comprise thousands of components, such as penstock, valve, dam, generator, exciter, etc. Thus, modeling of whole hydropower plant will be a large project. Therefore, this thesis focuses on the electrical part, especially the modeling and simulation of an excitation control system in the hydropower controller, which should represent the actual hydropower controller HYMAREG 10's excitation control system.

1.1 Background

A hydropower controller, such as HYMAREG 10, consists of several functionalities as an excitation control system, turbine regulation, generator synchronizing, etc. Modeling and simulations of such a controller required to analyze and predict the behavior of the controller for various operations scenarios. In addition, the behavior of the controller may help to analyze and predict the behavior of the generator or turbine through modeling and simulations to improve the design and deployment process. In this thesis, the excitation control system part of the hydropower controller shall be implemented using the real hydropower controller HYMAREG 10 as a reference. Additionally, the model should be documented, and simulation results shall be compared with empirical data.

The previous work of this thesis is initially started as a master project during fall 2019 by USN's students Kahled Aleikish, Okbe Kifle Habte, and Hector C. Zambrano H. In that project, a waterway model of the Sølia hydropower plant was modeled based on the provided data from Småkraft AS. And the simulation results were compared with the real data measurements to verify the results, and the analysis showed some positive results.[6]

Further, the project was continued by Hector C. Zambrano H. as a Master's thesis. In that thesis, the previous model was further developed by implement HYMAREG 10 controller functions. The implemented HYMAREG 10 controller functions are water-level control, speed control, phase control, synchronization control, and frequency control. They have also added a signal to the main circuit breaker. The work was summarized to be working, but some tuning and developments are necessary to achieve more accuracy.[7]

Finally, in fall 2020, the model was improved by a project group of three students from the master program in electrical power engineering, Khemraj Bhusal, Jonatan Hellborg, and Tonje Tollefsen. This group has developed water-level, frequency, and power factor controllers. And further divided hydropower controller into several sub-controllers as a level controller, frequency controller, power factor controller, synchronization controller, and excitation controller, and fitted into a finished HYMAREG 10 controller. And the group concluded that the models behave as desire, and some functions from the HYMAREG 10 controller are still missing.[1]

This thesis reimplements the particular excitation controller from the master project 2020 [1] based on HYMAREG 10 controller functionalities. However, the final implemented excitation controller model shall fundamentally consist of functionalities such as automatic voltage regulation, field current regulation and limitation, active and reactive current control, volts-per-hertz limitation, and power factor control. And finally, the results shall be compared with the real data.

1.2 HYMAREG 10

HYMAREG 10 is one of Hymatek Controls AS' products. Hymatek Controls AS is one of the leading providers of turbine governors and excitation equipment for hydropower plants in Norway. Also, they provide services as hydropower plant analysis as well as protection and control of waterways. In particular, They also supply control systems for small-scale hydropower plants. [8]

The hydropower controller HYMAREG 10 is primarily intended for a small-scale hydropower plant that consists of several functions as follows [9]:

- Turbine regulation
- Voltage regulation
- Water level regulation
- Generator synchronization
- Speed monitoring

There are mainly two types of HYMAREG 10 controllers, HYMAREG 10B and HYMAREG 10S. Where HYMAREG 10B is primarily intended for brushless synchronous generators, but it can also be used for static excitation systems for small generators. Whereas the HYMAREG 10S controller is for larger generators with static excitation systems.[9]

1.3 Hogstad Hydropower Plant

Hogstad power plant is located in Opdalen in the Siljan municipality, and it is the second power plant in the Siljan string. The power plant produces 40 GWh yearly, with an installed generator of 9 MW or 10 MVA (A in Figure 1.1) and another with 0.6 MW (B in Figure 1.1). The Hogstad plant was initially built and commissioned by Trescow in 1912. Both generators are equipped with Francis turbines with a gross head of 136 m and a flow rate of 8 m^3/s.[10]

Figure 1.1: Generators in the Hogstad hydropower plant. A: 9 MW generator, B: 0.6 MW generator. [10]

1.4 Objectives and Scope

The purpose of the Master's thesis is to model an excitation control system of a hydropower controller and then verify the model by comparing simulated values to the real plant data from the Hogstad power plant. The objective then is to end up with a final excitation controller model consisting of various controllers and limiters that should represent and behave similarly to the actual excitation system controller part in the HYMAREG 10.

The original task description can be found in Appendix A. It has been adapted and will cover the following items:

1. Investigate the functionality of a typical hydropower control unit for small hydropower systems, especially wrt voltage regulation.
2. Make yourself familiar with the excitation options as offered by the HYMAREG 10.
3. Create a typical power system model in Modelica using the OpenIPSL(openipsl.org) in order to serve as a test bench for the voltage regulation functionality of the hydropower controller.
4. Model, implement and simulate an excitation control system with the following functionalities:
    a. Current limitation
    b. Active and reactive current control (droop and compensation)
    c. V/Hz limitation
    d. Reactive power or power factor control
5. Test the model for different operation scenarios and test against empirical data provided by the external partner.
6. Document the models.

1.5 Report Outline

This Master's thesis paper consists of six chapters. After chapter one, the introduction, and the next following six chapters are briefly described:

- ***Chapter 2*. Theory**
  At the beginning of this chapter, the relevant fundamental theory of the electric generator and excitation control system is introduced. Further, it describes characteristics of different types of excitation systems, protective limiters, and then functionalities of voltage droop/compensation and reactive power or power factor controllers.

- ***Chapter 3.* Software**
  Chapter 3 contains a brief description of the Modelica modeling language, Dymola software, and simulation library OpenIPSL used during this study.

- ***Chapter 4.* Modeling**
  This chapter mainly contains information about how the controllers and limiter in the excitation control systems were modeled in Dymola using standard and OpenIPSL library components. It also describes the user interfaces that were implemented in the models.

- ***Chapter 5.*** **Simulation Results**
  Mainly presents the simulation results from all the models as well as the comparisons between the simulated and the real data.

- ***Chapter 6.*** **Discussion**
  This chapter presents a general discussion about possible issues with the models and the simulation results compared to the expected results.

- ***Chapter 7.*** **Conclusions and Future Work**
  Finally, the conclusions regarding the results, as well as comments on recommendations for further work, are presented.

2 Theory

This chapter provides the fundamental theory of the excitation control system to get an overview of inherent components in the excitation control system and how they are principally working. Also, the different types of standard excitation systems and limiters, as well as the HYMAREG 10's voltage droop/compensation function and Norwegian requirement for excitation system performance, are presented.

2.1 Electric Generator

A generator is an Alternating Current (AC) machine that converts mechanical energy to electrical energy. There are mainly two types of generators used to produce electrical energy synchronous generator and induction generator, which is also called an asynchronous generator. The main differences between these generators are the construction of the rotor (rotating part), rotational speed, and how the field current is supplied. Among these two generators, synchronous generators are the most used generators in hydropower due to their ability to control reactive power and keep the grid stable.[11]

A typical synchronous generator mainly consists of the following parts, which is also indicated in Figure 2.1 [11]:

1. Rotor: Rotating element of the generator that rotated by a mechanical source as water in hydropower plant.
2. Stator: Stationary element of the generator that produces electrical energy.
3. Rotor/Field winding: Winding that produces a main magnetic field in the generator using an excitation system.
4. Stator/Armature winding: Where the rotational magnetic field from the rotor induces a three-phase voltage.
5. Excitation system: The system that provides and controls the Direct Current (DC) to the field windings to control the terminal voltage.

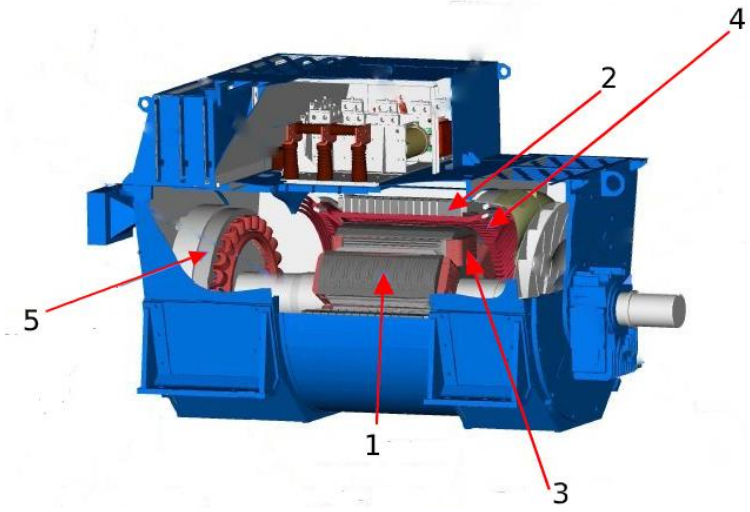

Figure 2.1: Cutaway diagram of the Synchronous generator, 1. Rotor, 2. Stator, 3. Rotor/Field windings, 4. Stator/Armature windings, and 5. Excitation system. [12]

In hydropower plants, the potential energy of the water head is converted to kinetic energy by letting the water flowing through the penstock. That kinetic energy is harvested by water

turbines and converted into rotational energy as the shaft of the generator is connected to the turbine. Then, the rotational energy causes the generator's rotor to rotate. In order to convert rotational energy to electrical energy, the excitation system should supply DC to field winding to produce the desired magnetic field. The produced magnetic field then induces the voltage in the armature windings, and at the end of the windings, at the terminals, the electrical power grid can be connected to harvest the electrical energy.[1]

As mentioned above, the excitation system plays a vital role by controlling the magnetic field of the generator to produce electrical power. More about the excitation system will be covered in the next coming sections.

2.2 Excitation System

An excitation system acts as a source of electrical power for the field winding of the synchronous generator. The rotational magnetic field induces the voltage in the armature windings to produce a sinusoidal AC voltage in the generator terminals. The amount of output voltage at the generator terminals depends on the strength of the magnetic field as produced by the field winding. The magnetic field is mainly controlled by an excitation system that supplies the field voltage to the rotor winding. The induced voltage can be expressed in a simple formula to emphasize the crucial variables during the generation operation [11]:

$$E_A = K\phi\omega \tag{2.1}$$

where

E_A	:	Induced voltage	$[V]$
K	:	Generator's construction constant	[-]
ϕ	:	Magnetic flux	$[T]$
ω	:	Rotational speed	$[rad/s]$

As Eq. (2.1) shows, the induced voltage E_A is proportional to magnetic flux ϕ and rotational speed ω. This means, during the normal operation, the rotational speed of the synchronous generator is locked into the synchronous speed of the power system. Thus, the rotational speed will be kept constant, and the only possibility to change the magnitude of the induced voltage is by varying the magnetic flux. This can be acquired by controlling the field current I_{FD} in the exciter. [1], [11]

Since the excitation system produces the field current in the rotor that rotates continuously during electricity production, a special arrangement is essential for transferring the DC to field windings. There are plenty of types in excitation systems, and this leads to most of the complexities involved, and these various excitation systems are explained in Section 2.3.

In addition, an excitation system comprises several components that inherent control and protective functions to secure the adequate performance of the generator and power system. An overview of these components is briefly described in Section 2.2.1.

2.2.1 Excitation Control System

The fundamental function of an excitation control system is to automatically adjust the DC to the field winding of the synchronous generator in order to maintain the generator within its capability as well as to provide effective voltage control and stability enhancement of the power system. Therefore, some additional functions are essential, e.g., controllers, to control the voltage or reactive power output and stabilizers to enhance the power system's stability. Also, the protectors protect the generator, excitation system, and other components in the power system. Figure 2.2 depicts a block diagram of the typical components of an excitation control system.[13]

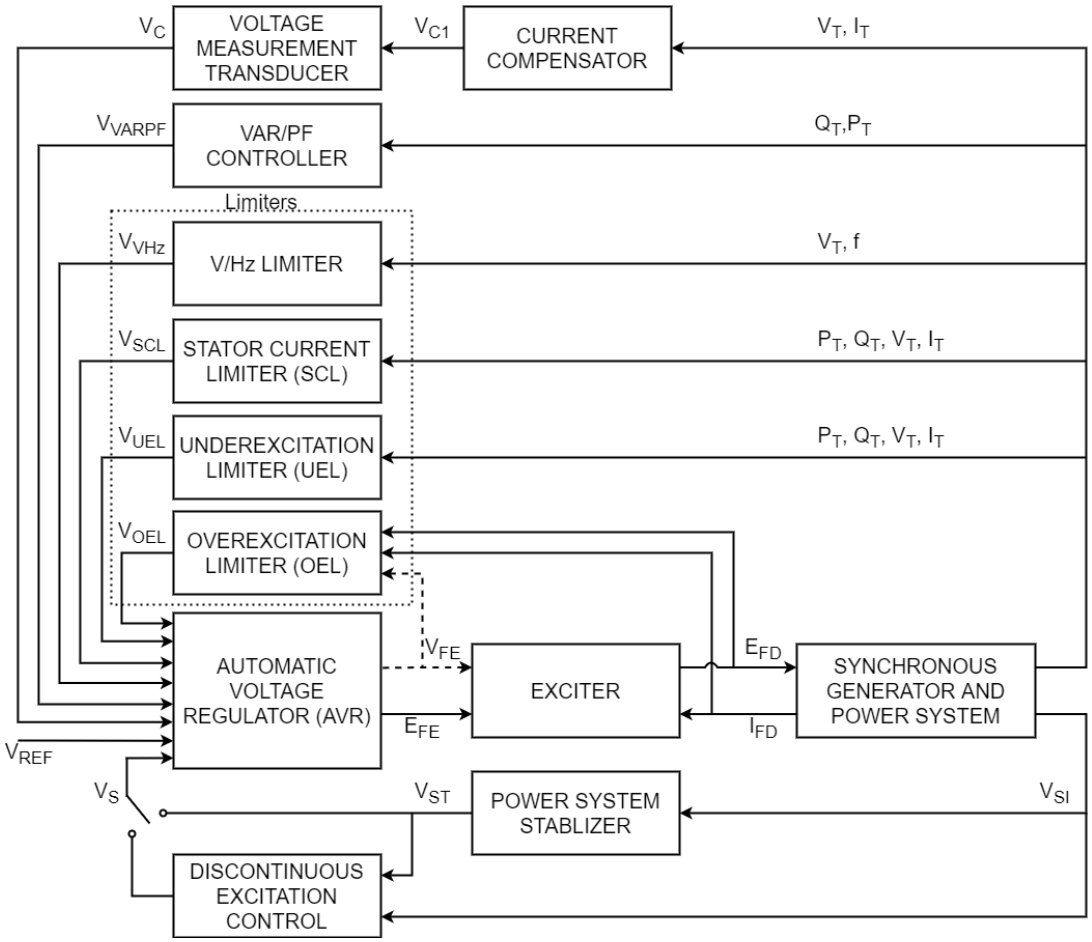

Figure 2.2: Functional block diagram of a synchronous generator excitation control system.[14](modified)

Where the purpose of components indicated in the block diagram above are the following [14]–[17]:

- Automatic voltage regulator (AVR): Amplifies and processes the input control signals to control the amount of current and voltage produced by the exciter. A typical AVR includes functions as:
  - AC regulator: Maintains voltage in the stator.
  - DC regulator: Keeps constant generator field voltage when the AC regulator is failed and uses for testing and startup.
  - Stabilizing circuit: Stabilize AVR itself during disturbances or abnormal situations.

Besides, the AVR may also be configured to provide reactive power or power factor regulator.

- Exciter: Provides required DC for the field windings of the synchronous generator to produce the desire terminal voltage.
- Synchronous generator and power system: Converts mechanical energy to electrical energy and delivers power to the power grid.
- Power system stabilizer (PSS): Enhance the system stability by compensating for low frequency (0-3Hz) oscillations in the power system. Also, to obtain a more stable generator output.
- Voltage measurement transducer: Measures the output voltage of the generator using potential transformers and converts and filter out to DC to compare with the reference voltage and the error signal in the AVR.
- Current compensator: Provides active and reactive current compensation using either droop and/or line drop compensation to keep a constant voltage at a point external to the generator.
- Overexcitation limiter (OEL): Limit the excessive field current to avoid overheating of the field winding. The limits can be obtained using the generator capability curve (GCC).
- Underexcitation limiter (UEL): Act as a boost excitation to increase the field current to prevent loss of synchronism, overheating in stator end region, and loss-of-excitation relays.
- Stator current limiter (SCL): Prevents overheating of the stator winding due to operations such as significant changes in system voltage or increase in turbine power without any upgrade in generator stator windings.
- Volt-per-hertz (V/Hz) limiter: Reduce the excitation to protect the synchronous generator against excessive magnetic flux resulting from low frequency and/or overvoltage.
- Reactive power and power factor (VAR/PF) controller: Automatically adjust the generator output reactive power (VAR) or power factor (PF) concerning user specification.
- Discontinues excitation control: Enhance the stability during the large transient disturbances. Also, to reduce the full exploit the potential of the excitation system with continuous excitation control with terminal voltage and PSS.

This thesis does not look deeply into PSS and discontinues excitation control function since these are neither implemented in HYMAREG 10.

2.3 Types of Excitation System

The excitation system of the synchronous generator can be mainly classified into three types, as follows [14]:

- Direct Current Commutator Rotating Excitation System
- Alternator Supplied Rectifier Excitation System
- Static Excitation system

2.3.1 Direct Current Commutator Rotating Excitation System (DC Type)

This type of excitation system utilizes DC generators to produce excitation power to provide field current through slip rings of the generator (alternator in Figure 2.3). DC excitation system consists of two exciters, where the first one is known as the main exciter, which is a separate excited DC generator that provides field current to the generator. And the second one is known as the pilot exciter, which is comprised of a Permanent Magnet Generator (PMG) in order to provide field current to the main exciter (see Figure 2.3). Both exciters can be either driven by a separate motor or through the shaft of the main generator. [18], [19]

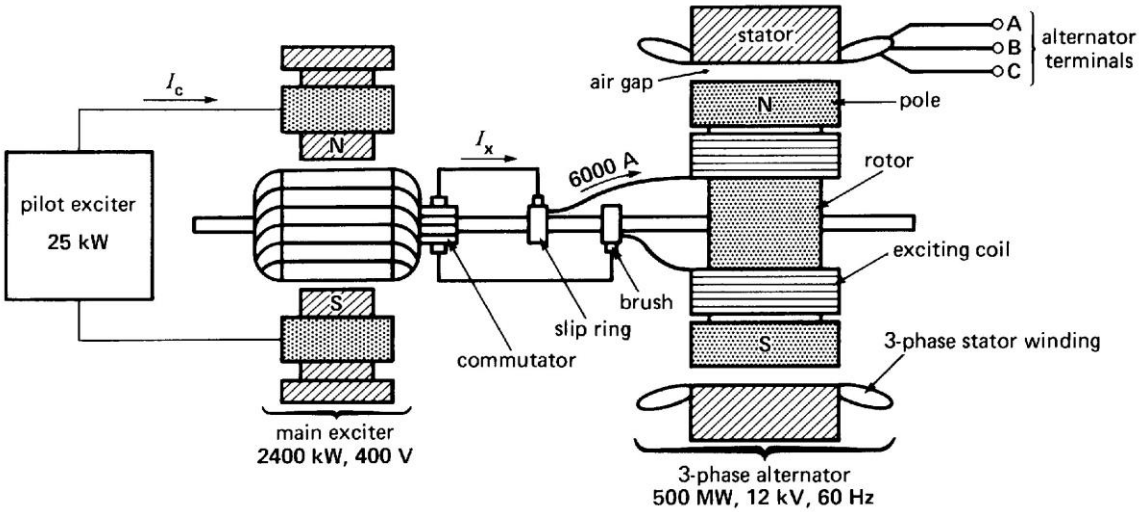

Figure 2.3: Illustration of a DC excitation system concept with the pilot exciter. [20]

A single-line diagram of the typical DC type excitation system with an amplidyne voltage regulator is shown in Figure 2.4. An amplidyne is a special type of rotating amplifier that provides incremental changes to the exciter field. The produced DC in the exciter is controlled by amplidyne and supplied through the commutator (an electrical switch that reverses the field current direction) and slip rings to the main generator. DC excitation has the advantage of being more reliable and compact in size. However, the disadvantage of this system is complex voltage regulation, very slow response (time constant in the range from 0.02 to 0.25 sec). Thus, currently, the DC excitation systems have been replaced by AC excitation systems and static excitation systems. [13], [18], [21]

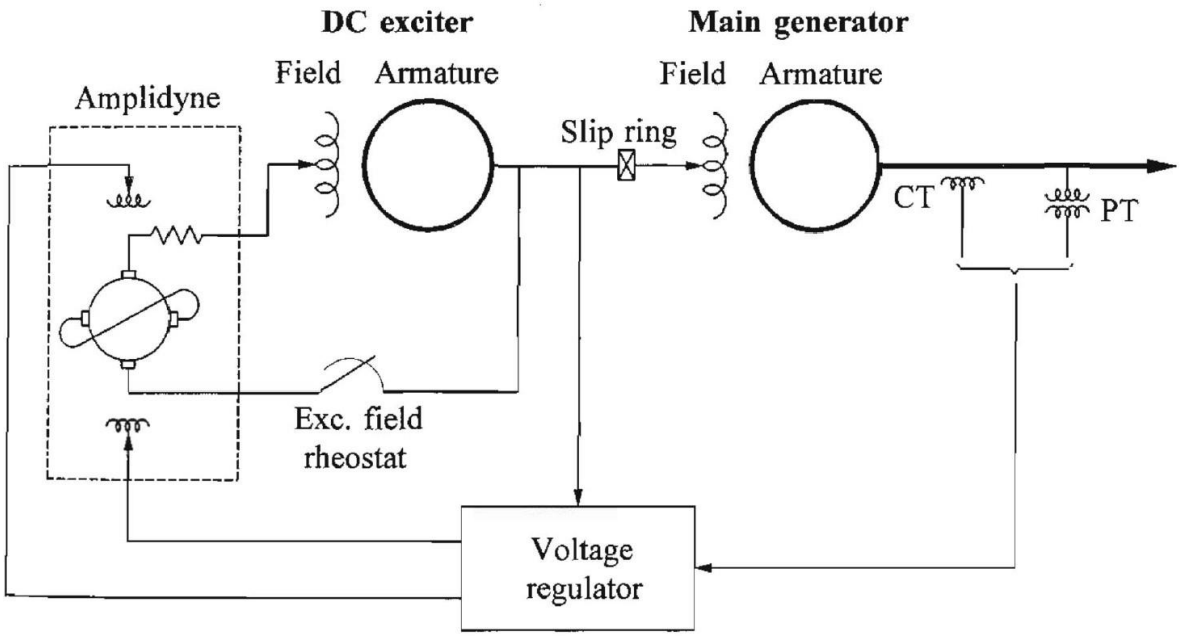

Figure 2.4: Single-line diagram of the DC excitation system with amplidyne voltage regulator. [13]

2.3.2 Alternator Supplied Rectifier Excitation System (AC Type)

An AC type excitation system mainly consists of an AC exciter that is connected to the same shaft as the generator to produce excitation power to the field winding of the generator. However, the AC exciter produces only AC, while the field winding needs DC to produce the magnetic field. This problem is solved by conducting the AC output through a thyristor rectifier bridge (controllable) or a diode rectifier bridge (uncontrollable) to the field winding of the main generator. This excitation system can be classified concerning rectifier arrangement, exciter output control method, and excitation source of the exciter. The AC excitation system is currently categorized as a stationary excitation system and a rotating excitation system, and these are briefly described in Section 2.3.2.1 and 2.3.2.2, respectively. [13], [18]

2.3.2.1 Stationary Excitation System

This system consists of stationary field windings and a rotating armature winding, where the DC output from the rectifier is conducted through the slip rings to the field winding of the generator. When controlled rectifiers are used, the regulator directly controls the DC output of the exciter. But when non-controlled rectifiers are used, the DC output is controlled by control the AC exciter field current. Figure 2.5 shows the single-line diagram of the system, where the AC exciter field current is controlled by the controlled rectifier to control the generator field. [13], [18]

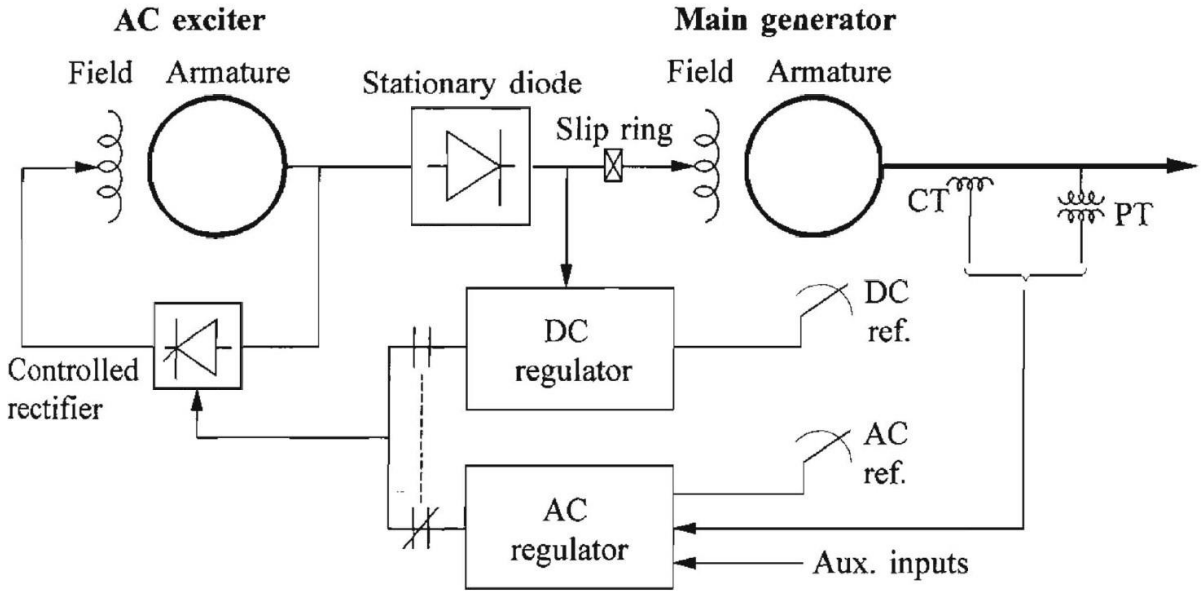

Figure 2.5: Single-line diagram of the non-direct main field-controlled stationary excitation system. [13]

Figure 2.6 depicts a single-line diagram of the direct main field-controlled stationary excitation system, which has a thyristor rectifier that directly controls the main generator's field current by controlling the firing angle of the thyristor. Thus, this type of controller has a short response time than the latter type. [13]

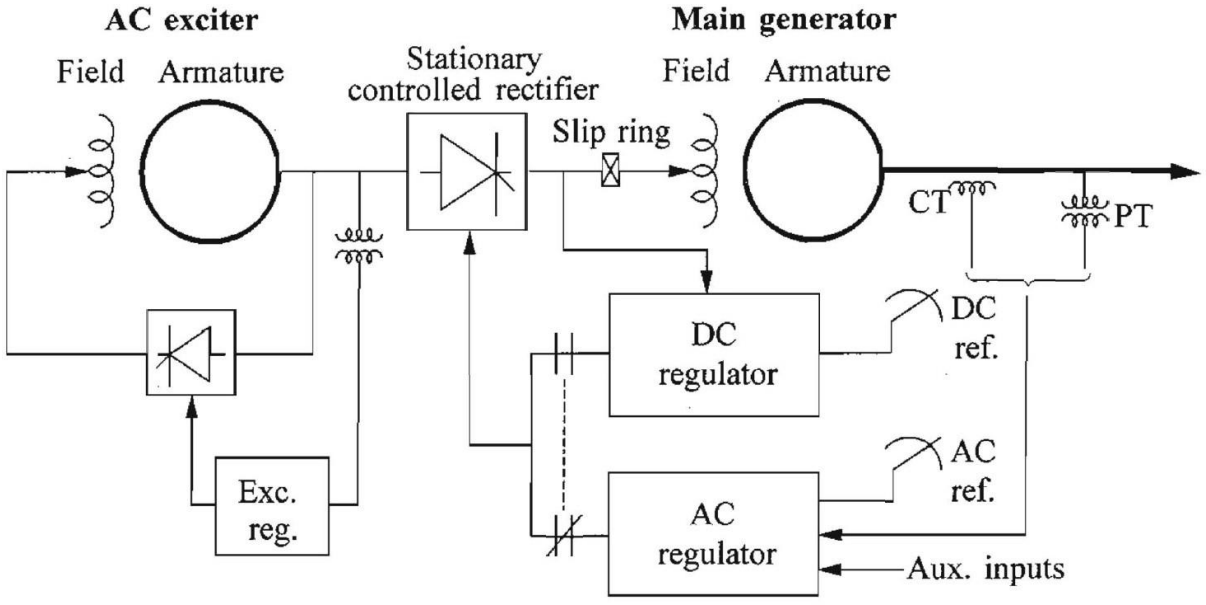

Figure 2.6: Single-line diagram of the direct main field-controlled stationary excitation system. [13]

The voltage controller in both controllers gains power from exciter output. The voltage regulator consists of two types of regulators, where the AC regulator keeps the terminal voltage at the desired value as determined by AC reference. And the DC regulator keeps the main field voltage at the desired level corresponds to the DC reference. The AC regulator is the primary regulator, while the DC regulator is a secondary controller that takes control of the excitation system when the AC regulator is faulty or needs to be disabled. The advantages of this system

are fast response and low cost, but the disadvantage is that it requires a slip ring and brush. [13], [18], [21]

2.3.2.2 Rotating Excitation System

The rotating excitation system does not require slip rings and brushes because the rotating rectifier is directly connected to the generator (alternator) field winding (see Figure 2.7). Such systems are developed to avoid problems with the brushes when a high field current is applied to a larger generator. Thereby, this system is also known as a brushless excitation system. [18], [19]

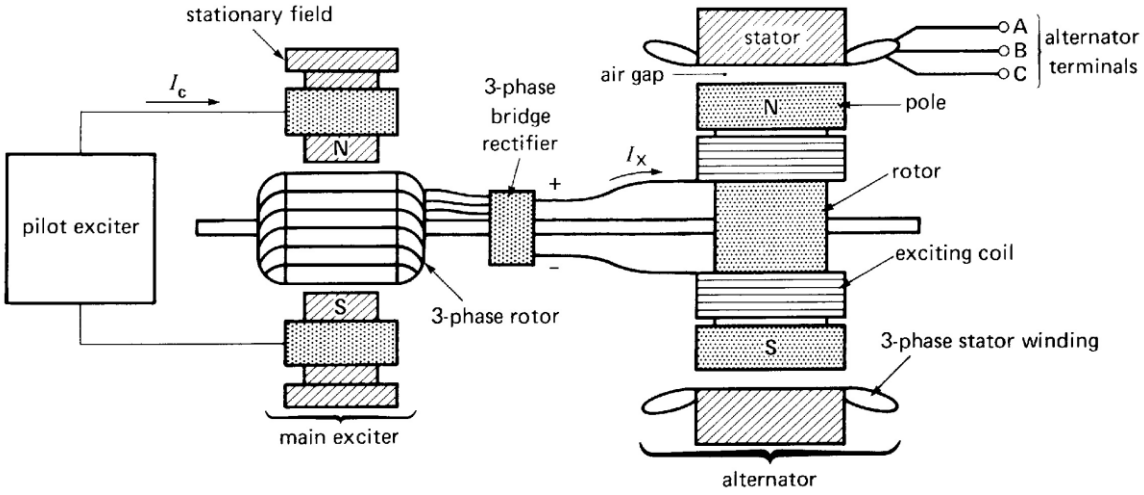

Figure 2.7: Illustration of a rotating excitation system concept. [20]

Figure 2.8 depicts a single-line diagram of the rotating excitation system, where a dashed rectangle indicates the rotating part. This system is consists of a regulator, rectifier, main exciter, and a PMG pilot exciter. Both the main and pilot exciter is driven directly from the main shaft. The generator field is directly connected through silicon rectifiers and the rotating armature of the main exciter. The pilot exciter is a shaft-driven PMG that has permanent rotational magnets on the shaft and a three-phase stationary armature. The produced power from the pilot exciter is transferred to the AC exciter through the thyristor bridges. Then, the AC exciter produces the main field current and fed through an uncontrolled rectifier to the generator's field winding. This system's advantages are high in reliability, provides flexible operation, faster in response, and has low maintenance due to the elimination of slip rings and brushes. Also, this system has a short time constant that affords a major advantage in small-signal dynamic performance and power system stabilizing signals enhancement. However, this system has the disadvantage of slow de-excitation.[13], [19], [21]

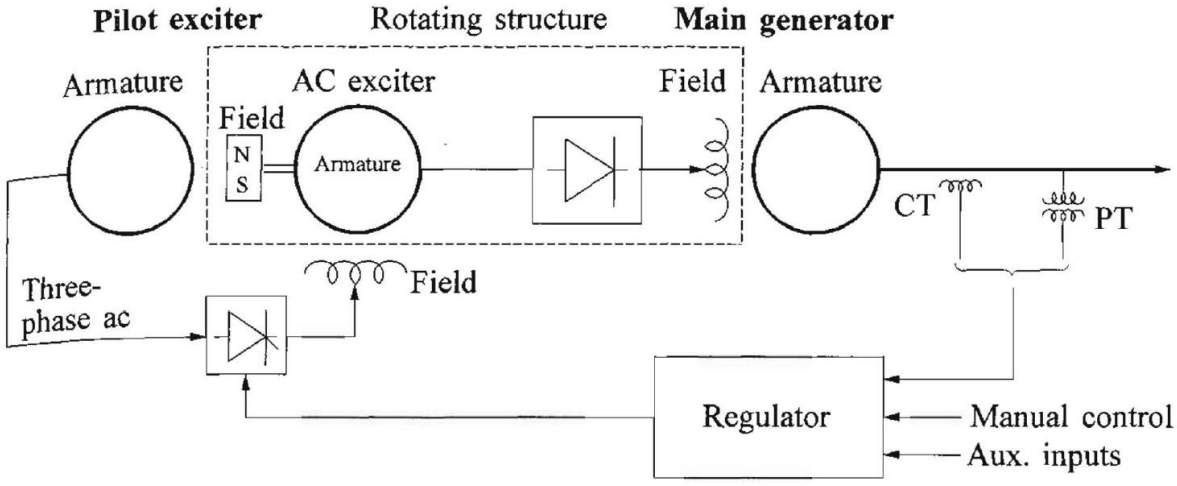

Figure 2.8: Single-line diagram of the rotating excitation system (brushless excitation system). [13]

2.3.3 Static Excitation System (ST Type)

In this system, all the components are either static or stationary, and the generator itself provides excitation power, meaning the generator is a self-exciter. The reason for that is that the static excitation system does not comprise the main exciter as DC and AC excitation systems. The derived power from the generator is fed through a step-down transformer, mercury-arc, or silicon-controlled rectifiers (SCR), then back to the field windings of the generator through slip rings. In some cases, excitation power is derived from the auxiliary windings in the generator. Since this system depends on the terminal voltage of the synchronous generator, the excitation ceiling voltage (maximum exciter output voltage) of this system is limited by the terminal voltage. However, during the system fault conditions, the terminal voltage is suppressed. Hence excitation ceiling voltage is reduced. This dependency causes instantaneous response and the high post-fault field-forcing capability. At the initial stage, the generator cannot produce voltage without any field current to solve this auxiliary power source to provide field current. The batteries are usually used as an external power source to initiate the field current, and this process is called field flashing. [13], [18], [19]

The advantages of this system are high-speed response (faster than AC excitation system), high reliability, excellent dynamics performance, small in size, simple system, low losses, reduced maintenance cost due to lack of windage loss, and commutator wearing. The disadvantage of this system is that it requires slip rings and brushes. [19], [21]

There are primarily three forms of ST-type excitation systems that have been widely used, and these are described in Section 2.3.3.1, 2.3.3.2, and 2.3.3.3.

2.3.3.1 **Potential-Source Controlled-Rectifier System**

These types of systems are usually called bus-fed or transformer-fed static systems. Meaning, excitation power is fed from the generator terminals or auxiliary buses through a step-down transformer (see Figure 2.9). [13]

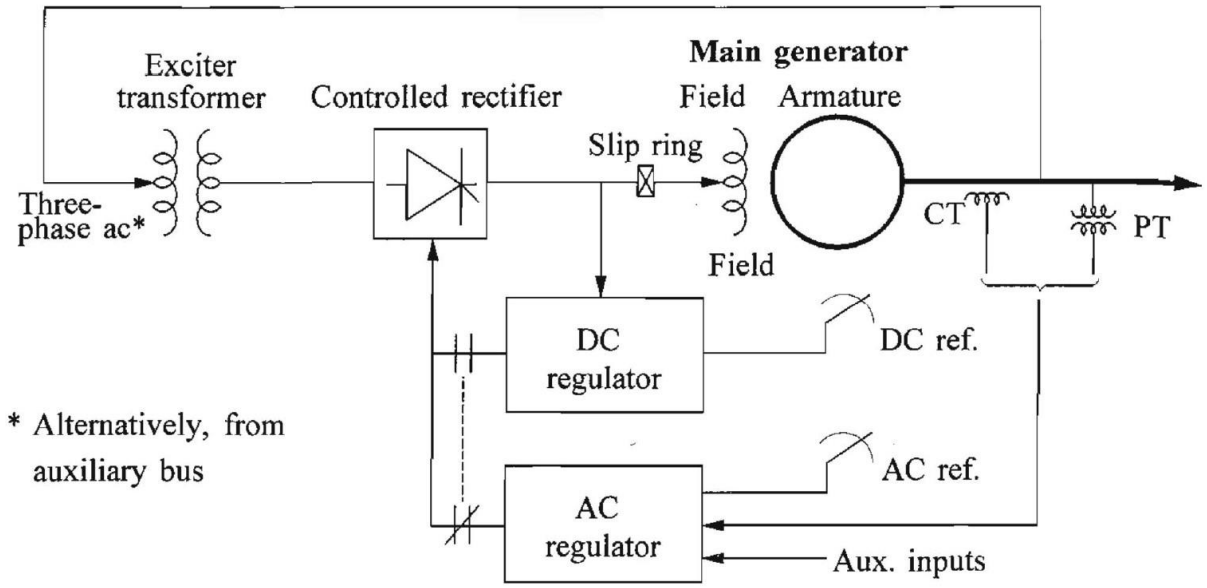

Figure 2.9: Single-line diagram of the potential-source controlled-rectifier excitation system. [13]

2.3.3.2 **Compound-Source Rectifier System**

This system utilizes the current and voltage from the generator using a power potential transformer (PPT) and a saturable-current transformer (SCT) or a saturable-current potential transformer (SCPT) to power the excitation system. Where Figure 2.10 shows a single-line diagram of the compound-source rectifier excitation system with PPT and SCT. The regulator controls the field current by control the SCT. During the loaded conditions, part of the excitation power is gained from the generator current through SCT and the rest from PPT. Unlikely, during the no-load condition, meaning the armature current is zero, the PPT supplies the entire excitation power.[13]

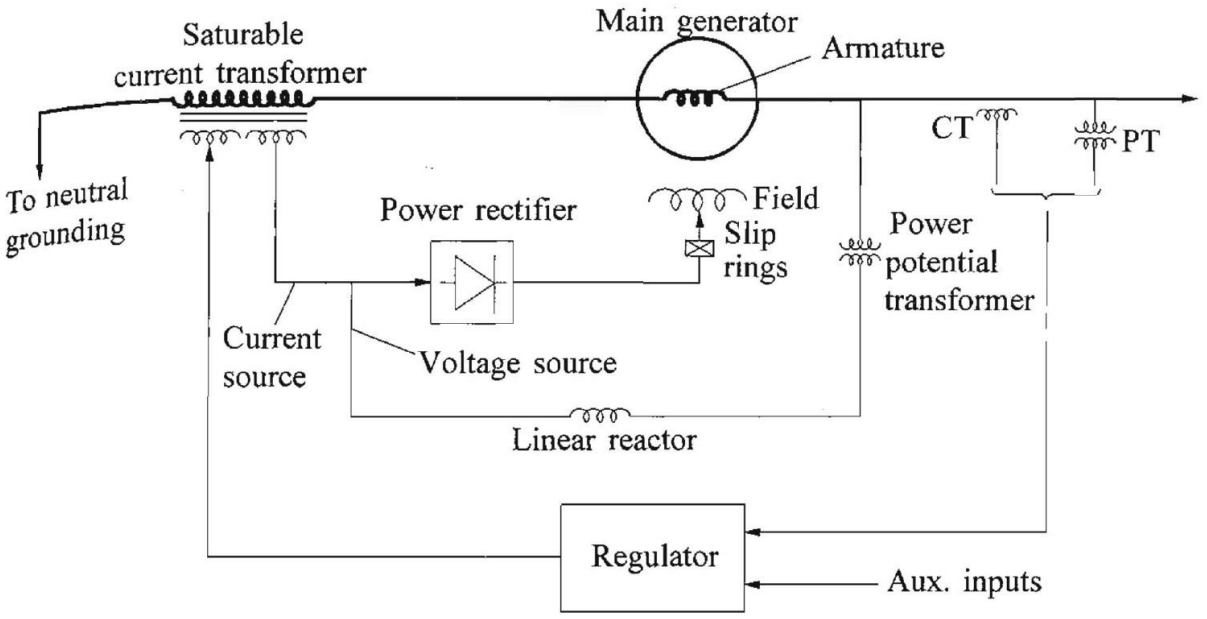

Figure 2.10: Single-line diagram of the compound-source rectifier excitation system.[13]

2.3.3.3 **Compound-Controlled Rectifier Excitation System**

The power to the excitation system is derived from the compounding of voltage and current sources within the generator stator using controlled rectifiers in the exciter output circuits (see Figure 2.11). Set of three-phase windings placed in the generator stator, and a series linear reactor is used to obtain voltage source. At the same time, the transformer placed in the neutral end of the stator winding is used as a current source. The resultant output from both these sources is rectified by a combination of diodes and thyristors connected to form a shunt bridge. And where the AC regulator controls the thyristors through the DC regulator. The notations "C", "P", and "F" mentioned in the Figure 2.11 are current and potential primary windings and corresponding secondary winding, respectively.[13]

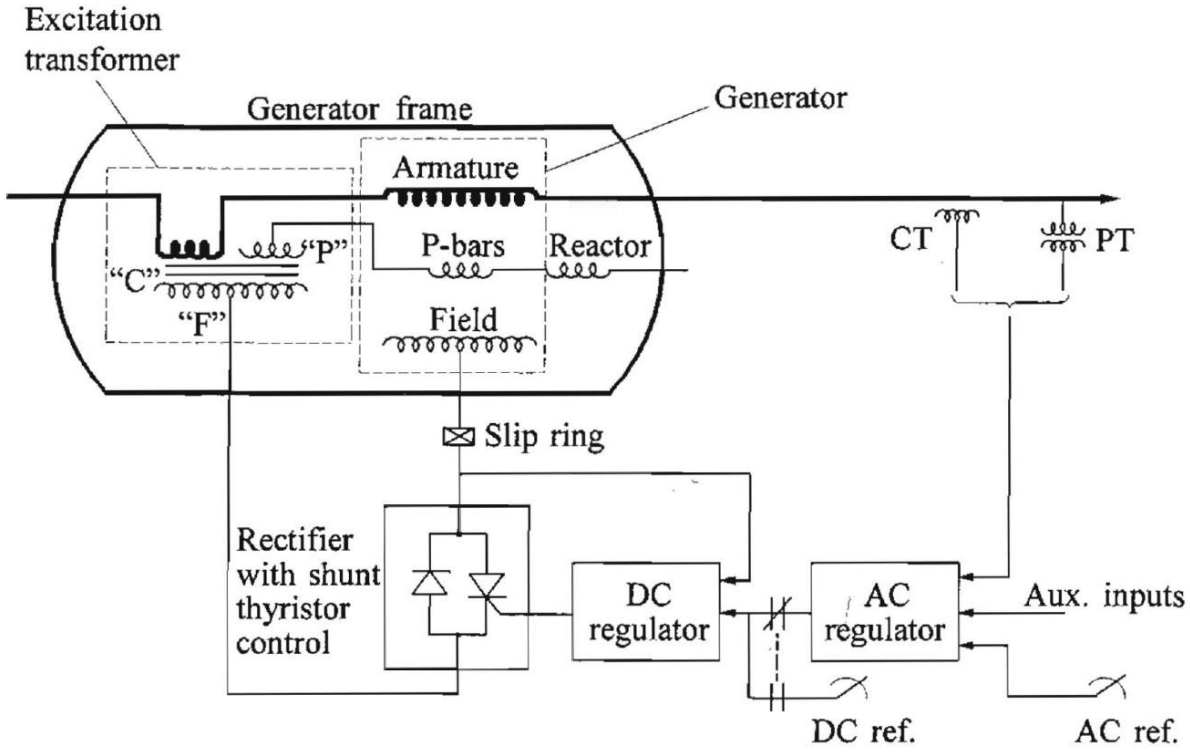

Figure 2.11: Single-line diagram of the compound-controlled rectifier excitation system. C: Primary current winding, P: Primary potential winding, F: Secondary winding [13]

2.4 Limiters

A synchronous generator must be operated within its limits for active and reactive power output in order not to exceed the thermal capability of different components. The limiters ensure that exciters and synchronous generators are not exceeding their capability limits during normal and abnormal operating conditions. Therefore, the limiters comprise several types of control and protective functions. Most common limiters are determined using the generator capability curve (GCC) of a specific generator. Figure 2.12 depicts the GCC of a synchronous generator, where curve A is an OEL that limits the field current during the overexcited (exporting reactive power to the grid) operation. And curve B is an UEL that prevents the excitation level from falling below the limit concerning active and reactive power or current during the underexcited (importing reactive power from the grid) operation. Curves C represents stator winding limits

that are protected by the stator current limiter. Also, there are plenty of other various limiters being used to protect equipment in the power plant as the volts-per-hertz limiter, and the functionality of some of these conventional limiters is briefly explained in this section.[13]

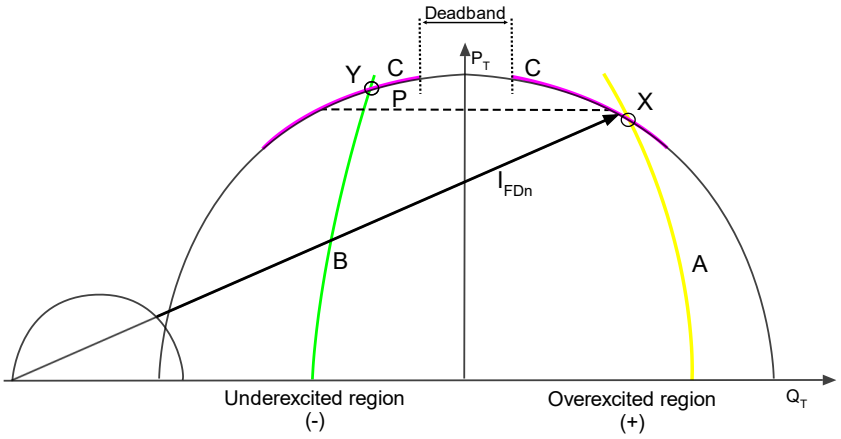

Figure 2.12: Synchronous generator capability curve with standard limits A: Field current limits, B: Stator end region limit and, C: Stator winding limit (between X and Y), I_{FDn}: Nominal field current, and P: Turbine power [22] (modified)

2.4.1 Overexcitation Limiters (OEL)

Overexcitation limiter, also commonly referred to as maximum excitation limiter and field current limiter, that protects the generator from overheating due to prolonged field overcurrent. Simultaneously, it allows the maximum field forcing for power system stability purposes. The generator field winding is designed to operate continuously at rated load conditions. But during voltage collapse or system islanding, the power system will be stressed and cause the generator to operate at high levels of excitation for a period. This limiter measures the field current, field voltage, or exciter field current or voltage to detects overexcitation. When the overexcitation is detected, it allows continuing the overexcitation for a certain period, defined as the time-overload period, and then reduce the excitation level to a safe level. If this function does not reduce the excitation to a safe value, the OEL limiter will trip the exciter field breaker.[13], [14]

The OELs have two types of time-overload periods that allow overexcitation, inverse time or fixed time. The inverse time limiters operate with the time delay matching the generator's field thermal capability, as shown in Figure 2.13. While the fixed time limiters operate when the field current exceeds the pickup value for a fixed set time, irrespective of the degree of overexcitation. Currently, a more common type of OEL is a combination of both instantaneous and inverse-time pickup characteristics. [13], [14]

The HYMAREG 10 also provides some specialized overexcitation limiters, such as Field Current Overexcitation Limiter (FCOEL) and Stator Current Overexcitation Limiter (SCOEL). The FCOEL is principally the same as OEL, but SCOEL protects the stator windings against thermal overload in case of excessive inductive load and assures that the machine always has a work point within given limits [22]. More information about these functionalities of the FCOEL and SCOEL can be found in Section 4.4.1 and 4.4.4, respectively.

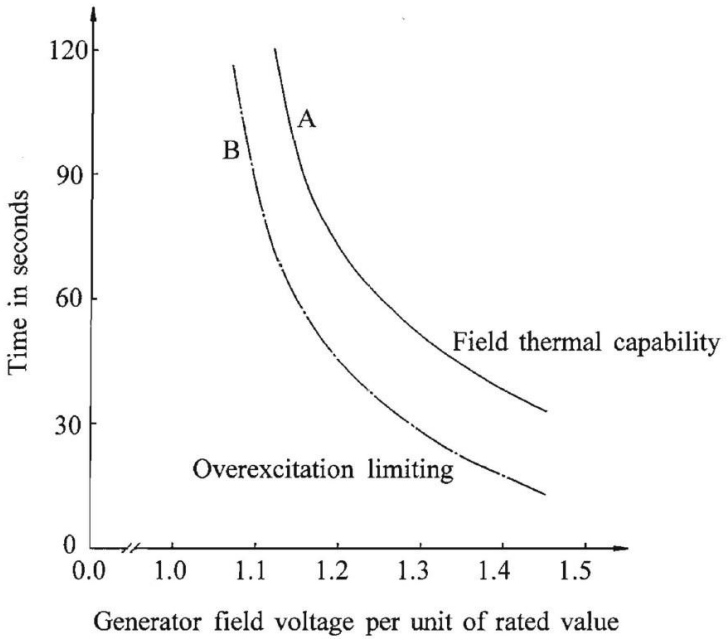

Figure 2.13: Coordination of overexcitation limiting with field thermal capability [13]

2.4.2 Underexcitation Limiter (UEL)

The underexcitation limiter prevents the reduction of the excitation level of the synchronous generator by increasing the excitation in the generator for one or more following purposes [14]:

- To prevent operating beyond the small-signal (steady-state) stability limit of the synchronous generator, which could lead to loss of synchronism.
- To prevent loss-of-excitation relays from operating during underexcited operation.
- To prevent overheating in the stator end region of the synchronous generator, typically defined by GCC.

The UEL limiter typically uses a combination of either voltage and current or active and reactive power of the synchronous generator to determine the control signal. Most importantly, the limiter should be coordinated with the required protection purposes as mentioned above to protect the generator adequately. Figure 2.14 demonstrates a coordination of the calculated small-signal stability limit (I) and loss- of-excitation relay characteristic (II), where the intention was to protect against small-signal stability (I). If the UEL is supposed to protect against overheating in the stator end region, the coordination will be the same, but the small-signal stability limit is replaced by the overheating limit.[13], [14]

The HYMAREG 10 also provides some specialized underexcitation limiters, such as Stator Current Underexcitation Limiter (SCUEL) and Field Current Underexcitation Limiter (FUEL). The SCUEL is a typical conventional UEL whereas, FCUEL maintains an excitation level above or equal to a defined level concerning the load to provide the generator with sufficient synchronizing torque and prevent the generator from falling out synchronous speed [22]. More information about these functionalities of the SCUEL and FCUEL can be found in Section 4.4.2 and 4.4.5, respectively.

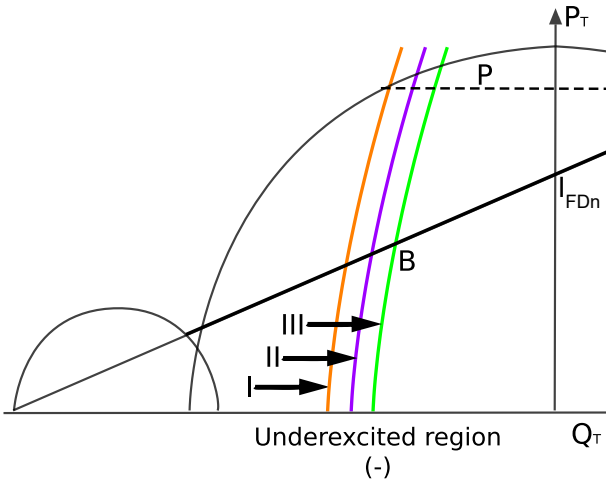

Figure 2.14: Coordination between UEL. I: Small-signal stability limit, II: Loss-of-excitation relay, III: Underexcitation limit set by the UEL, I_{FDn}: Nominal field current, and P: Turbine power [13]

2.4.3 Stator Current Limiter (SCL)

A stator current limiter is used to limit the high stator currents that cause overheating of the stator winding. High stator currents may occur due to significant changes in system voltage or increase in turbine power without considering the capability of generator stator windings. Here the SCL cannot directly limit the generator output current (stator current). It can only modify the excitation during the operation with the reactive stator current. Tab change of the main transformers or reduction of turbine power can be considered as an alternative to reduce the stator current. [14]

Common SCLs are mainly vary the excitation level to limit the stator current. The excitation level is varied based on whether the synchronous generator is operating inside the overexcited or underexcited region. When the generator is overexcited, the SCL should reduce the excitation to decrease the stator current. In contrast, when the generator is underexcited, the SCL should increase the excitation to reduce the stator current. [14]

The SCL is responsible for limiting the stator current between points *X* and *Y* on the GCC. As shown in Figure 2.12, the SCL limit or setpoint should be below the OEL's predefined limit and above the UEL's predefined limit. In addition, the SCL setpoint is usually set above the stator current corresponding to generator-rated apparent power to ensure that SCL does not reduce the excitation during the normal operation. The turbine capability limits the active power output of the generator in such a way that the reactive power output remains below the SCL characteristic. Thereby, the SCL would never become active under normal voltage conditions. If the turbine power increases, the generator stator windings should be upgraded; otherwise, the SCL might become active under normal operating conditions. [14]

2.4.4 Volts-per-Hertz (V/Hz) Limiters

V/Hz limiters protect the generator's core and step-up transformers from significant overheating and damage due to excessive magnetic flux. The excessive magnetic flux typically results from low frequency and overvoltage. This limiter calculates the ratio of per unit voltage and per unit frequency and controls the field voltage to limit the generator voltage when the V/Hz value exceeds a preset value. The volts-per hertz limiters trip the generator by shutting

down the field voltage when the V/Hz value exceeds the preset value for a certain period. V/Hz limiter usually has two grades of settings, one with a higher V/Hz value and shorter time settings, another with a lower V/Hz value and longer time settings. This is due to terminal limitations of the generators and step-up transformer. [13]

2.5 Voltage Droop/Compensation Controller

The voltage droop/compensation controller is the additional function that is implemented in the HYMAREG 10 regulator. The purpose of this controller is to maintain constant generator terminal voltage concerning additional measurement signals from the generator, such as reactive, active current, and frequency. The voltage droop/compensation controller influences the voltage reference in the AVR to obtain the desired terminal voltage output. This controller consists of four control functions, reactive current droop, reactive current compensation, active current compensation, and frequency droop, the characteristics of each control function are described below.

2.5.1 Reactive Current Droop Control

Reactive current droop control is one of the functionality implemented to stabilize the distribution of reactive load between two or more generators on the same busbar. Alternatively, to reduce the reactive load changes at a small generator that is connected to an unstable grid with high voltage variations. This control function has a negative droop that reduces the terminal voltage as a function of increasing reactive current (see Figure 2.15), which gives the same effect as an inductor connected in series with the generator. [22]

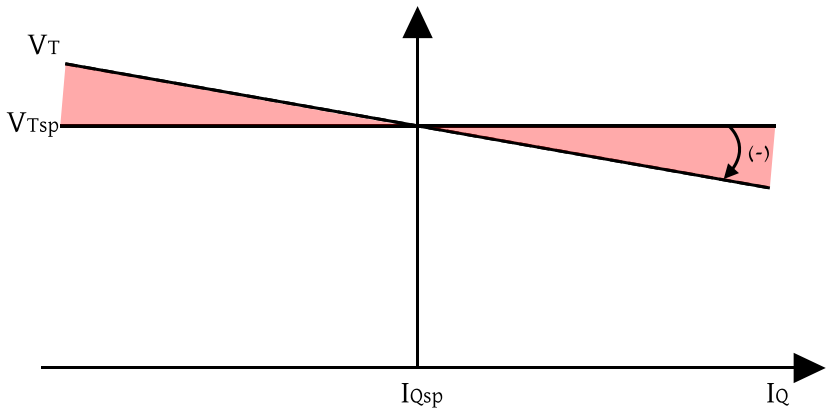

Figure 2.15: Characteristic curve of reactive current droop control function. V_T: Generator terminal voltage, I_Q: Generator terminal reactive current output, V_{Tsp}: Generator terminal voltage setpoint, I_{Qsp}: Reactive current setpoint.[22]

2.5.2 Reactive Current Compensation Control

This control function is used to compensate for the voltage drop due to reactive components as transformers or transmission lines in the gird. The reactive current compensation control function is quite the opposite of the reactive current droop control function, as depicted in

Figure 2.16. This control function has a positive droop, meaning the terminal voltage increases for increasing reactive current.[22]

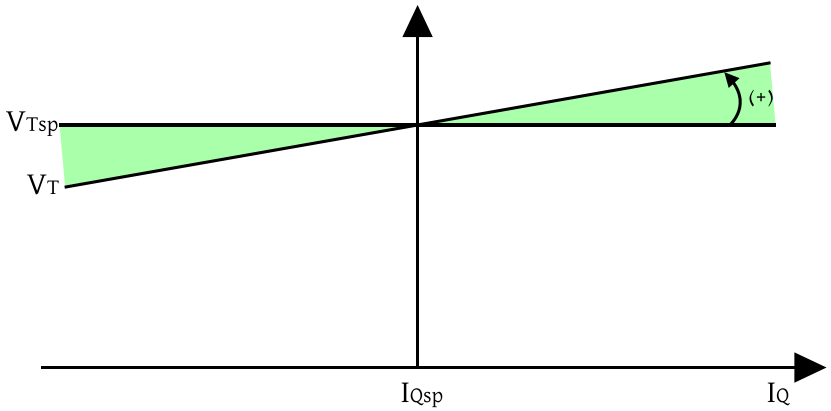

Figure 2.16: Characteristic curve of reactive current compensation control function. V_T: Generator terminal voltage, I_Q: Generator terminal reactive current output, V_{Tsp}: Generator terminal voltage setpoint, I_{Qsp}: Reactive current setpoint .[22]

2.5.3 Active Current Compensation Control

The active current compensation control function is used to compensate for voltage drop over transformers or transmission lines due to active power consumption. This control function increases the terminal voltage as a function of increasing active current, see Figure 2.17. [22]

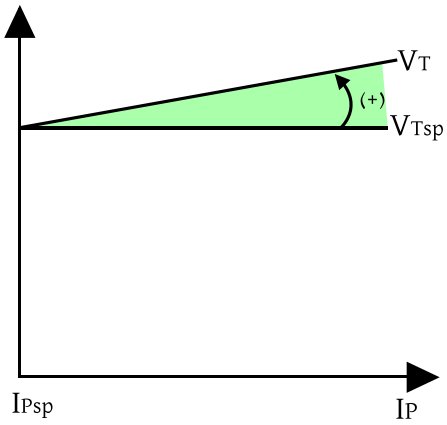

Figure 2.17: Characteristic curve of active current compensation control function. V_T: Generator terminal voltage, I_P: Generator terminal active current output, V_{Tsp}: Generator terminal voltage setpoint, I_{Psp}: Active current setpoint.[22]

2.5.4 Frequency Droop Control

This control function can be used to help the turbine regulator to stabilize the frequency at the local grid. The frequency droop control function increases or decreases the terminal voltage as a function of increasing or decreasing frequency within a limited span (see Figure 2.18). As a consequence, active power consumption in the resistive load increases if the generator runs at a higher speed. This control is only active if the circuit breaker is closed. [22]

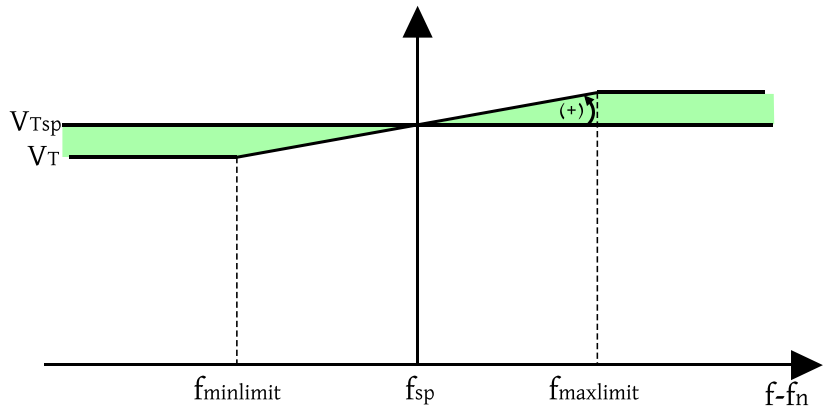

Figure 2.18: Characteristic curve of frequency droop control function. V_T: Generator terminal voltage, f: Actual frequency of the generator, V_{Tsp}: Generator terminal voltage setpoint, f_{sp}: Frequency setpoint. [22] (modified)

2.6 Reactive Power (VAR) or Power Factor (PF) Controllers and Regulators

Reactive power (VAR) or power factor (PF) controllers or regulators are optional methods to control or regulate the generator output reactive power (VAR) or power factor (PF) to a desired preset value. The VAR/PF *controller function* is defined in IEEE Std 421.5-2016 [14] as "A control function that acts through the reference adjuster to modify the voltage regulator setpoint to maintain the synchronous machine steady-state power factor or reactive power at a predetermined value.". Which means that the *control function* is mainly using the error between the desired and measured PF, VAR, or reactive current to control (increase or decrease) the AVR's setpoint to obtain the predefined reactive output. The VAR/PF controller is equipped with AVR as a slow-acting outer loop control, which takes the right action during the disturbance right after immediate reaction of the AVR to set back the setpoint to a normal position. On the other hand, the VAR/PF *regulator function* is defined in IEEE Std 421.5-2016 [14] as "A synchronous machine regulator that functions to maintain the power factor or reactive component of power at a predetermined value.". Which means the *regulation function* directly controls the field voltage to regulate the VAR/PF to the user-defined reference setpoint by eliminating the AVR terminal voltage feedback loop. The lack of the feedback loop causes insufficient dynamic voltage support during the faults. Hence the *controller function* is desired instead of the *regulator function* during the faults.[14]

VAR/PF controllers and regulators are often used in industrial applications where the machine voltages are expected to follow any variation in the system voltage. They are also popular among small independent power producers in the interest of elimination of one operator.

However, these controllers and regulators are not desirable for larger synchronous machines as they reduce the amount of voltage regulation, which may lead to power system instability. VAR/PF controllers and regulators may also contribute to system overvoltage or undervoltage if they are improperly configured. Despite this, VAR/PF controllers and regulators can provide an alternative mode of operation to avoid problems with the coordination of multiple voltages controlled generators or other devices when they are located on a single busbar or line. [14]

2.7 Legal Requirement for Excitation System

The legal requirement for excitation system is given in the National Guide for Functional Requirements in the Power System, NVF 2020 [23]. It is a guideline for the power system administrators to build, maintain or operate their system in order to fulfill the functional requirements set by the Norwegian Energy Regulatory Authority. The NVF 2020 [23] contains requirements for the Norwegian grids, production power plants, High Voltage Direct Current (HVDC), consumers, protections, and measuring equipment.[23]

The production power plant part in NVF 2020 [23] describes requirements for synchronous power plants and power parks. Several requirements are described under synchronous power plants, such as turbine regulation, excitation system, maximum reactive power, etc. Where the excitation system section describes the requirement for excitation system response time, VAR/PF control or regulation (Section 2.6), voltage droop/compensation control (Section 2.5), limiters (Section 2.4), PSS, and reset functionality (not considered in this thesis). [23]

Since the excitation system response time is one of the crucial requirements to verify the excitation system performance, therefore the requirement for excitation system response time as described in Section 2.7.1 will be compared with the simulation results later in this thesis.

2.7.1 Excitation System Response Time

This section briefly describes the national requirements for excitation system time response according to NVF 2020 [23]. Table 2.1 describes the requirement for synchronous generator voltage response time after the 5 % change in the generator terminal voltage setpoint (ΔV_{Tsp}) in the excitation system. More importantly, the circuit breaker should be closed during the response time test. Further, the "t_1" in Table 2.1 is the time from the change in setpoint applied to 90 % of ΔV_{Tsp} is reached as depicted in Figure 2.19. Whereas "t_2" is settling time, the time duration from the change in setpoint applied to the steady-state value with ±5 % of ΔV_{Tsp} is reached as illustrated in Figure 2.19. [23]

Table 2.1: Requirement for voltage response time for various power-plant with open circuit breaker.[23]

Nominal power	Response time at 90 % of ΔV_{Tsp}, t_1 $[s]$	Response time at steady-state (with ±5 % of ΔV_{Tsp}) t_2 $[s]$	Overshoot
$P_{max} > 30\ MW$	$<0.5\ s$	$< 2.5\ s$	$< 0.15 \cdot \Delta V_{Tsp}$
$P_{max} < 30\ MW$	$<1.0\ s$	$< 2.5\ s$	$< 0.15 \cdot \Delta V_{Tsp}$
$P_{max} < 30\ MW$, with PSS.	$< 0.5\ s$	$<2.5\ s$	$< 0.15 \cdot \Delta V_{Tsp}$

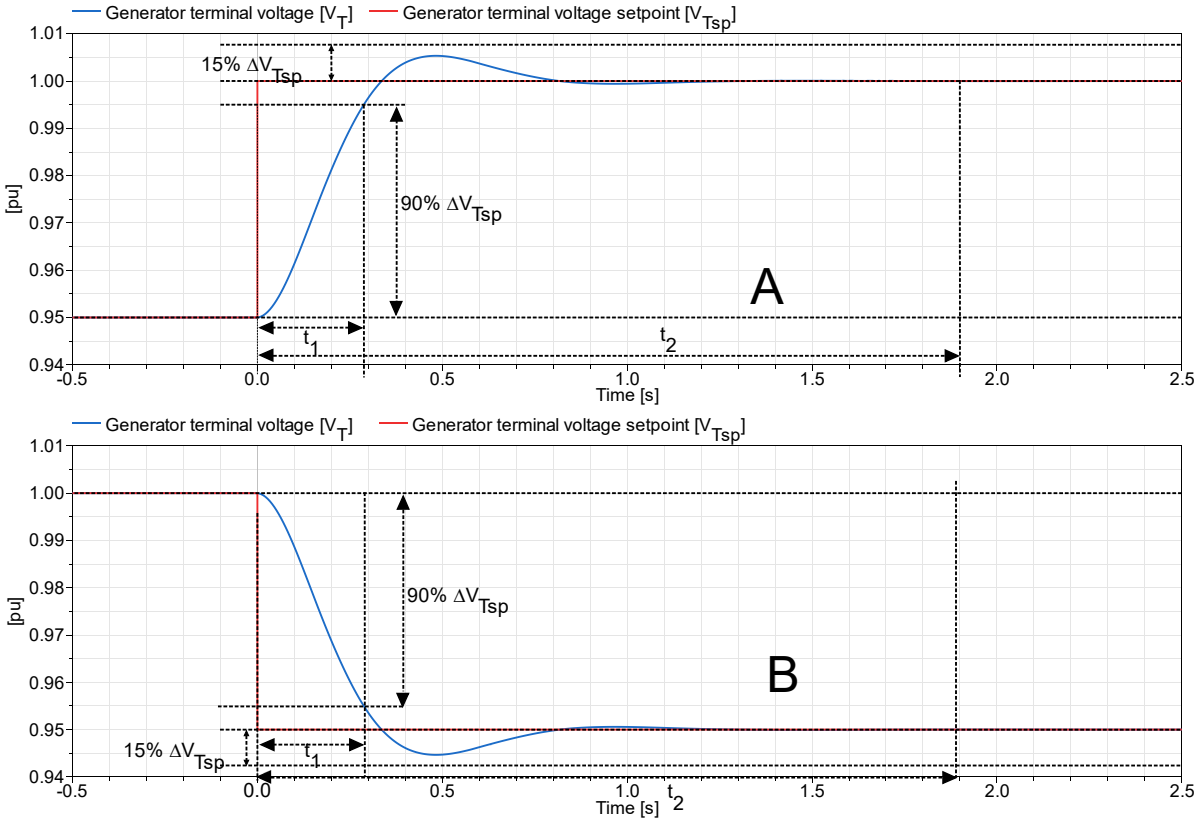

Figure 2.19: Illustrates the requirement for the response time of the excitation system for a synchronous generator with an open circuit breaker. A: Step-up response for +5 % change in voltage setpoint, B: Step-down response for -5 % change in voltage setpoint. [23]

3 Software

Software and programming or modeling languages are the most used terms over the past few decades. Software is the tool that helps the user with different programming or modeling languages to intact with the computers or machine to execute different tasks. Among these different tasks, modeling and simulations are some of the increasing tasks in recent decades. The modeling language Modelica and the software Dymola are used in this thesis to model and simulate the excitation control systems. More about the Modelica, Dymola, and OpenIPSL library are described in this chapter.

3.1 Modelica

Modelica is a modern non-proprietary, object-oriented, and equation-based modeling language that can be used to model large complex physical systems as electrical, mechanical, thermal, etc. This language translates any model or blocks to a flat Modelica structure later transforms further into a set of differential, algebraic and discrete equations [24]. The Modelica contains an open-source Modelica library with 1600 model components and 1350 functions from different domains. Modelica can be used with compatible software as OpenModelica, Dymola, MapleSim, SimulationX, etc. Many automotive companies such as Audi, BMW, etc., and power plant providers, such as ABB, EDF, and Siemens, use Modelica language and Modelica Libraries. Modelica is also used to model and simulate the industrial control system, chemical processes, photovoltaic cells and modules, and buildings [25].[26]

3.2 Dymola

Dynamic Modeling Laboratory, known as Dymola, is complete modeling, testing, simulation, and post-processing tool of integrated and complex systems. This tool has been broadly used for many applications as automotive, aerospace, robotics, and other applications. The Dymola has key advantages as follows [27]:

- Inherent compatible model libraries for many engineering fields.
- Using a powerful, object-oriented, and formally defined modeling language, Modelica.
- Users can either build their own libraries or use free and commercial libraries to adapt to their needs.
- Equation-oriented models allow a component or a model to be used and reused in different contexts and studies.
- Symbolic equation processing helps the user to eliminate the process of converting equations to assignment statements or block diagrams. Also, it helps the user with efficient and robust simulations.
- Compatible for real-time simulation on software dSPACE and xPC.
- Powerful interoperability options with full FMI (Functional Mock-up Interface) support and interfaces to Python, the SIMULIA tools Abaqus and iSight, as well as Simulink.
- Support also the real-time 3D animation and import of CAD (Computer-Aided Design) files for visualization.

3.3 OpenIPSL

OpenIPSL, which stands for Open-Instance Power System Library, is an open-source power system library implemented in Modelica. This library contains power system components that can be used for various power system analyses as phasor time-domain simulations. The aim of the OpenIPSL is to be used freely for researchers, teachers/professors, and students. Therefore, it is also highly compatible with OpenModelica. The OpenIPSL fundamentally contains a large number of models from two different software, Power System Analysis Toolbox (PSAT) and Power System Simulator for Engineering (PSS®E). It also contains examples, nonelectrical components such as continuous control blocks and logic blocks, interfaces, etc., as shown in Figure 3.1. Note that the components used in this thesis to model the excitation control system are obtained from the OpenIPSL version 2.0.0. [28]

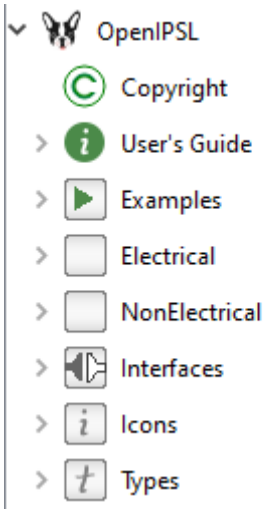

Figure 3.1: Screenshot of OpenIPSL library

4 Modeling

This chapter gives an overview of the modeling of various components in excitation control systems based on the information from the HYMAREG 10 user manual [22] together with IEEE Std 421.5 2016 [14] and Kundur [13]. In addition, it provides a parameterization of the models and information about implemented user interfaces in the models. Indeed, most variables name and their descriptions in each model originates in IEEE Std 421.5-2016 [14]. However, some variables' names and descriptions are modified due to modeling purposes. Moreover, all the model's inputs are in the per unit except the frequency in Hz.

4.1 Components of the Test Setup

This section presents the components used to model the simulation setup where most of the components are obtained from the OpenIPSL Library.

4.1.1 Generator

The GENSAL model from OpenIPSL Library is used as a generator model in this thesis. In order to represent the 10 MVA generator in the Hogstad power station (see A in Figure 1.1), the GENSAL model has to be parameterized with 10 MVA generator parameters. Some of the generator's parameters are obtained from the datasheet [29] and the test report [30] given by Skagerak. The rest of the parameters are estimated based on supervisor Dietmar Winkler's advice and by using a scaling factor to convert parameters from the example "Single machine infinite base system with one load and GENSAL model" in OpenIPSL. The parameters of the 100 MVA machine from the example are described in Table 4.1.

Table 4.1: Parameters of 100 MVA machine from example "Single machine infinite base system with one load and GENSAL model" in OpenIPSL

Parameters	Description	Values	Units
M_b	Machine base power	100	MVA
T'_{d0}	d-axis transient open-circuit time constant	5	s
T''_{d0}	d-axis sub-transient open-circuit time constant	0.07	s
T''_{q0}	q-axis sub-transient open-circuit time constant	0.09	s
H	Inertia constant	4.28	s
D	Speed damping	0	–
X_d	d-axis reactance	1.84	pu

X_q	q-axis reactance	1.75	pu
X'_d	d-axis transient reactance	0.41	pu
X''_d	d-axis sub-transient reactance	0.2	pu
X''_q	q-axis sub-transient reactance	0.2	pu
X_l	Leakage reactance	0.12	pu
$S_{1.0}$	Saturation factor at 1.0 pu	0.11	pu
$S_{1.2}$	Saturation factor at 1.2 pu	0.39	pu
R_a	Armature resistance	0	pu

The machine base is 10 MVA, which is given in the datasheet provided by Skagerak [29]. The d-axis transient open-circuit time constant T'_{d0} is guessed to 1 s, reference to the parameter in Table 4.1 and suggestions from the supervisor. The d-axis sub-transient open-circuit time constant T''_{d0} and q-axis sub-transient open-circuit time T''_{q0} are chosen to use the same as 100 MVA machine.

The inertia constant is calculated using Eq. (4.1) [13]:

$$H = \frac{1}{2} \cdot \frac{J\omega_r^2}{M_b} \tag{4.1}$$

where

H : Inertia constant [s]

J : Moment of inertia [$kg \cdot m^2$]

ω_r : Rated rotation speed [rad/s]

M_b : Rated power of the machine [VA]

By assuming the generator's rotational part as a rotating cylinder, the moment of inertia can be calculated using Eq. (4.2) [13].

$$J = m \cdot r^2 \tag{4.2}$$

where

J : Moment of inertia [$kg \cdot m^2$]

m : Mass of rotating part $[kg]$

r : Distance between axis and rotation mass $[m]$

The mass of the generator's rotating parts is given in the datasheet, where the rotor is 29 tons, and the flywheel is 7.15 tons [29]. After inspecting some pictures of the generator in the Hogstad and the supervisor's suggestions, the generator's diameter is estimated approximately to 1.8 m [31]. Further, the generator's rotational speed is 500 RPM, which is also given in the generator's datasheet.[29] However, it should be converted to rad/s by using Eq. (4.3) [13]:

$$\omega_r = \frac{2\pi}{60} \cdot RPM \tag{4.3}$$

Consequently, the inertia constant will be:

$$\begin{aligned} H &= \frac{1}{2} \cdot \frac{m \cdot r^2 \cdot \left(\frac{2\pi}{60} \cdot RPM\right)^2}{M_b} \\ &= \frac{1}{2} \cdot \frac{(29 + 7.15) \cdot 10^3 \cdot \left(\frac{1.8}{2}\right)^2 \cdot \left(\frac{2\pi}{60} \cdot 500\right)^2}{10 \cdot 10^6} \\ &= 4.01\ s \end{aligned} \tag{4.4}$$

The speed damping D is decided to keep as notated in Table 4.1. The d-axis reactance X_d, is given in the test report, and based on this value and the X_d of 100 MVA machine, a scale value is determined. Thereby, the q-axis reactance X_q, d-axis transient reactance X'_d, and d-axis sub-transient reactance X''_d are estimated. Reference to the PSS®E model library [32], the X''_d has to be equal to q-axis sub-transient reactance X''_q, hence X''_q is set equal to X''_d. The leakage reactance is also estimated using the scaling factor again.

The saturation factor at 1.0 and 1.2 pu can be determined using the magnetizing curve (see Figure 4.1) given in the test report [30], where the saturation factor at 1.0 pu can be calculated using Eq. (4.5)[14].

$$S_{1.0} = \frac{I_{FD1} - I_{FD0}}{I_{FD0}} \tag{4.5}$$

where

$S_{1.0}$: Saturation factor at 1.0 pu $[pu]$

I_{FD0} : Field current of the air-gap line at stator voltage 1.0 pu $[A]$

I_{FD1} : Field current of the open circuit characteristics (OCC) at stator voltage 1.0 pu $[A]$

Studying Figure 4.1, the I_{FD0} and I_{FD1} is found to be 2.9 and 3.1 A, respectively. Thus, the saturation factor at 1.0 pu is calculated to be roughly 0.07 pu. Similarly, the saturation factor at 1.2 pu can be calculated using Eq. (4.6) [14]. And, field current at I_{FD2} = 3.5 A and I_{FD3} = 4.1 A, thus the $S_{1.2}$ is calculated to be approximately 0.17 pu.

$$S_{1.2} = \frac{I_{FD3} - I_{FD2}}{I_{FD2}} \tag{4.6}$$

where

$S_{1.2}$	:	Saturation factor at 1.2 pu	$[pu]$
I_{FD2}	:	Field current of the air-gap line at stator voltage 1.2 pu	$[A]$
I_{FD3}	:	Field current of the open circuit characteristics (OCC) at stator voltage 1.2 pu	$[A]$

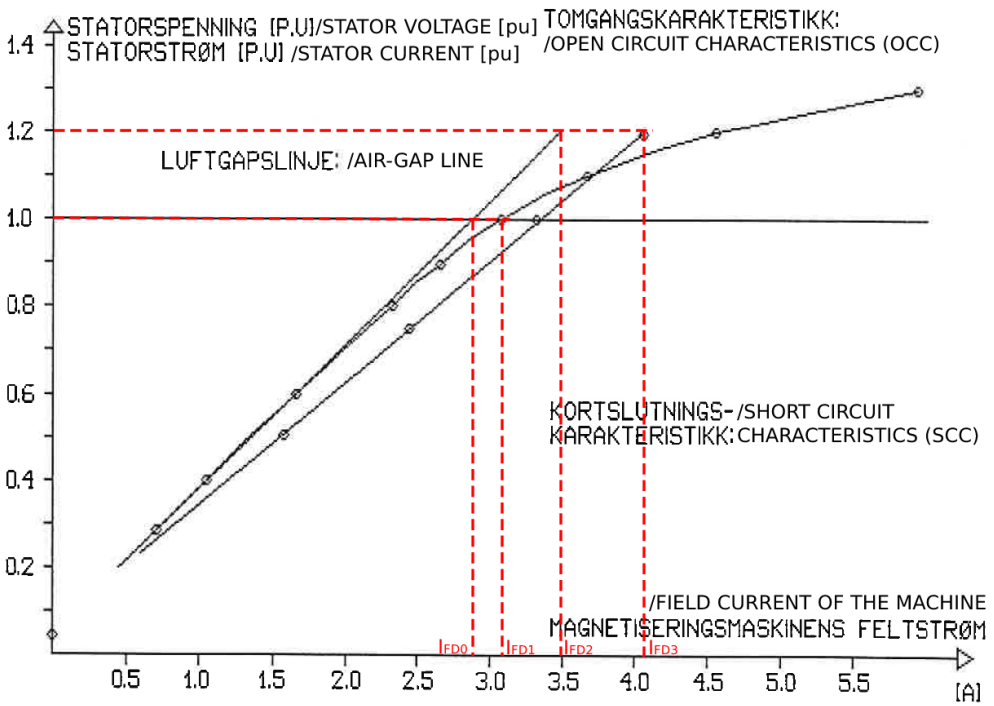

Figure 4.1: Magnetizing curve of the 10 MVA generator in Hogstad power station. I_{FD0} : field current of the air-gap line at stator voltage 1.0 pu, I_{FD1}:field current of OCC at stator voltage 1.0 pu, I_{FD2}: field current of the air-gap line at stator voltage 1.2 pu, and I_{FD3}: field current of OCC at stator voltage 1.2 pu.

Finally, the armature resistance R_a is specified in the test report [30], and it can be converted to per unit value by dividing with the base impedance. And the base impedance can be calculated using Eq. (4.7).

$$Z_b = \frac{V_b^2}{M_b} \tag{4.7}$$

where

Z_b	:	Base impedance	$[\Omega]$
V_b	:	Base voltage	$[kV]$
M_b	:	Machine base power	$[MVA]$

Using base power M_b and base voltage V_b, from the datasheet [29], the base impedance Z_b can be calculated to 3.136 Ω. Consequently, the per unit value of R_a is determined by dividing R_a in Ω by Z_b. However, the value of R_a seems to be huge, so after examining simulation results and a small discussion with the supervisor, the value is set equal to zero as in Table 4.1.

Finally, all the generator's estimated variables are summarized in Appendix B, and these values are used for further simulations.

4.1.2 Circuit Breaker

The circuit breaker component called Breaker in OpenIPSL (see Figure 4.2), is placed under the Electrical package, so in the Events package in the OpenIPSL library. This breaker uses a defined time or an external Boolean signal to open or close the breaker. If the external signal is "true", the breaker is open; otherwise, it will be closed. For this reason, only the external signal is used to trigger the breaker.

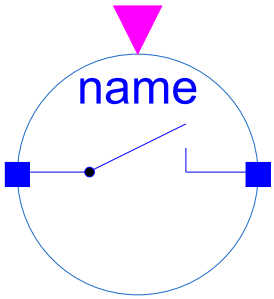

Figure 4.2: Symbol of the Breaker component in OpenIPSL

4.1.3 Transmission Line

To represent a transmission line, there is a component called "PwLine" used in the test grid. This transmission line is modeled based on the pi-equivalent circuit. The component can be found under the Electrical package then into Branches in the OpenIPSL library. The PwLine component's symbol is shown in Figure 4.3, while the parameters of the component are defined in Table 4.2.

Figure 4.3: Symbol of the PwLine component in OpenIPSL

Table 4.2: Transmission line parameters

Parameters	Description	Values	Units
R	Resistance	0.001	pu
X	Reactance	0.2	pu
G	Shunt half conductance	0.0	pu
B	Shunt half susceptance	0.0	pu

4.1.4 Infinite Bus

The infinite bus GENCLS represents the rest of the infinite distribution grid in the test grid. This component can be acquired from OpenIPSL under the Electrical >Machines > PSSE package. An infinite busbar is a strong component that provides constant voltage and frequency at the given values, 1 pu, and 50 Hz. Figure 4.4 portrays the GENCLS infinite bus symbol.

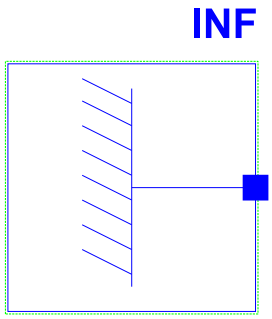

Figure 4.4: Symbol of the GENCLS infinite bus in OpenIPSL

4.2 Proportional-Integral-Derivative (PID) Controller

The PID controller is modeled based on reference to IEEE Std 421.5-2016 [14] with non-windup limits. Non-windup or anti-windup conveys that the output of the integral part in the PID controller is internally limited by the defined maximum and minimum limits to avoid unnecessarily large accumulated control errors after a setpoint change [13], [33]. The typical transfer function of the PID controller is often described as Eq. (4.8). [14]

$$K(s) = K_P + \frac{K_I}{s} + \frac{sK_D}{1 + sT_D} \tag{4.8}$$

where

$K(s)$	:	The output of the PID controller	$[pu]$
K_P	:	Proportional gain	$[pu]$
K_I	:	Integral gain	$[pu/s\ ]$
K_D	:	Derivative/differential gain	$[pu]$
T_D	:	Derivative/differential time constant	$[s]$

A simple non-windup PID controller block diagram (a) and implemented model (b) is depicted in Figure 4.5. If the sum y is greater-equal than the maximum limit B, the output x becomes B and the integration stoppes. Whereas, when the sum y is less-equal than minimum limit A, the output x becomes A and, the integrator stops. Otherwise, the x is equal to y, and the integrator integrates the error signal u.

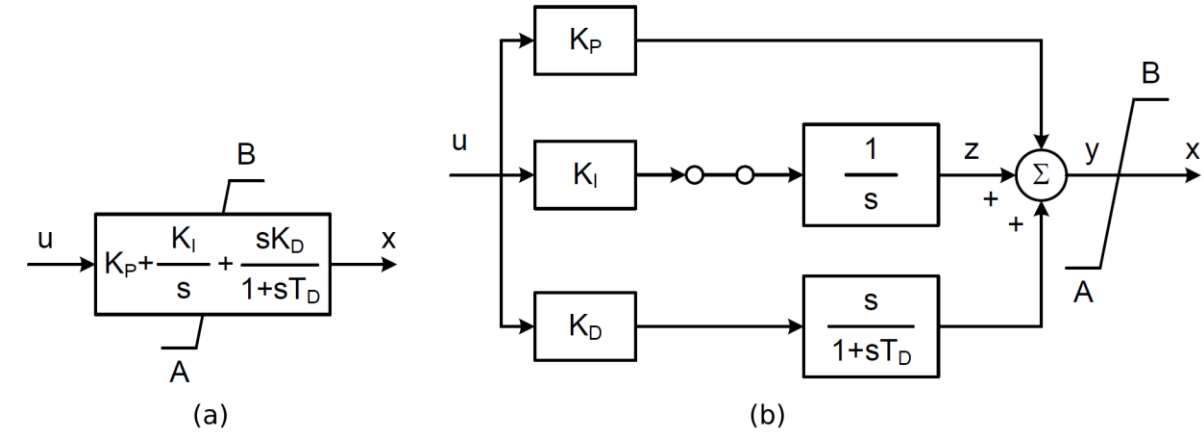

Figure 4.5: Proportional-integral-derivative block with the non-windup limit. a: Block diagram of the PID controller and, b: Modeling of PID controller.

Two types of PIDs exist in the Modelica library. In order to follow the IEEE Std 421.5-2016 [14] guidance, the non-windup PID is modeled as displayed in Figure 4.6. As shown in the figure below, the PID controller's integral block is used integrator with limited value.

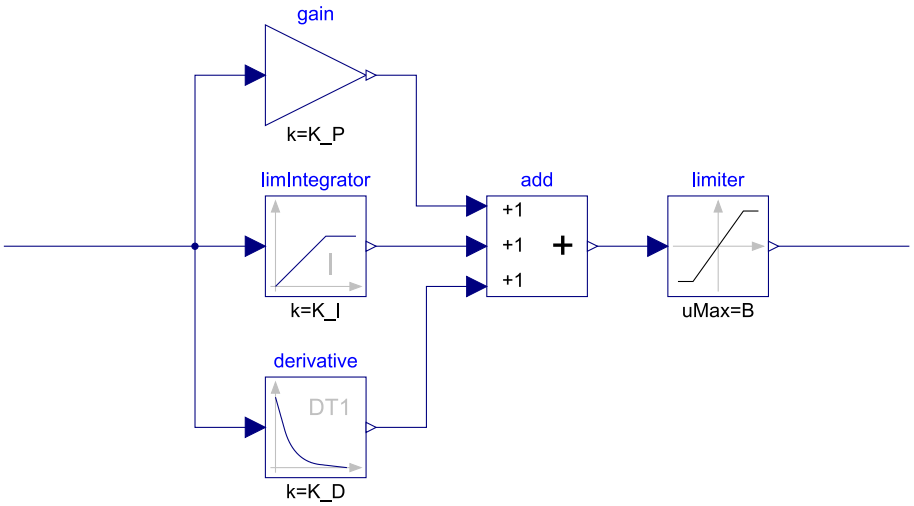

Figure 4.6: Implementation of a non-windup proportional-integral-derivative block in Modelica

4.3 Excitation System

The excitation system in the HYMAREG 10 could be represented by a static excitation system model *ST7C* or alternator-supplied rectifier excitation systems model *AC8B* from IEEE Std 421.5-2016 [14] based on the information from the external partner Hymatek Controls AS. Therefore, the *ST7C* model has been used in this work.

ST7C is a static potential source excitation system, where the excitation power of this system is obtained from the generator's terminals or auxiliary buses, as mentioned in Section 2.3.3. The AVR in *ST7C* type contains a proportional-integral (PI) voltage regulator. And this system contains a phase lead-lag filter in series to allow derivative function, to obtain a PID type voltage regulator (see Figure 4.7).[14]

The AVR mainly compares the terminal voltage transducer output (V_C) and PSS or discontinues excitation control output (V_S) against the voltage reference. The voltage reference can be influenced by the limiter's inputs such as OEL, UEL, SCL, V/Hz limiter, voltage droop/compensation controller, and VAR/PF regulator. However, the UEL could be connected to the alternate input locations such as $V_{UEL}(a)$, $V_{UEL}(b)$, and $V_{UEL}(c)$. Similarly, the OEL could be connected to the alternate input locations $V_{OEL}(a)$, $V_{OEL}(b)$, and $V_{OEL}(c)$ (see Figure 4.7). The output of the stator current limiter can be connected to all the latter six inputs. The locations "a" and "b" are called summing point inputs, while the location "c" is called the takeover junction inputs, which controls the output of the excitation model by removing the AVR loop. This is due to the high-value (HV) and low-value (LV) gate that generates output from the highest and lowest value of the inputs, respectively. Finally, the signal V_{FB} can be used as an input only for the UEL type *UEL2C* model.[14]

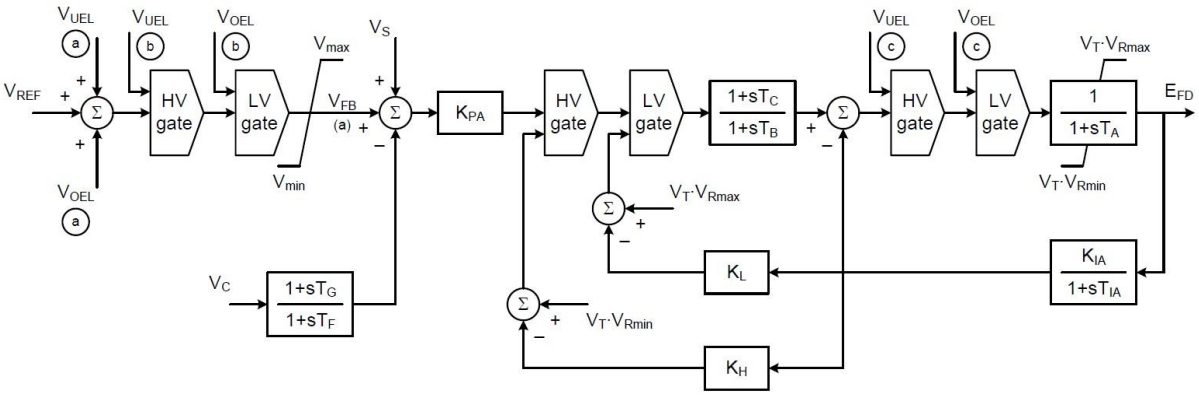

Figure 4.7: Static potential source excitation system, type *ST7C* [14]

Figure 4.8 shows an exciting model of the *ST7C* type developed in the OpenIPSL library. The model can be found under Electrical > Controls > PSSE > ES in OpenIPSL.

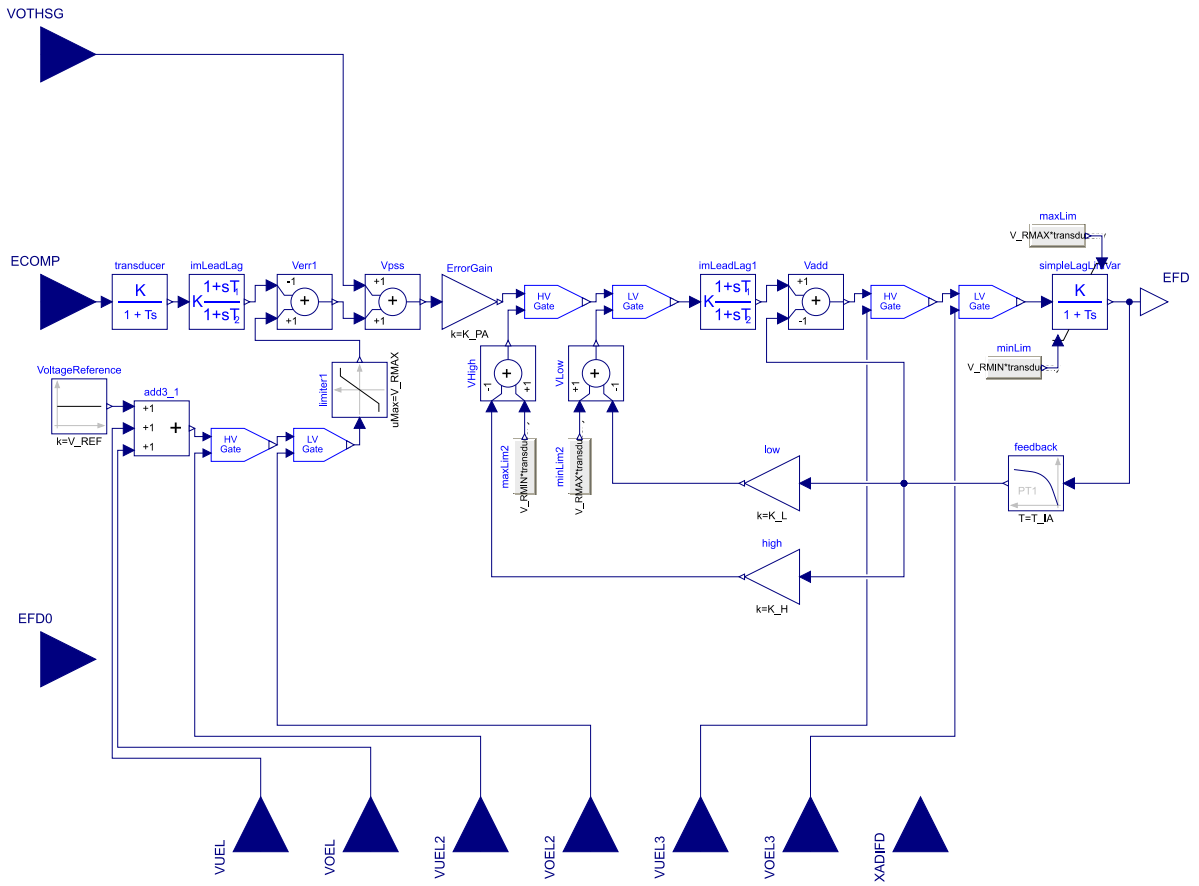

Figure 4.8: Excitation system *ST7C* developed in OpenIPSL

There is a small notable difference between the *ST7C* block diagram provided in IEEE Std 421.5-2016 [14] (Figure 4.7) and the model in OpenIPSL (Figure 4.8). Where the model in OpenIPSL uses constant block as a voltage reference instead of real input. This solution may cause some drawbacks regarding the lack of direct connection of the control signals to the reference input. This issue is solved by connecting control signals to ECOMP, which corresponds to the input of terminal voltage transducer output V_C in Figure 4.7.By connecting

the control signals to ECOMP, the measured terminal voltage will be varied. Hence the AVR regulator tries to compensate for the voltage variations by increasing or decreasing the field voltage. The input VOTHSG, where the output from the PSS or discontinues excitation control interacts, corresponding to V_S as shown in Figure 4.7. Moreover, the EFD0 represents the initial generator field voltage input, and XADIFD is the field current input.

To represent the HYMAREG 10 controller in the Hogstad power plant, the *ST7C* model needs to be tuned. Appendix C presented the parameters of the *ST7C* model, which are tuned with respect to the real HYMAREG 10 controller's parameters in the Hogstad power plant. And the real HYMAREG 10 controller's parameters are converted to the *ST7C* model by using scaling or tuning factors that are provided by the Hymatek Controls AS.

4.4 Limiters

There are plenty of limiters being used in hydropower plants to protect their components. The limiters are modeled with reference to the HYMAREG 10 user manual [22]. There are six limiters in the HYMAREG 10, and these are the following[22]:

A. Field current overexcitation limiter (FCOEL)
B. Stator current underexcitation limiter (SCUEL)
C. Stator current limiter (SCL), which follows the generator maximum current limit
D. Stator current overexcitation limiter (SCOEL)
E. Field current underexcitation limiter (FCUEL)
F. Volts-per-Hertz (V/Hz) limiter

The above-mentioned A-E limiters are field current or stator current limiters, determined using GCC as depicted in Figure 4.9. But, the last V/Hz limiter is the voltage limiter, limiting the voltage for under frequency and/or overvoltage as mentioned in Section 2.4.4.

The field current limiters, FCOEL and FCUEL, provides the necessary protection of the generator, which also takes care of the necessary limitation provided by the stator current limiters. The FCOEL and FCUEL are faster and uses fewer measurement systems than the stator current limiters, SCUEL, SCOEL, and SCL. Therefore, the stator current limiters are often deactivated during the commissioning. Unlike field current limiters are often permanently activated to protect against overload. [22]

Two conditions may make the stator current limiters desirable to use [22]:

- The amount of variation of field current and non-ideal cooling causes the resistance in the field winding to vary up to 20 % with the temperature on the field winding. These may lead field current in the GCC to vary, whereas the stator current limiters stay robust.
- The relationship between the field current and reactive power output is highly non-linear due to a larger saturation effect of the generator design.

And this section contains the modeling of A-F limiters in Modelica.

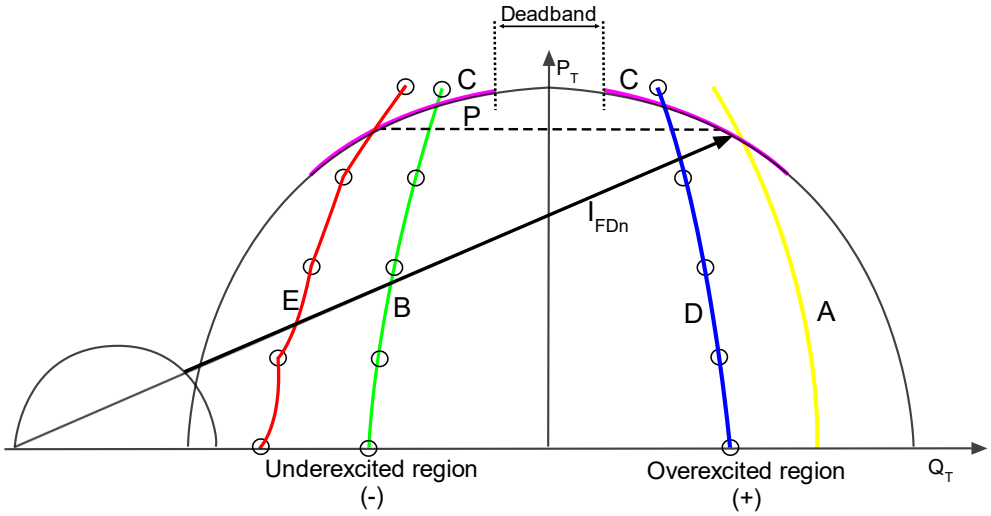

Figure 4.9: Synchronous generator capability curve with all limiters provided by the HYMAREG 10. A: Field current overexcitation limiter (FCOEL), B: Stator current underexcitation limiter (SCUEL), C: Stator current limiter (SCL), D: Stator current overexcitation limiter (SCOEL), E: Field current underexcitation limiter (FCUEL), I_{FDn}: Nominal field current, and P: Maximum turbine power [22]

4.4.1 Field Current Overexcitation Limiter (FCOEL)

The FCOEL is a conventional OEL, modeled based on *OEL2C* in IEEE Std 421.5-2016 [14]. The fundamental function of FCOEL is to detect overexcitation conditions, and it allows to continue for a defined time-overload and reduce the excitation level to a safer level. [14]

The block diagram of the FCOEL shown in Figure 4.10 can interact with the AVR either as an addition to the summation point or at the takeover junction. If the FCOEL model is connected to the summation point, the maximum output limit should be set to zero, while the minimum output limit should be set to a negative value corresponding to the maximum reduction. When the FCOEL is connected to the takeover junction point, the maximum output limit of the FCOEL should be set to larger values, whereas the minimum output limit should be set to a positive value that maintains the minimum excitation level. And the input to the limiter could be the generator field current I_{FD}, generator field voltage E_{FD}, or a signal proportional to exciter field current V_{FE}. [14]

Besides, the FCOEL's output is limited by the PID controller's maximum and minimum limit if the lead-lag function is turned off. Otherwise, the output is limited by $V_{FCOELmax1}$ and $V_{FCOELmin1}$ or $V_{FCOELmax2}$ and $V_{FCOELmin2}$.

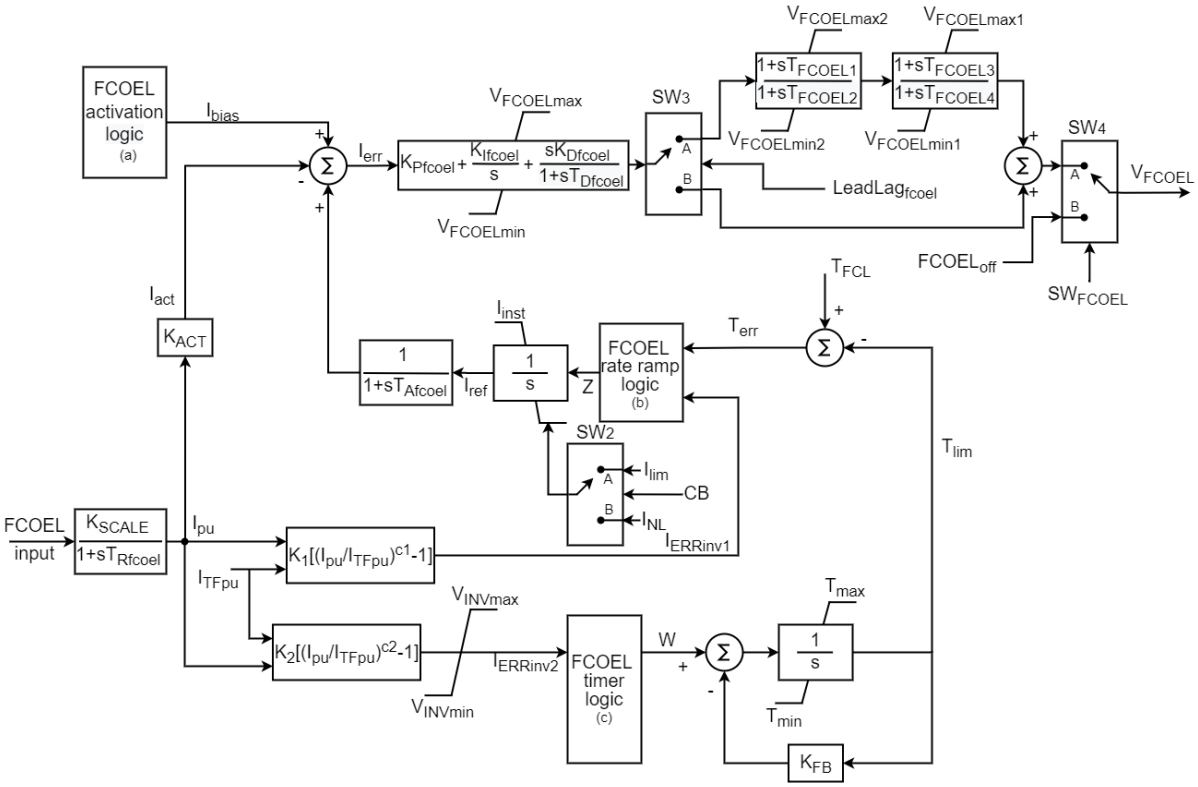

Figure 4.10: Block diagram of the field current overexcitation limiter (FCOEL) [14] (modified)

The activation logic (a) in Figure 4.10 allows the user to specify an activation delay time $T_{enFCOEL}$, this time delay will disable the instantaneous FCOEL responses for a certain time to allow very high transient forcing capability. Also, it allows defining the reset threshold value and time delay to reset the limiter. [14]

If the timer error signal $T_{err} = T_{FCL} - T_{lim}$ is less or equal than zero, or if the actual feedback field current I_{act} is greater or equal than the reference I_{ref} for longer or equal than the activation delay time $T_{enFCOEL}$, or if the $T_{enFCOEL}$ is equal to zero, then the output of the activation logic I_{bias} becomes zero. Thus, the error I_{err}, the input to the PID controller is reduced; consequently, the output of the FCOEL V_{FCOEL} reduces towards the limiter minimum until the field current reaches the preset limit. The preset limit could be instantaneous field current limit I_{inst}, or thermal (long-term) value I_{lim} or no-load limit I_{NL} level. While, when the I_{ref} is less-equal than I_{inst} and the error ($I_{ref} - I_{act}$) is larger or equal than the reset-threshold value $I_{THoffFCOEL}$ for longer or equal than the reset time delay $T_{offFCOEL}$, then the output I_{bias} becomes the reset reference value $I_{resetFCOEL}$. As a consequence, the output V_{FCOEL} will reach back to maximum limits set by the PID controller or double lead-lag function.

This model comprises both instantaneous and timed responses, where the timed response could follow inverse-time or fixed ramp rates (defined time). The inverse-time characteristic of the FCOEL is calculated using the filtered actual field current I_{pu} and parameters (K_2,c_2, and I_{TFpu}), then the output signal $I_{ERRinv2}$ is applied to the timer logic (c) in Figure 4.10. While the fixed ramp characteristic is determined by the ramp rates $Fixed_{ru}$ and $Fixed_{rd}$. The inverse-time characteristic can be disabled by either set the parameter K_2 to zero or by setting the limits V_{INVmax} and V_{INVmin} to zero. The fixed ramp characteristic can be disabled by setting the ramp rates $Fixed_{ru}$ and $Fixed_{rd}$ equal to zero. In addition, the timed response could be represented

by both the inverse time characteristic and fixed ramp rates to represent a bias in the response.[14]

The timer logic determines the input signal to the timer integrator by using defined fixed time ramp rates, $Fixed_{ru}$ and $Fixed_{rd}$ together with $I_{ERRinv2}$. Whereas, the timer integrator output T_{lim} and fixed-parameter T_{FCL} determine the timed action of FCOEL.[14]

The ramp rate logic (b) in Figure 4.10 uses the T_{err} signal to determine if the reference field current I_{ref} should be ramped up to the I_{inst} value or ramped down to the I_{lim} or I_{NL}. The ramp rate can be constant values as K_{ru} (ramp-up) and K_{rd} (ramp-down) or can be given by $I_{ERRinv1}$. Where the signal $I_{ERRinv1}$ is calculated similarly to $I_{ERRinv2}$ with parameters (K_1,c_1, and I_{TFpu}). Switching from instantaneous limit I_{inst} to timed limit I_{lim} or I_{NL} is represented by setting the SW_1 to false and K_{ru} and K_{rd} to large values. Or, if it is a desire to have a ramp down at a rate calculated from overexcitation can be obtained by setting the SW_1 to "true" and select a proper parameter for K_1 and c_1. During the no-load condition (circuit breaker is in the open position), the switch SW_2 is changed to position "B", meaning the lower limit of the integrator is changed to the no-load limit I_{NL}. Otherwise, during the normal operating condition (circuit breaker is in the closed position), the lower limit is set to I_{lim}. [14]

There is a PID controller and double lead-lag compensator at the output of the FCOEL, which determine the FCOEL's dynamic response. If the PID controller is desirable, the double lead-lag function can be disabled by changing the position of the switch SW_3 to "B". Alternatively, if the lead-lag function is desirable, the gain K_{Ifcoel} and K_{Dfcoel} should be set to zero, simultaneously the position of the switch SW_3 should be set to "A".[14]

Finally, the switch SW_4 at the output of the FCOEL is used to disable the limiter's output by the user command. And then, the output of the FCOEL will be the user-defined parameter $FCOEL_{off}$.

Figure 4.11 shows modeled FCOEL in Modelica, while Figure 4.12 depicts implemented user interfaces. The red circle (I) in Figure 4.12 indicates radio buttons that shall be chosen to switch the SW_1 to alternate from fixed time ramp rate to the calculated ramp rate from overexcitation. Whereas the red circle (II) in Figure 4.12 represents the checkbox that shall be checked to change the position in SW_3 to "A" to enable the lead-lag function. Moreover, the double lead-lag should be enabled to parameterize the lead-lag function; else, the parameter boxes are locked. The Modelica code for FCOEL activation logic and FCOEL ramp rate logic FCOEL timer logic can be founded in Appendix L, M, and N, respectively.

The parameters of FCOEL are presented in Appendix D, and these parameters and their values are obtained from both IEEE Std 421.5-2016 [14] and the commissioning report [34] from the Hogstad power station. The overexcitation field current limits given in the commissioning report were in percentage with respect to the rated field current. Since the GENSAL generator model rated field current is slightly differing from the actual field current, a simulation is performed under the no-load condition with only the generator. According to the simulation results, the generator needed 1.07 pu field current under no-load condition, which corresponds to 55 %, according to the commissioning report. Thereby, the field current 1.07 pu is used as a reference to determine the rest of the limits in FCOEL. Moreover, some of the parameters, such as parameters of the PID controller, are tuned under the simulations.

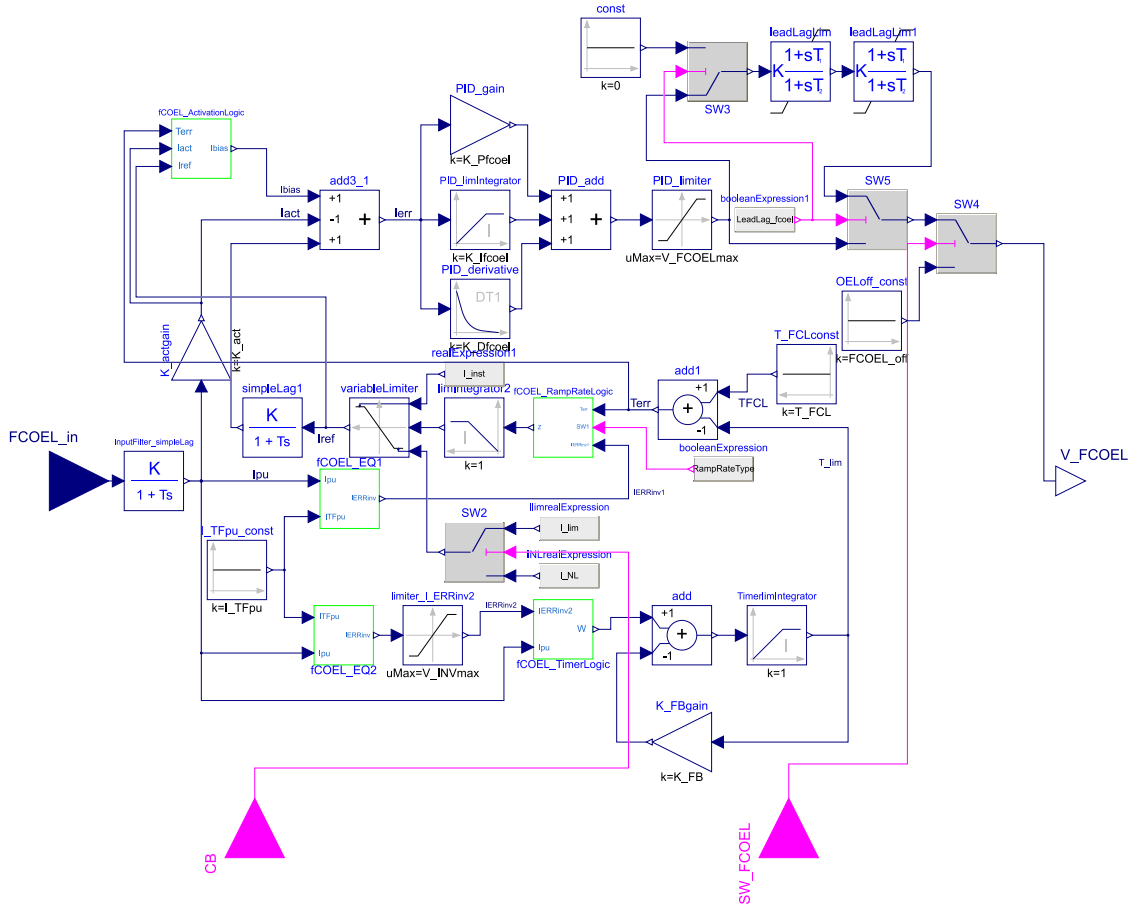

Figure 4.11: Implementation of field current overexcitation limiter (FCOEL) in Modelica

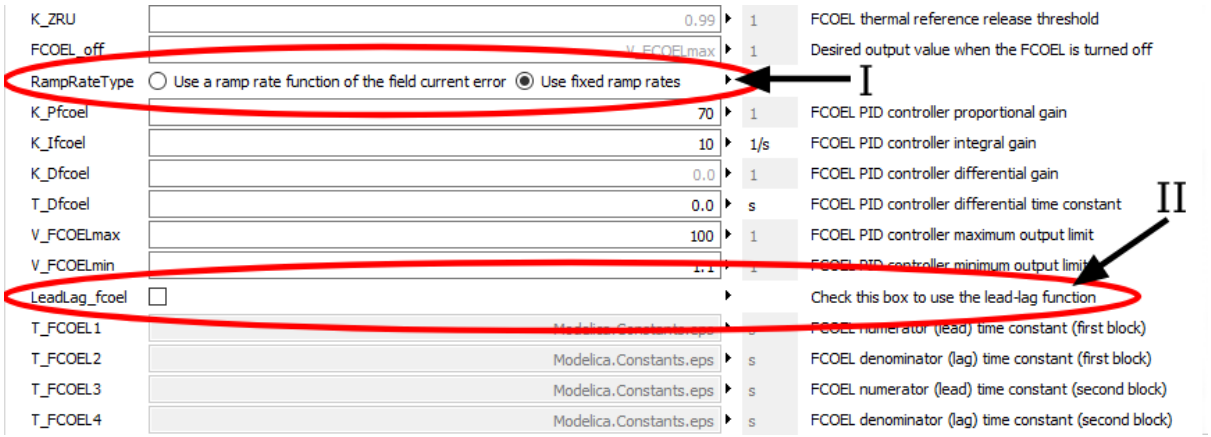

Figure 4.12: Implemented user interface in the FCOEL model. I: Radio buttons to choose the type of ramp rates. II: Checkbox to enable the lead-lag function.

4.4.2 Stator Current Underexcitation Limiter (SCUEL)

The block diagram of the SCUEL shown in Figure 4.13 is based on the type *UEL2C* in IEEE Std 421.5-2016 [14]. The limiter senses the active power P_T and reactive current I_Q and increases the excitation when the generator runs at underexcitation below the defined characteristic value. Since the limiter is a separate circuit, the output signals of this limiter can

interact either with the summing point or the HV gate input of the excitation system. The interaction with the summing point leads to normal voltage control, whereas interaction with the HV gate (takeover junction) will overwrite the normal action of the AVR. Be aware that the inputs could also be the active current I_P instead of active power P_T, but it should be a positive value and also reactive power Q_T can be used instead of reactive current I_Q. The excitation stabilizer signal from the AVR shall be provided to the input V_F, and it helps to damp the oscillations. The input V_{FB} can only be used in conjunction with the excitation system *ST7C* model. [14]

If the SCUEL interacts with the summation point, the minimum output limit should be set to zero, while the maximum output limit should be set to a large positive value. On the contrary, if the SCUEL is connected to the takeover junction, the maximum output limit of the SCUEL output should be set to 0, while the minimum output limit should be set to a significant negative value. Besides, the SCUEL's output maximum and minimum limit are set by the PID controller's limit if the double lead-lag function is turned off. Otherwise, the output is limited by $V_{SCUELmax1}$ and $V_{SCUELmin1}$ or $V_{SCUELmax2}$ and $V_{SCUELmin2}$.

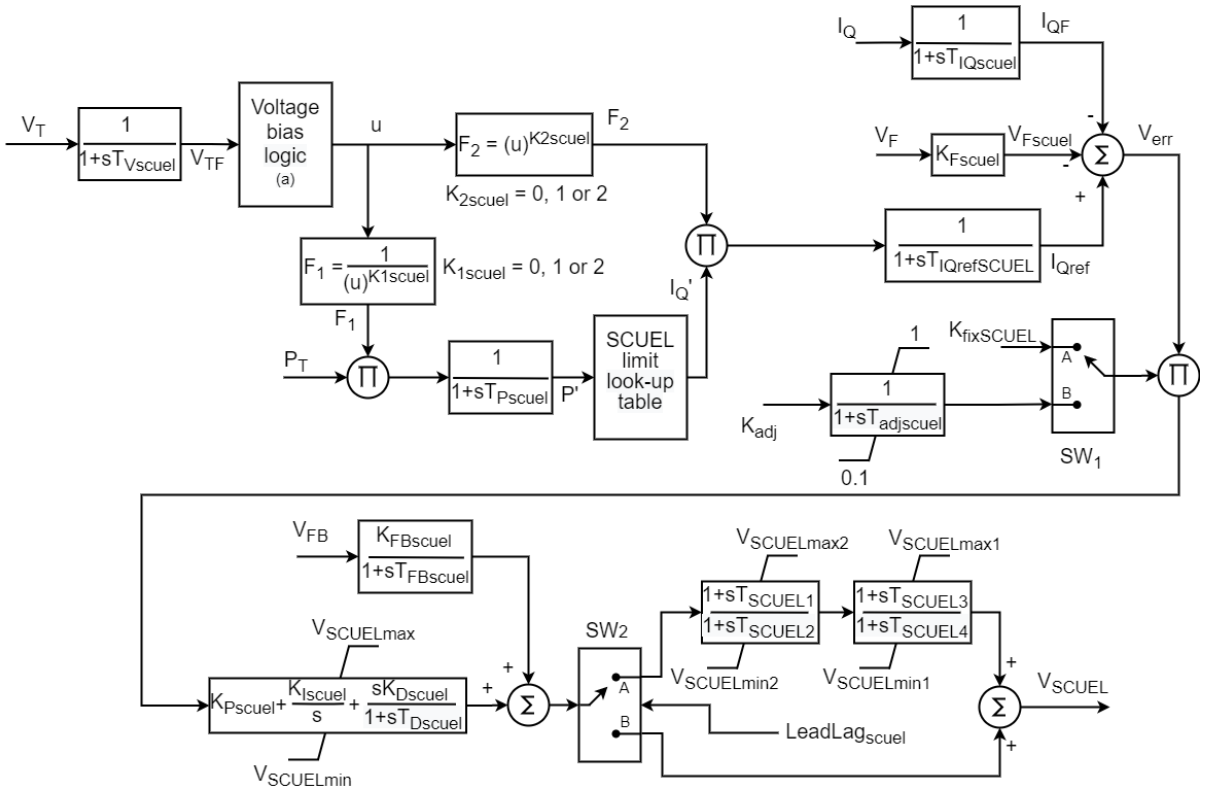

Figure 4.13: Block diagram of the stator current underexcitation limiter (SCUEL) [14] (modified)

The voltage bias logic (a) in Figure 4.13 provides an adequate voltage ratio to be used in equation blocks F_1 and F_2. And, the logic can be bypassed by setting the parameter $V_{biasSCUEL} = 1$. The equation blocks F_1 and F_2 in the SCUEL block diagram provide appropriate adjustments so that the effects of the terminal voltage V_T on the limiter are taken into account. The adjustments provided by the F_1 and F_2 are based on limiting characteristics of SCUEL and determined by constants K_{1scuel} and K_{2scuel}. If SCUEL configured to be influenced by the active and reactive currents, the limiter characteristic is set proportional to V_T by using the $K_{1scuel} = K_{2scuel} = 1$. While, if the limiter is influenced by the active and

reactive components of the apparent impedance looking from the machine terminals, the characteristic can be set to proportional to the V_T^2 by using $K_{1scuel} = K_{2scuel} = 2$. However, the latter limiting characteristic requires proper coordination with generator protection functions such as loss-of-excitation relays. And, this function can be disabled by using $K_{1scuel} = K_{2scuel} = 0$. [14]

The SCUEL model shown in Figure 4.13 takes active power P_T and multiplies it by F_1, further filters it and the resulting normalized value P' is sent to the look-up table. The limiting characteristic defined in the lookup table determines the corresponding normalized reactive current value $I_Q{}'$ related to P'. The reference I_{Qref} is determined by multiplying the $I_Q{}'$ and F_2 and compared with the filtered actual reactive current I_{QF}. Under normal conditions, the error signal $V_{err} = I_{Qref} - I_{QF} - V_{Fscuel}$ becomes negative, the limiter's output will be the minimum PID or lead-lag limits, meaning no actions are taken. When the error signal becomes positive, the output of the SCUEL drives in the positive direction and boosts the excitation to move the operating point back towards the SCUEL limit. [14]

The SCUEL reduction gain can be either automatically adjusted (depending on V_T, P_T and I_Q) or can have a fixed constant gain value. To enable the automatically adjusted gain, the logic switch SW_1 should be selected to position "B", where the automatic adjustable gain reduction K_{adj} is calculated using Eq. (4.9), while the fixed constant gain, given by the parameter $K_{fixSCUEL}$ value, is enabled by switching the SW_1 to position "A". The gain reduction can be disabled by setting $K_{fixSCUEL} = 1$. [14]

$$K_{adj} = \frac{\frac{V_T^2}{X_q} + I_Q}{\sqrt{\left(\frac{V_T^2}{X_q} + I_Q\right)^2 + P_T^2}} \tag{4.9}$$

where

K_{adj}	:	Automatic adjustment gain	$[-]$
V_T	:	Generator terminal voltage	$[pu]$
P_T	:	Generator active power output	$[pu]$
I_Q	:	Generator terminal reactive current output	$[pu]$
X_q	:	q-axis synchronous reactance	$[pu]$

As mentioned in Section 4.4.1, the lead-lag compensation can be disabled by changing the position of the switch SW_2 to "B", and the PID controller can be disabled by set gain K_{Iscuel} and K_{Dscuel} to 0. If the double lead-lag function is desirable, the position of SW_2 should be changed to "A", and the time constants should be appropriately adjusted to provide sufficient damping.[14]

The limiting characteristic of the SCUEL is depicted in Figure 4.14, where the limit is composed of four straight line segments. All five endpoints should be defined in terms of P_i

and I_{Qi} values in order to determine the limiter characteristic. For any values of P', the corresponding value of $I_Q{}'$ between the segment endpoints is determined using linear interpolation. [14]

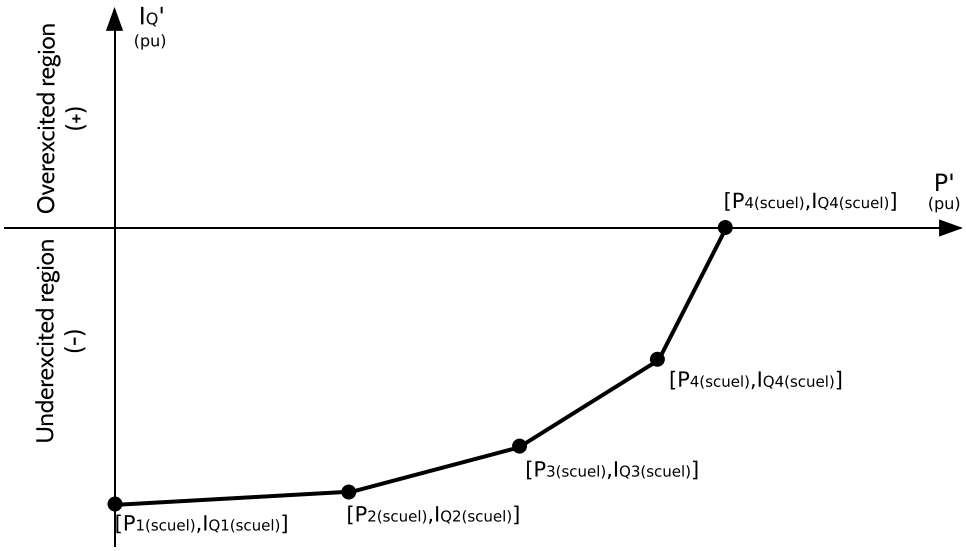

Figure 4.14: Normalized limiting characteristic for the SCUEL [14]

Figure 4.15 displays modeled SCUEL in Modelica, while Figure 4.16 shows modeled user interfaces to change the position of the switches SW_1 and SW_2. The notation (I) in the Figure 4.16 represents the checkbox that changes the position of SW_2 from "B" to "A" by checking it to enable the lead-lag function. The checkbox in notation (II), alternates switch position "A" to "B" in order to enable the adjustable gain reduction by checking it. Additionally, by enabling the lead-lag and adjustable gain reduction function, their parameter boxes will be enabled to allow the user to define the parameters; otherwise, the parameter boxes are locked. Besides, when the automatically adjustable gain reduction enables, the parameter box for $K_{fixSCUEL}$ will be locked. Alternatively, by unchecking the checkbox, the parameter box for fixed gain $K_{fixSCUEL}$ will be opened, and the switch is back to the position "A".

The parameters of this model are described in Appendix E, and these are obtained from both IEEE Std 421.5-2016 [14] and the commissioning report [34] from the Hogstad power station. Please note that the parameters are given in percentage in the commissioning report, but they are converted to per unit values in the model. In addition, the PID controller's parameters are acquired from the simulation tests.

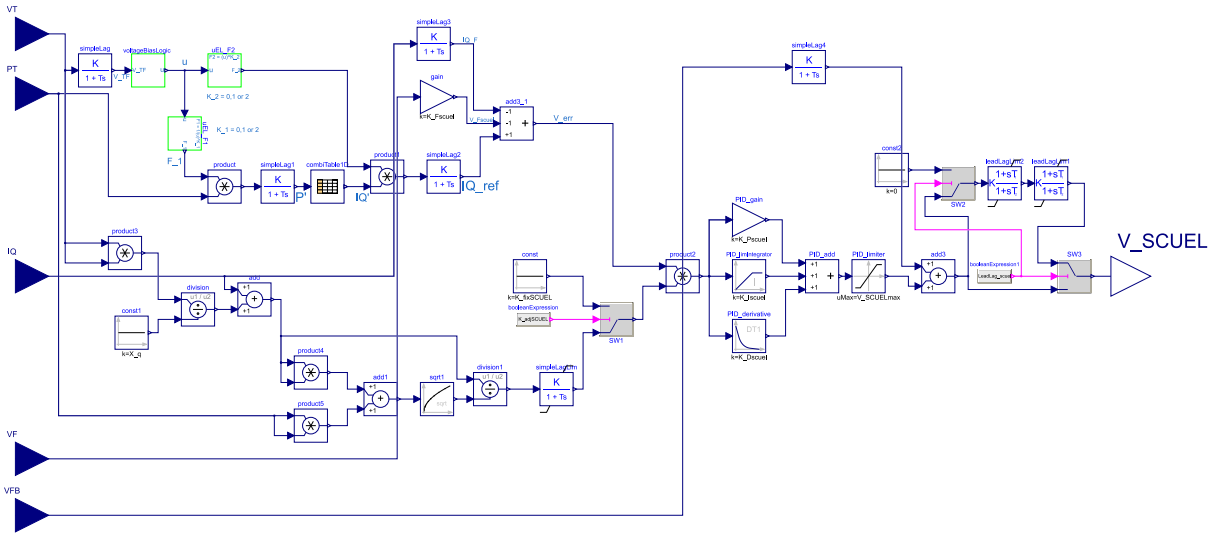

Figure 4.15: Implementation of stator current underexcitation limiter (SCUEL) in Modelica

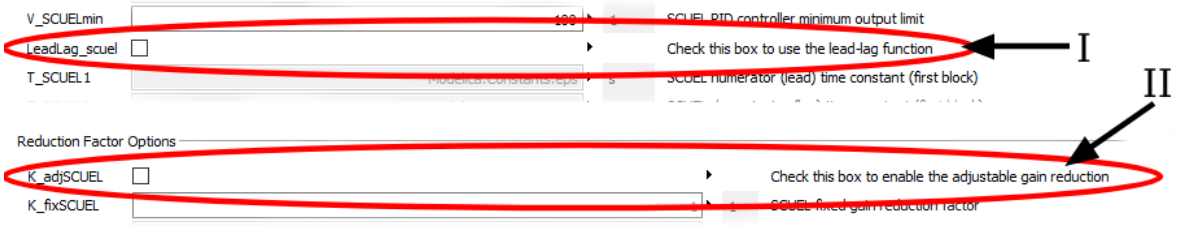

Figure 4.16: Implemented user interface in the SCUEL model. I: Checkbox to enable the lead-lag function, II: Checkbox to enable the automatically adjusted reduction gain function.

4.4.3 Stator Current Limiter (SCL)

A stator current limiter modifies the excitation level to reduce the reactive component of the stator current. As a consequence, the stator current will be limited. Figure 4.17 shows a block diagram of the SCL based on the type *SCL1C* in IEEE Std 421.5-2016 [14]. This limiter uses stator current I_T, reactive current I_Q, and reactive power Q_T at the generator terminal as inputs. Further, the output signal V_{SCL} from the SCL can only interact with the summing point of the excitation system.[14]

When the magnitude of the I_T becomes greater than the adjustable pickup value I_{SCLlim}, then the SCL starts to influence the excitation after the time delay. The time delay before limiting allows a short-term increase of stator current during a system disturbance or startup. There are three types of time delay functions implemented in this limiter. One of the time delay functions caused by the transducer delay in the measurement of the stator current is represented by the time constant T_{IT}. The second and third type time delay functions are enabled if the switch SW_1 on position “B”, and the time delays are determined by an inverse time characteristic T_{INV} or a fixed-time T_{DSCL}. The switch SW_2 in the delayed reactive power logic (c) in Figure 4.17 should be set to “true” to enable the inverse time delay. Else, the fixed-time delay will be applied.[14]

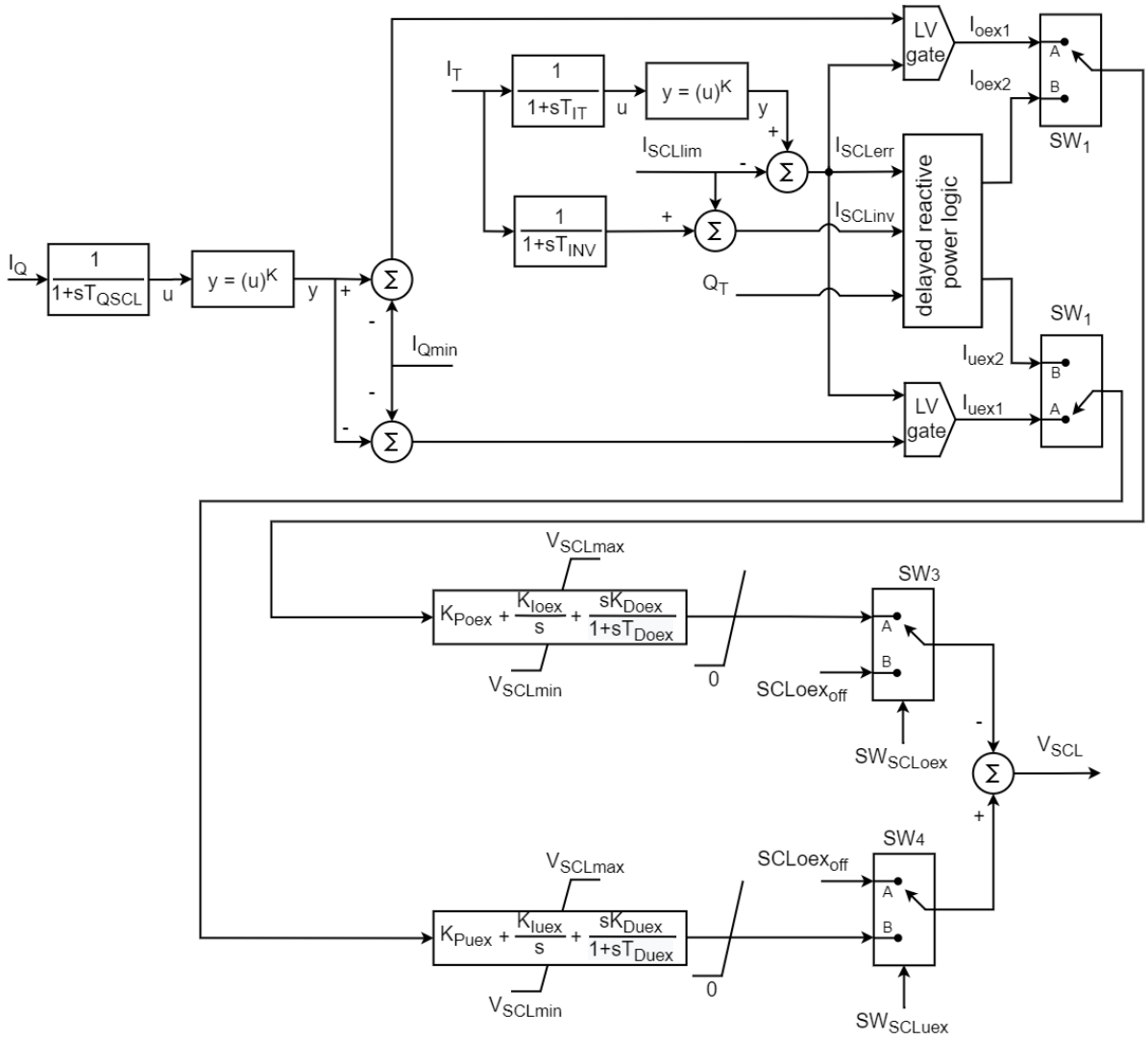

Figure 4.17: Block diagram of the stator current limiter (SCL) [14] (modified)

A deadband is implemented at unity PF because the SCL does not affect active power, so modifying the excitation level does not benefit at unity PF. There are two options to provide the deadband to the limiter. If the reactive current is used to modify the excitation, the deadband zone can be defined by the parameter I_{Qmin}. If the reactive power is used, then the deadband can be defined by the parameter V_{SCLdb}.[14]

When the SW_1 is in position "A", the reactive current is used to determine if the generator is operating in an overexcited or underexcited condition. When the SW_1 is in position "B", the reactive power is used to determine the generator's operating condition. During the underexcited condition, the field current is increased, unlike during the overexcited condition, the field current is decreased.[14]

There are two individual PID controllers for overexcited and underexcited control loops, which can be individually adjusted for proper tuning of the PID controllers. If I_Q or Q_T within the deadband, the input to the PID controller becomes zero, and the PID controller's output will be held constant. Also, during the normal operation condition (when the I_T is lower than the I_{SCLlim}), the outputs of the overexcited and underexcited range will be zero. Consequently, the output of the output V_{SCL} will be zero. When the I_T is higher than the I_{SCLlim}, the output V_{SCL}

reduces during the overexcited range, while V_{SCL} increases during the underexcited range. Under both ranges, the output decreases or increases until the reactive current or power reaches the deadband zone or until the I_T or Q_T becomes equal to the I_{SCLlim}. And there are two switches SW_3 and SW_4 at the output of the overexcited and underexcited range used to switch off each range's output, respectively, where the user shall give the command. When the outputs of the overexcited and underexcited range are switched off, the user-defined parameters $SCLoex_{off}$ and $SCLuex_{off}$ will be the output of each region, respectively.

The modeled stator current limiter in Modelica is displayed in Figure 4.18, where the switches at the output SW_3 and SW_4 should have a Boolean signal to enable the limiter's output.

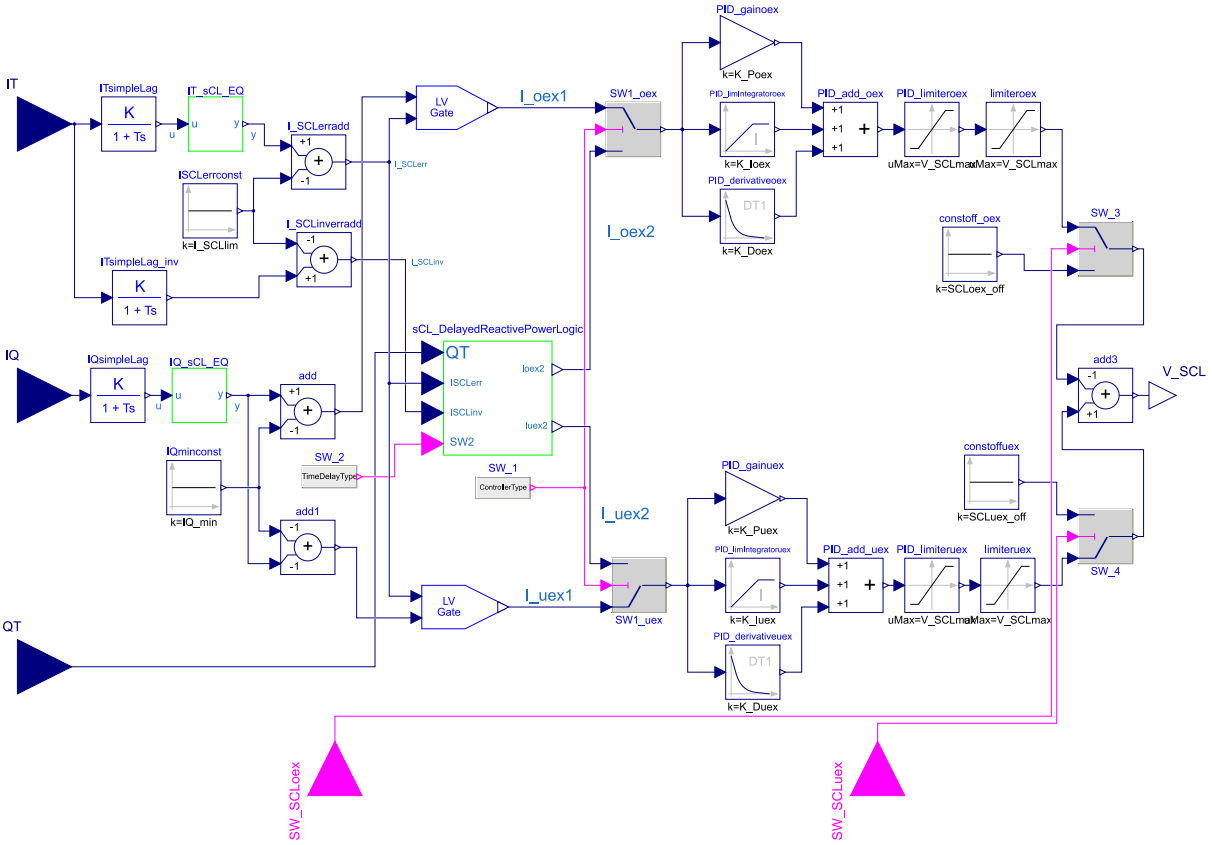

Figure 4.18: Implementation of stator current limiter (SCL) in Modelica

Furthermore, Figure 4.19 depicts a screenshot of the implemented user interface for the switches, SW_1 and SW_2, as indicated in I and II in the figure, respectively. If the controller type is selected to "Reactive current controller", then the SW_1 is changed to position "A". Whereas, if the controller type is selected to "Reactive power controller", then the SW_1 is shifted to position "B", and the SCL uses the reactive power to determine the operating condition of the generator. As well, the switch SW_2 can be set to "true" by selecting the radio button "Enable inverse time delay", while it can be set to "false" by selecting the "Enable fixed-time delay".

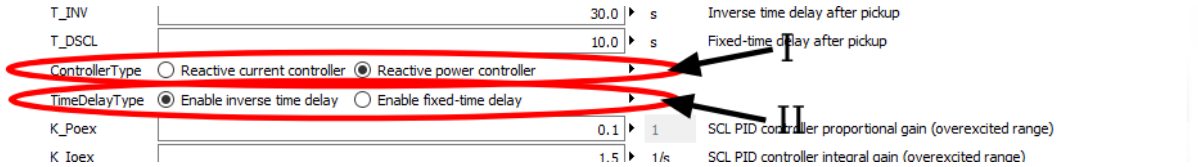

Figure 4.19:Implemented radio buttons in Modelica for switch SW_1 and SW_2 of the SCL

Moreover, the SCL's parameters are described in Appendix F, and these are also obtained from both IEEE Std 421.5-2016 [14] and the commissioning report [34] from the Hogstad power station. The parameters I_{SCLlim} and integral time T_I are given in the commissioning report, where the I_{SCLlim} is converted from percentage to per unit to apply in the SCL model. While the integral time is converted to integral gain K_{Ioex} and K_{Iuex} by using the Eq. (4.10) [22]. However, other the PID controller's parameters are acquired from the simulation tests. Finally, the Delayed Reactive Power Logic script is attached in Appendix O.

$$K_I = \frac{K_P}{T_I} \tag{4.10}$$

where

K_I : Integral gain $[pu]$

K_P : Proportional gain $[pu]$

T_I : Integral time $[s]$

4.4.4 Stator Current Overexcitation Limiter (SCOEL)

The SCOEL is one of the nonconventional limiters that is implemented in HYMAREG 10. This limiter is modeled based on type *UEL2C* in IEEE Std 421.5-2016 [14]. In addition, the activation logic from type *OEL2C* is also implemented in this limiter. This limiter protects stator windings against thermal overload during the overexcited condition. The limiter takes the generator's active power output P_T and reactive current I_Q and compares them with the preset characteristic to decreases the excitation when the generator runs above the limiting characteristic during the overexcited region. Figure 4.20 portrays the block diagram of the SCOEL.

Note that the inputs could also be the active current I_P instead of active power P_T but, it should be a positive value and also reactive power Q_T can be used instead of reactive current I_Q. This limiter's output can interact either with the summing point or the excitation system's takeover junction. The maximum output limit should be set to zero for the summation point connection, while the minimum output limit should be set to a negative value corresponding to the maximum reduction. Alternatively, suppose the SCOEL interacts with the takeover junction. In that case, the maximum output limit should be set to larger values, whereas the minimum should be set to a positive value to maintains the minimum excitation level. Besides, the limiter's output is limited by the PID controller's maximum and minimum limit if the lead-lag function is inactive. Else, the output is limited by $V_{SCOELmax1}$ and $V_{SCOELmin1}$or $V_{SCOELmax2}$ and $V_{SCOELmin2}$.

The activation logic (a) in Figure 4.20 allows the user to specify an activation delay time $T_{enSCOEL}$, this time delay allows very high transient forcing capability for a particular time. Also, it allows defining time delay to reset the limiter and reset threshold value as FCOEL.[14]

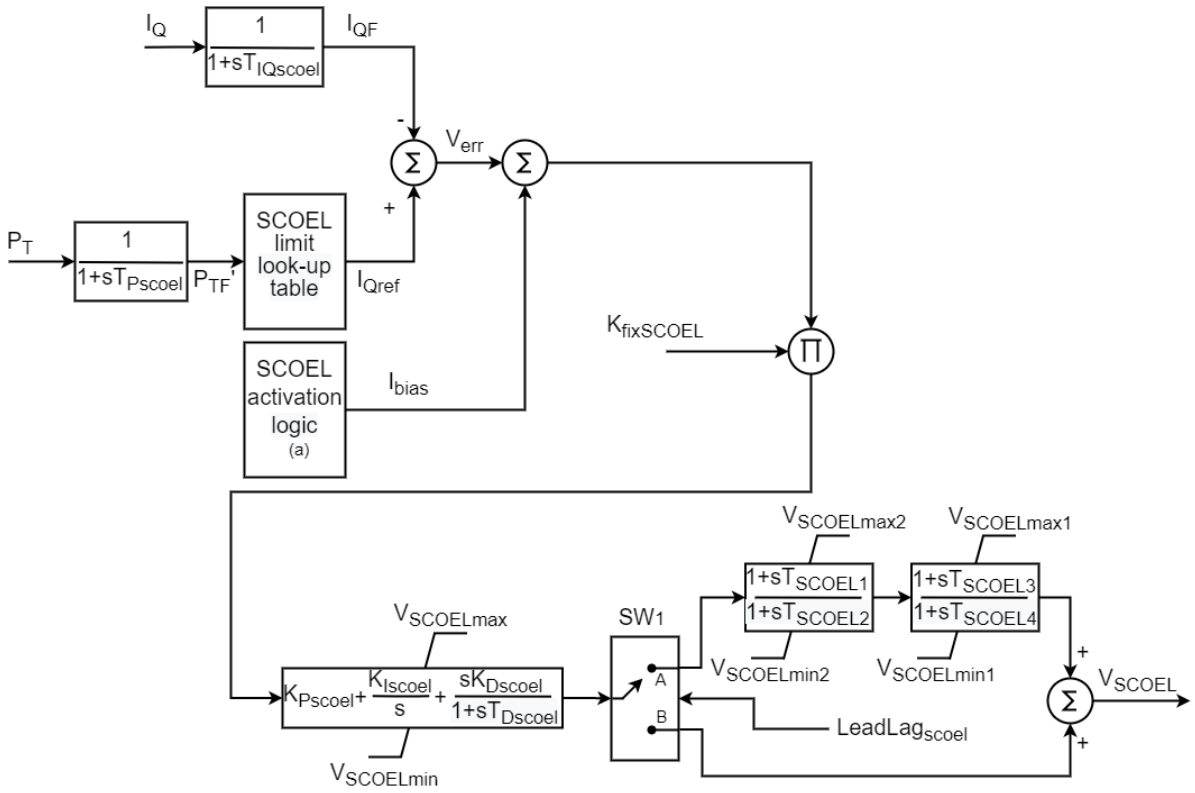

Figure 4.20: Block diagram of the stator current overexcitation limiter (SCOEL)

Firstly, the SCOEL model filtered out the active power input P_T and applied it to the look-up table. The limiting characteristic defined look-up table will then determine the corresponding reference reactive current I_{Qref} value relative to P_T. After that, the reference is then compared with the actual reactive current I_Q, and then the error $V_{err} = I_{Qref} - I_{QF}$ is added to the output signal from the activation logic I_{bias}.

Simultaneously, the activation logic output I_{bias} senses the filtered reactive current I_{QF}, V_{err}, and I_{Qref}. When the error V_{err} is less-equal than zero or the I_{QF} is larger or equal than I_{Qref} for longer or equal than the activation delay time $T_{enSCOEL}$, or $T_{enSCOEL} = 0$, then the output of the activation logic becomes zero. Else, if the I_{Qref} is less-equal than I_{QF} and ($I_{Qref} - I_{QF}$) is greater equal than the reset threshold value $I_{THoffSCOEL}$ for longer or equal than the reset delay time $T_{offSCOEL}$, the output becomes $I_{resetSCOEL}$.

The output I_{bias} and V_{err} added together and multiplied with a fixed gain reduction factor $K_{fixSCOEL}$ before the signal reaches the limiter's output V_{SCOEL} throughout the PID controller and lead-lag compensators. As well, the lead-lag function can be disabled by switching the SW_1 to position "B", while PID controller can be disabled by setting the gain K_{Iscoel} and K_{Dscoel} to zero.

When the limiter is inactive, meaning the I_{bias} is equal to $I_{resetSCOEL}$, the SCOEL output V_{SCOEL} will be the defined maximum limits of the PID controller or lead-lag compensators. When the

I_{bias} is zero, the limiter activates. Then the output V_{SCOEL} will be reduced towards the minimum limits until the I_Q reaches the defined limiting characteristic, where minimum limits also are set by the PID controller or lead-lag compensators.

Figure 4.21 illustrates the limiting characteristic of the SCOEL with five endpoints. All five endpoints should be defined in terms of P_i and I_{Qi} values to determine the limiter characteristic. The I_{Qref} is determined using linear interpolation for any values of P_{TF} between the segment endpoints.

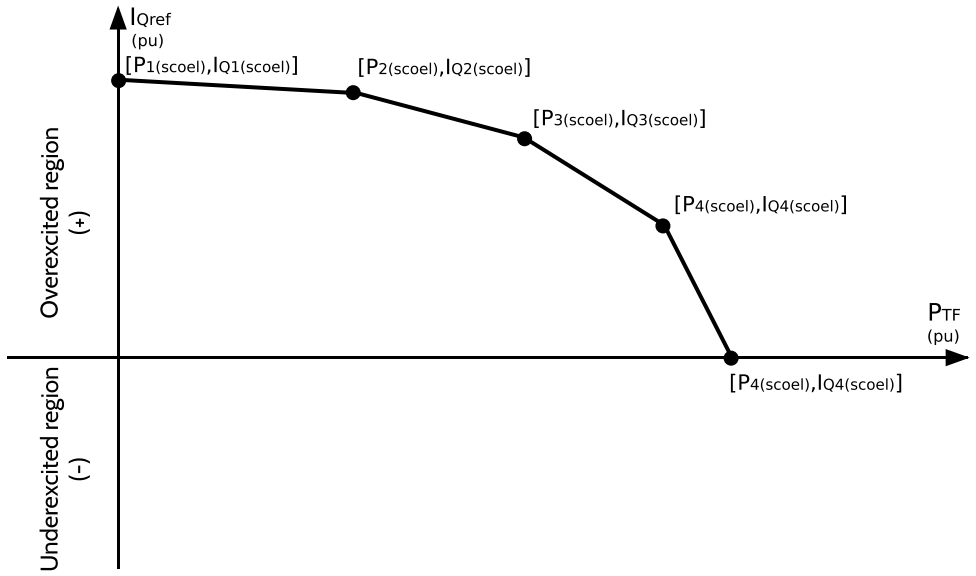

Figure 4.21: Limiting characteristic for the SCOEL

A modeled SCOEL in Modelica is portrayed in Figure 4.22, and implemented user interface to enable or disable the lead-lag function is depicted in Figure 4.23. The checkbox $LeadLag_{scoel}$ shall be checked to change the position in SW_1 to "A" in order to activate the lead-lag function. Moreover, the lead-lag should be enabled to parameterize the lead-lag function; else, the parameter boxes are locked.

Further, the SCOEL's parameters are described in Appendix G, where most of the parameters are obtained from IEEE Std 421.5-2016 [14], while some parameters such as the stator current limits and time delays are obtained from the commissioning report [34] from the Hogstad power station. The parameters are given in percentage in the commissioning report, but they are converted to per unit values in the model. However, the PID controller's parameters are acquired from the simulation tests. Lastly, the Modelica script for SCOEL activation logic is presented in Appendix P.

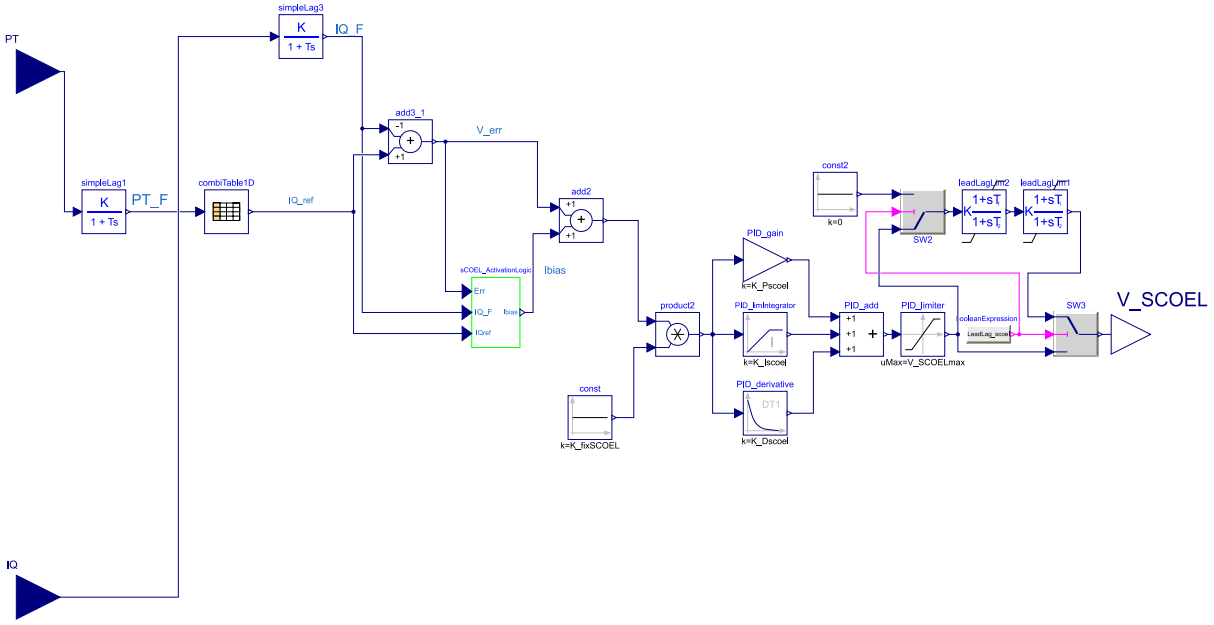

Figure 4.22: Implementation of stator current overexcitation limiter (SCOEL) in Modelica

Figure 4.23: Implemented checkbox in Modelica to enable the lead-lag function in the SCOEL

4.4.5 Field Current Underexcitation Limiter (FCUEL)

The field current underexcitation limiter (FCUEL) is fundamentally modeled based on the type *UEL2C* in IEEE Std 421.5-2016 [14] (see Figure 4.24). This limiter senses the active power P_T and field current I_{FD} and keeps the field current above the predefined characteristic during the underexcited region to provide sufficient synchronous momentum and prevent the loss of synchronism [22].

The active power input P_T could also be replaced with an active current I_P, but it should be a positive value, and the field current I_{FD} can also be replaced with a field voltage E_{FD} instead. This limiter can also interact either with the summing point or the HV gate input of the excitation system [14].

Like the SCUEL in Section 4.4.2, if the FCUEL model interacts with the summation point, the minimum output limit should be 0, while the maximum output limits a large positive value. Unlike, if the FCUEL concatenates with the takeover junction, the maximum output limit of the FCUEL output should be set to 0, whereas the minimum output limit should be set to a large negative value. Besides, the FCUEL's maximum and minimum limit is set by the PID controller's limit if the double lead-lag compensator is disabled. Otherwise, the output is limited by $V_{FCUELmax1}$ and $V_{FCUELmin1} or\ V_{FCUELmax2}$ and $V_{FCUELmin2}$.

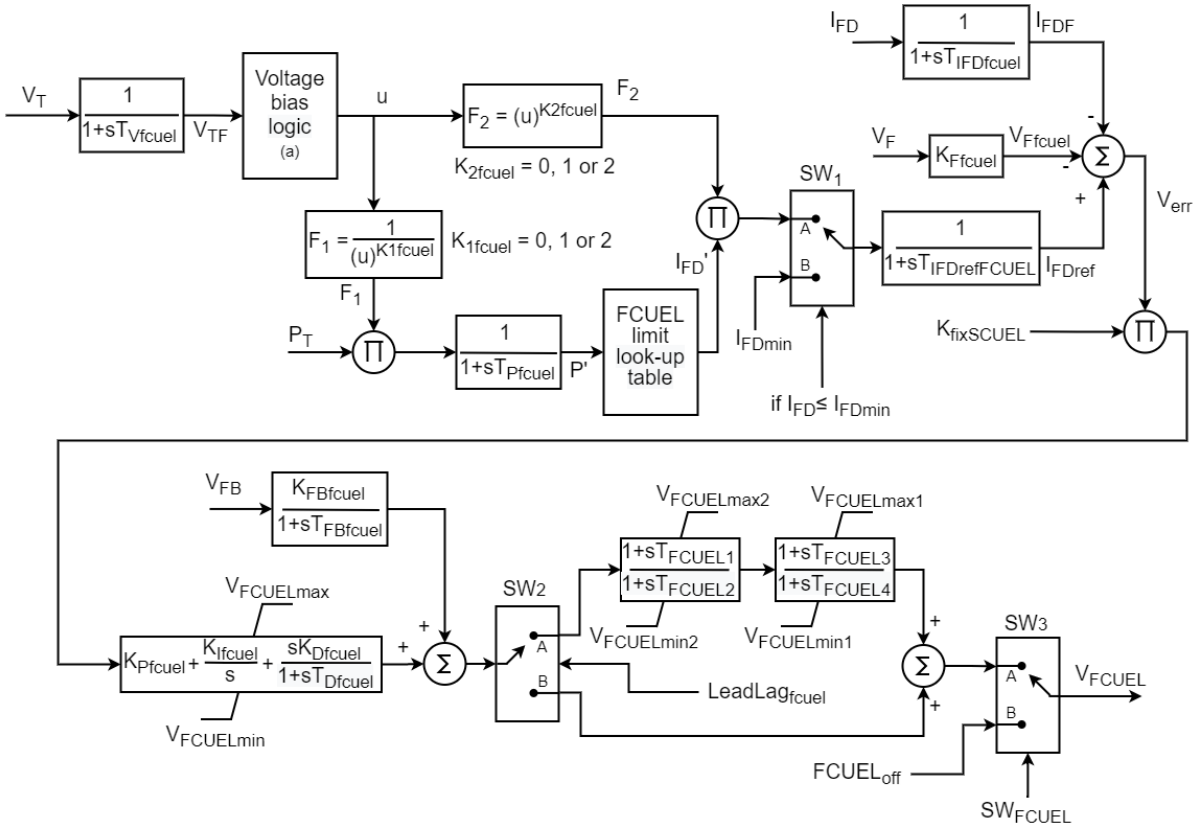

Figure 4.24: Block diagram of the field current underexcitation limiter (FCUEL) [14] (modified)

FCUEL model contains the voltage bias logic (a) in Figure 4.24 that provides the appropriate voltage ratio to determine the limiting characteristics to be set to unaffected by V_T or affected by V_T or V_T^2 by setting parameters K_{1fcuel} and K_{2fcuel} as 0, 1, and 2, respectively. Also, by setting the parameter $V_{bias} = 1$, the voltage bias can be disabled.[14]

The FCUEL works similar to the SCUEL in Section 4.4.2, except that the limiting characteristic defined lookup table determines the corresponding normalized generator field current I_{FD}' instead of reactive current I_Q'. The reference I_{FDref}, determined by multiplying the I_{FD}' and F_2 and then compared with the filtered generator field current I_{FDF} and excitation stabilizer signal V_{Ffcuel}. In addition, the adjustable reduction gain is eliminated. Thus, only the fixed reduction gain shall be used to increase the reduction.

There is a switch SW_1 that switches to position "B" if the field current goes below or equal to a defined absolute minimum field current I_{FDmin}. The limiter increases the field current to the I_{FDmin}.

The excitation stabilizer signal from the AVR shall be provided to the input V_F, to damp the oscillations. The input V_{FB} can only be used in conjunction with the excitation system *ST7C* model. The lead-lag function can be disabled by changing the position of the switch SW_2 to "B", and the PID controller can be disabled by set gain $K_{Ifcuel} = K_{Dfcuel} = 0$. Besides, if the lead-lag compensation is desirable, change the SW_2 to position "A", and the time constants should be properly adjusted to provide sufficient damping.[14]

As well, the switch SW_3 at the output that enables or disables the output when the SW_{FCUEL} changes to "true" or "false", respectively, and when the limiter is disabled, the output of the FCUEL will be the user-defined parameter $FCUEL_{off}$.

The limiting characteristic of the FCUEL shall be defined as illustrated in Figure 4.25. A total of five points of active power output P_i and the corresponding field current I_{FDi} in the underexcited region should be defined. For any values of P' and the corresponding value of I_{IFD}' between the segment endpoints is determined using linear interpolation. [14]

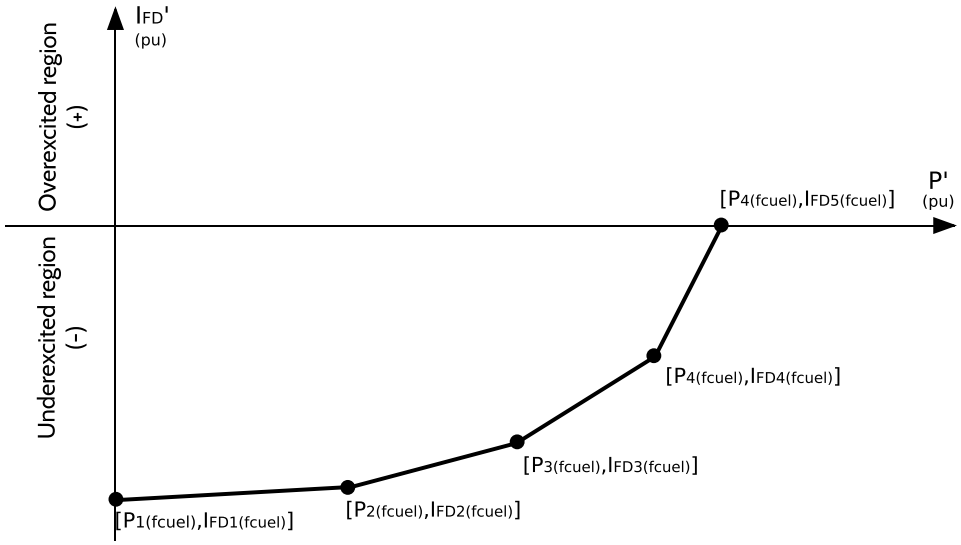

Figure 4.25: Normalized limiting characteristic for the FCUEL [14] (modified)

Figure 4.26 portrays modeled the FCUEL in Modelica, while Figure 4.27 depicts implemented user interface to enable or disable the lead-lag function. Where the checkbox $LeadLag_{fcuel}$ shall be checked to change the position of the SW_2 to "A" in order to activate the lead-lag function. As well, the parameter boxes of the lead-lag function are usually locked when the checkbox is unchecked; otherwise, these are open to parameterize.

Finally, the FCUEL's parameters are presented in Appendix H, where most of the parameters are obtained from IEEE Std 421.5-2016 [14], whereas the field current limits are obtained from the commissioning report [34] from the Hogstad power station. The parameters in the commissioning report are given in percentage, but they are converted to per unit values to parameterize the model. Despite this, the PID controller's parameters are acquired from the simulation tests.

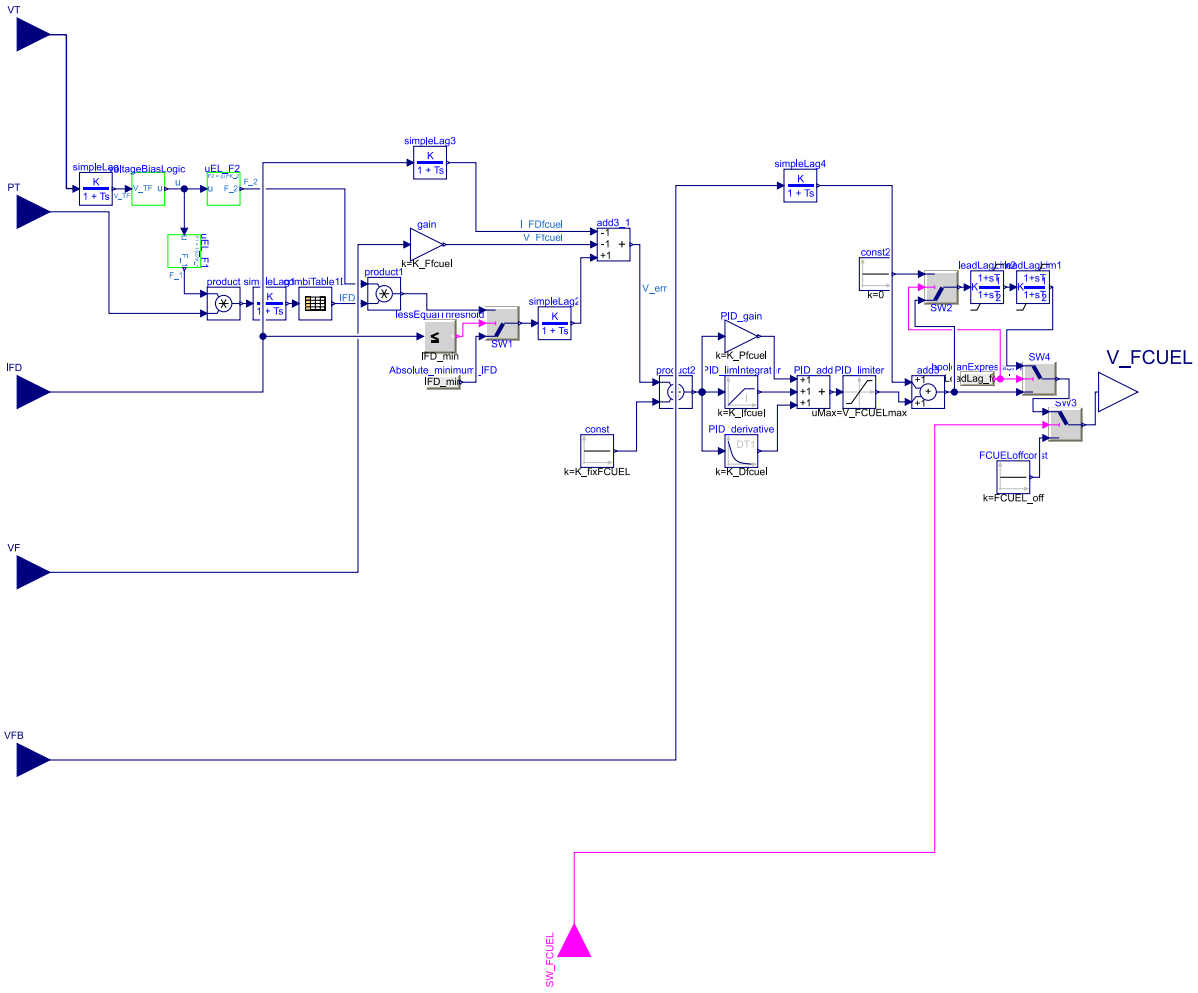

Figure 4.26: Implementation of field current underexcitation limiter (FCUEL) in Modelica

Figure 4.27: Implemented checkbox in Modelica to enable the lead-lag function in the FCUEL

4.4.6 Volts-per-Hertz (V/Hz) Limiter

V/Hz limiter is a voltage limiter that limits the voltage function of frequency. This model is build based on Kunder [13] and information from HYMAREG 10 user manual [22]. This limiter interacts with the AVR at the summing point and reduces the reference so that the terminal voltage reduces with respect to the frequency reduction. A block diagram of the V/Hz limiter is shown in Figure 4.28, where the limiter takes inputs as terminal voltage V_T and frequency f. The limiter calculates the ratio between the terminal voltage and the frequency in per unit, which is compared with the limiting value V_{ZLM} to determine the error E_{rr}. If the E_{rr} is greater than zero, a timer will start to count, and when the time is greater than T_d, then the E_{rr} signal will be sent further to the PID controller. During the normal operation (when the limiter is inactive), the E_{rr} is a negative value, and thus, the output is zero. When the limiter is active, and the E_{rr} becomes greater than the zero, the output starts to increase until the voltage

reduces and the E_{rr} becomes less-equal than the zero. Additionally, this limiter can be activated and deactivated by the Boolean signal, and when the limiter is deactivated, the output will be zero.

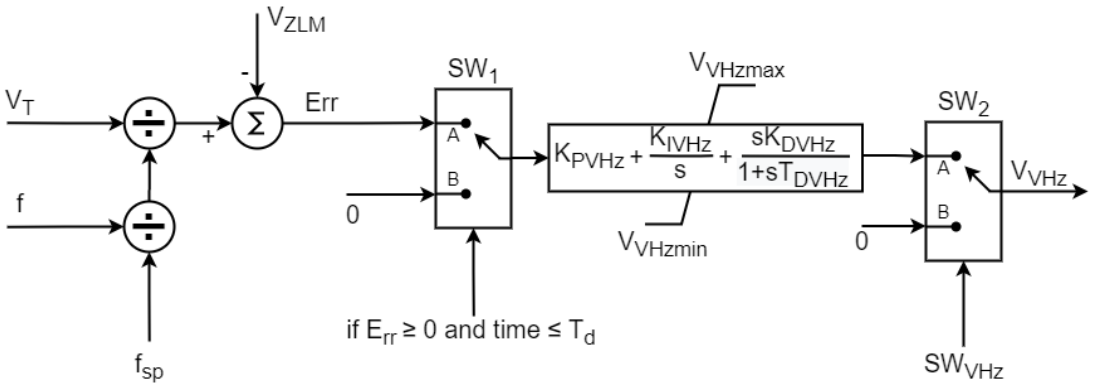

Figure 4.28: Block diagram of the volts-per-hertz (V/Hz) limiter [13] (modified)

A V/Hz limiter modeled in Modelica is shown in Figure 4.29, where the dashed lines illustrate the conditional connections that the user can either activate the constant frequency setpoint f_{sp} or variable frequency setpoint input f_{vsp}. By checking the checkbox $Enable_{f_{vspt}}$ seen in Figure 4.30, the real input f_{vsp} is enabled so the variable frequency input can be connected to the limiter, and simultaneously the f_{sp} will be disabled. Contrarily, when the checkbox is unchecked, the real input f_{vsp} dissipates, and the f_{sp} enabled. Additionally, the switch SW_2 at the output allows the user to activate and deactivate the limiter by a Boolean signal. Besides, a constant epsilon is added with the frequency to protect against division by zero problems. Further, the V/Hz limiter's parameters are presented in Appendix I, where limiting value and time delay are obtained from the commissioning report [34] from the Hogstad power station. And, the rest of the parameters are obtained from the simulation tests.

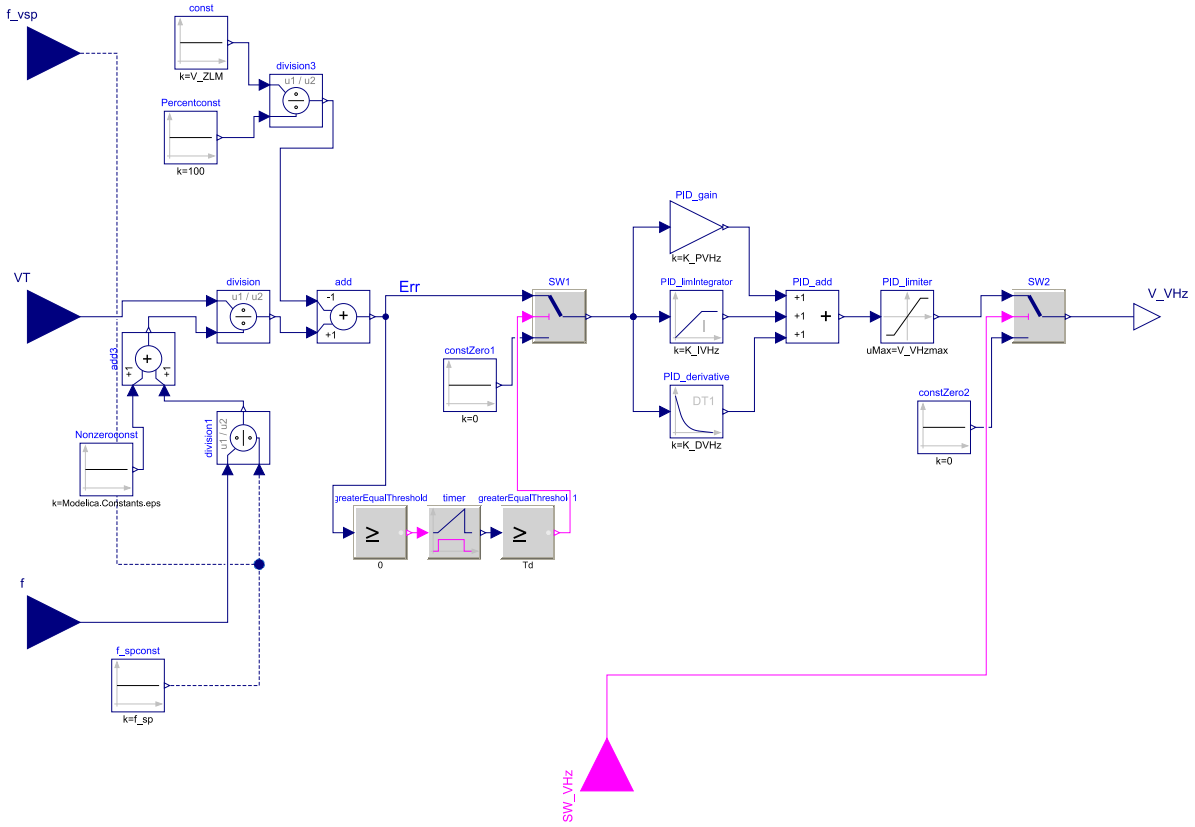

Figure 4.29: Implementation of V/Hz limiter in Modelica

Figure 4.30: Implemented checkbox for frequency setpoint options in the V/Hz limiter

4.5 Voltage Droop/Compensation Controller

This controller varies the generator terminal voltage considering the changes in active and reactive current and frequency. The controller's output interacts with the summing point to modify the voltage reference signal V_{REF}, and consequently, the generator terminal voltage will be regulated. The voltage droop/compensation controller consists of four control functions or three controllers. These controllers are modeled based on the particulars from the hydropower controller HYMAREG 10's user manual [22], and the modeling of the controllers is described below.

4.5.1 Reactive Current Droop and Compensation Controller

This controller inherent a combination of reactive current droop and reactive current compensation control functions. The controller is fundamentally modeled based on the formula given in Eq. (4.11) [35]. This formula is used to calculate the new generator terminal voltage

setpoint considering the droop/compensation value and actual generator reactive current output. The E_{rr} obtained by subtracting the measured terminal voltage V_T from the calculated generator terminal voltage value V_{Tcal}. And then the E_{rr} is applied through the PID controller to the output. Additionally, the droop (regulation) value should be given in percent, and most importantly, it should be a negative value "-" for the droop control function and a positive value "+" for the compensation control function. Figure 4.31 illustrates the block diagram of the reactive current droop/compensation controller. The Boolean signal $IQ_{controller}$ should be "true" in order to activate the output of the controller, else the output will be zero.

$$V_{Tcal} = \left\{\left[\left(\frac{I_Q - I_{Qsp}}{I_{Qn}}\right) \cdot \frac{R_{IQ}}{100}\right] + 1\right\} \cdot V_{Tsp} \tag{4.11}$$

where

R_{IQ}	:	The droop (regulation) value	[%]
I_Q	:	The actual generator reactive current output	$[pu]$
I_{Qsp}	:	The generator reactive current setpoint	$[pu]$
I_{Qn}	:	Generator nominal reactive current	$[pu]$
V_{Tcal}	:	The calculated new generator terminal voltage setpoint	$[pu]$
V_{Tsp}	:	The generator terminal voltage setpoint	$[pu]$

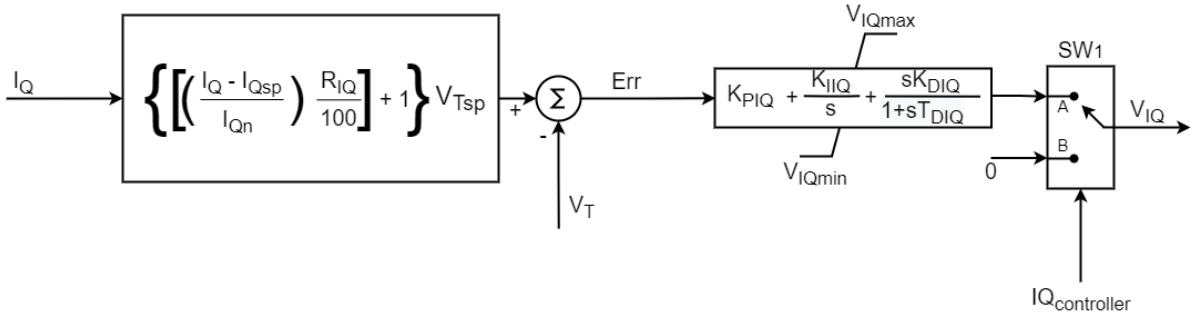

Figure 4.31: Block diagram of reactive current droop/compensation controller

4.5.2 Active Current Compensation Controller

The active current compensation control function model uses the formula given in Eq. (4.12) to calculate the new generator terminal voltage setpoint [35]. This controller regulates the voltage only if the actual active current I_P is higher than the active current setpoint I_{Psp}. Meaning, if the I_P is less than the I_{Psp} the active compensation controller will not react. Furtherly, the E_{rr} is calculated by subtracting the V_T from V_{Tcal} then applied to the output through the PID controller. Moreover, the regulation value R_{IP} should be a positive value to obtain the compensation function. Otherwise, the controller will behave on the contrary. The block diagram of the active current compensation controller is presented in Figure 4.32. The

Boolean signal $IP_{controller}$ should be "true" to change the position in the switch SW_1 to enable the output of the controller, otherwise the it will be zero.

$$V_{Tcal} = \left\{\left[\left(\frac{I_P - I_{Psp}}{I_{Pn}}\right) \cdot \frac{R_{IP}}{100}\right] + 1\right\} \cdot V_{Tsp} \tag{4.12}$$

where

R_{IP}	:	The droop (regulation) value	[%]
I_P	:	The actual generator active current output	$[pu]$
I_{Psp}	:	The generator active current setpoint	$[pu]$
I_{Pn}	:	Generator nominal active current	$[pu]$
V_{Tcal}	:	The calculated new generator terminal voltage setpoint	$[pu]$
V_{Tsp}	:	The generator terminal voltage setpoint	$[pu]$

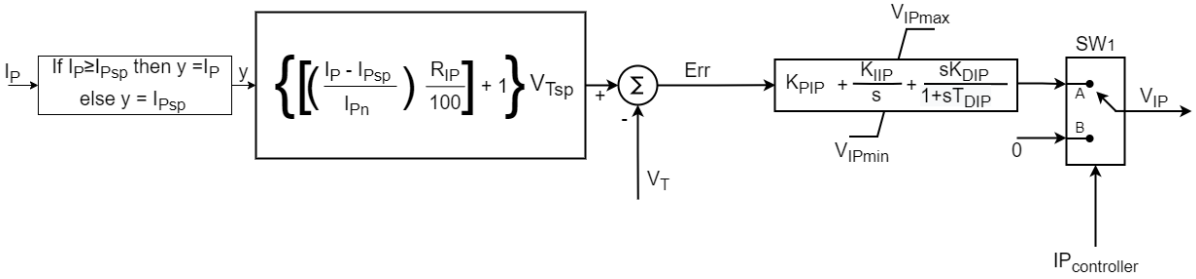

Figure 4.32: Block diagram of active current compensation controller

4.5.3 Frequency Droop Controller

This controller model is modeled based on Eq. (4.12) to determine the new generator terminal voltage setpoint [35]. And, this controller behaves similarly to the latter controllers, where the E_{rr} obtained by compare the V_T and V_{Tcal}, then applies through the PID controller to the output. The droop (regulation) value should be a positive value to obtain the compensation function. Besides, this controller has an additional function limiting the voltage support when the frequency exceeds the maximum and minimum limit, $f_{maxlimit}$ and $f_{minlimit}$, respectively. Meaning, the frequency droop controller will not increase or decrease the V_T when the frequency exceeds the latter limits. The Boolean signals $f_{controller}$ should be "true", and the circuit breaker should be closed in order to activate the output of the controller, else the output is zero. The block diagram of the frequency droop controller is depicted in Figure 4.33.

$$V_{Tcal} = \left\{\left[\left(\frac{f - f_{sp}}{f_n}\right) \cdot \frac{R_f}{100}\right] + 1\right\} \cdot V_{Tsp} \tag{4.13}$$

where

R_f	:	The droop (regulation) value	[%]
f	:	The actual frequency	$[Hz]$
f_{sp}	:	The frequency setpoint	$[Hz]$
f_n	:	Nominal frequency	$[Hz]$
V_{Tcal}	:	The calculated new generator terminal voltage setpoint	$[pu]$
V_{Tsp}	:	The generator terminal voltage setpoint	$[pu]$

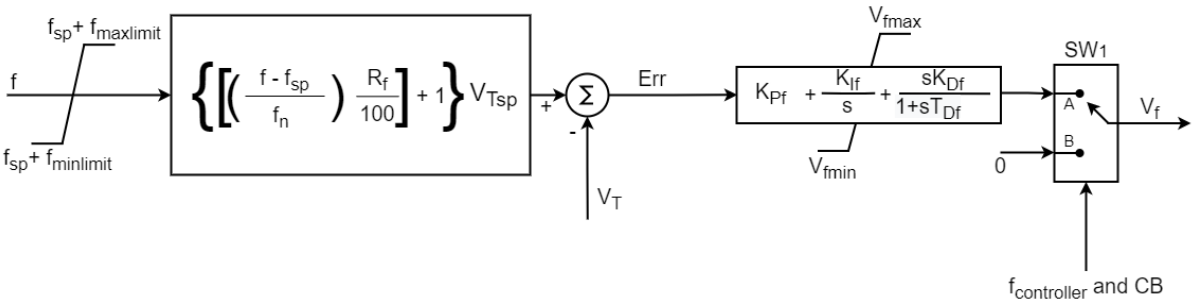

Figure 4.33: Block diagram of the frequency droop controller

4.5.4 Final Combined Controller

All three controllers mentioned in Section 4.5.1, 4.5.2, and 4.5.3 are added together into a voltage droop/compensation controller model (see Figure 4.34). The checkboxes III, V, and VII in Figure 4.35 shall be selected in order to enable the outputs of the reactive current droop/compensation, active current compensation, and frequency droop controllers, respectively. These checkboxes are associated with the switches, SW_{1IQ}, SW_{1IP}, and SW_{1f}. Thus, the controllers can either be used alone or in combination with others to regulate the voltage. All the setpoint values can be chosen as constant or variable setpoints by choosing the checkboxes indicated with II, IV, VI, and VIII in Figure 4.35. When the checkboxes II, IV, VI, and VIII are checked, variable setpoint inputs such as terminal voltage setpoint V_{Tvsp}, reactive current setpoint I_{Qvsp}, active current setpoint I_{Pvsp}, and frequency setpoint f_{vsp} will be enabled to connect, respectively. Simultaneously, when those are activated, the associated constant setpoints will be disabled. Moreover, conditional connections are visibly indicated with dashed lines in Figure 4.34. Note that the controller's parameters are placed in individual tabs as indicated with (I) in Figure 4.35, while the common terminal voltage setpoint options are placed in the tab called "General".

Further, in active compensation and frequency droop control functions, an absolute block is used to assure that a given negative droop (regulation) value (R_{IP} and R_f) does not change the characteristics of the control functions. The voltage droop/compensation controller's parameters are described in Appendix J, which is obtained from the commissioning report [34] from the Hogstad power station. And, parameters of the PID controllers are obtained during

the simulation tests. Be aware of the named parameters in the controller's block diagram and the model because they are changed due to modeling purposes.

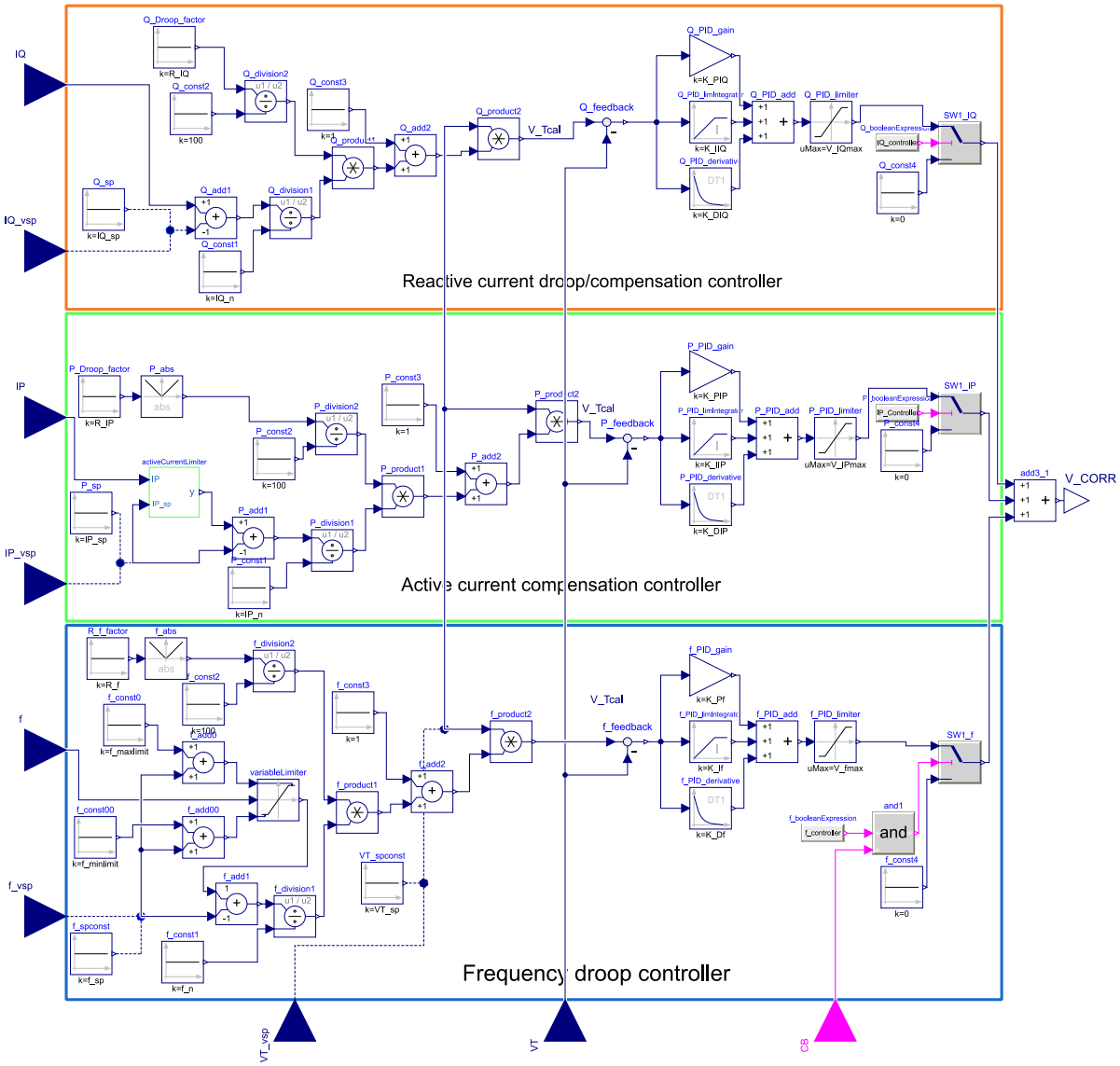

Figure 4.34: Implementation of voltage droop/compensation controller in Modelica

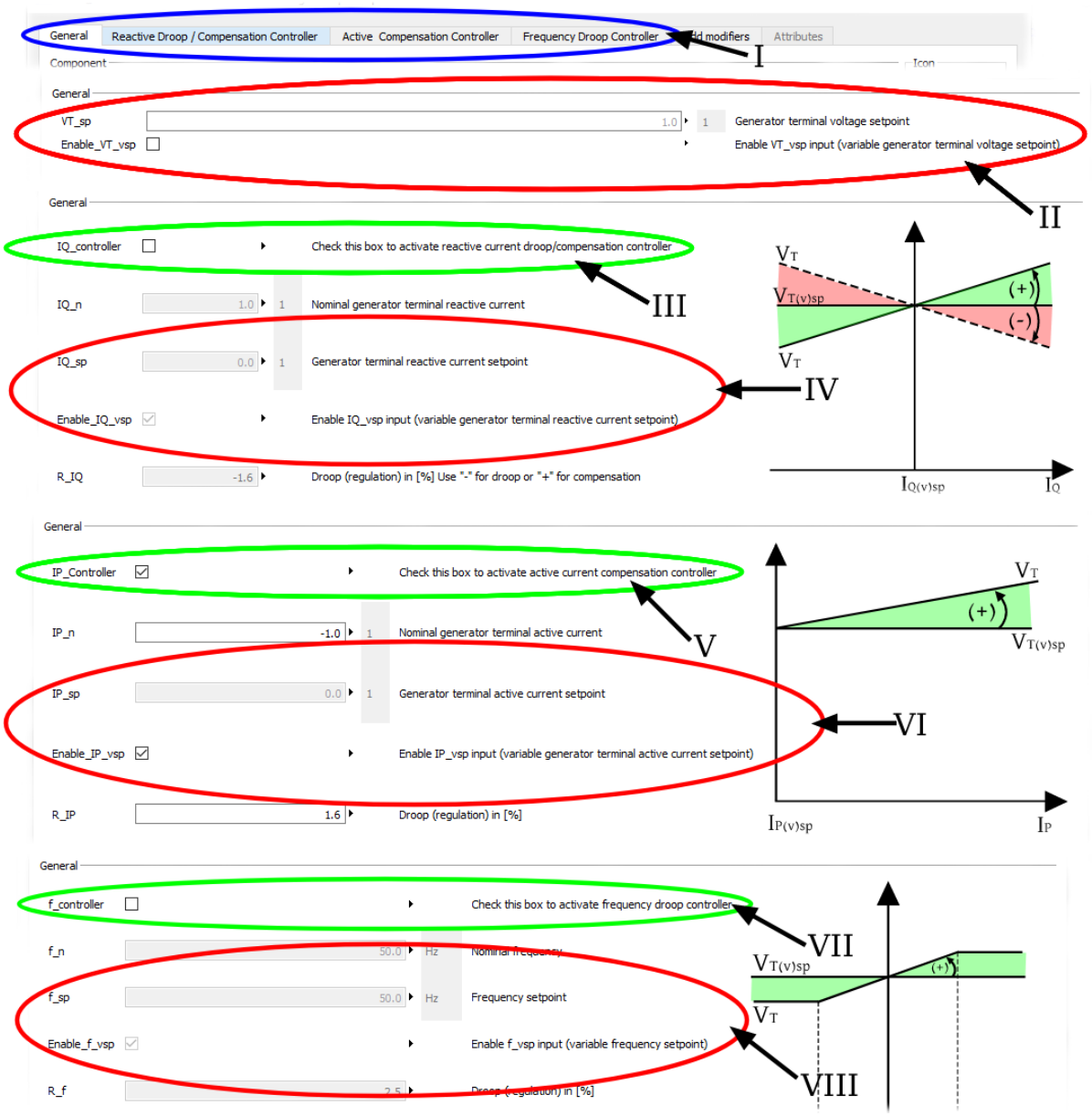

Figure 4.35: Implemented user interfaces in Modelica for voltage droop/compensation controller. I: Tabs for each controller. II: Checkbox to enable the variable generator terminal voltage setpoint. III: Checkbox to enable Reactive current droop/compensation controller. IV: Checkbox to enable the variable generator terminal reactive current setpoint. V: Checkbox to enable Active current compensation controller. VI: Checkbox to enable the variable generator terminal active current setpoint. VII: Checkbox to enable the Frequency droop controller. VIII: Checkbox to enable the variable frequency setpoint.

4.6 Reactive Power (VAR) or Power Factor (PF) Controller

The VAR/PF controllers and regulators have two main functions, as mentioned in Section 2.6. The regulator function is similar to the AVR, which can be modeled as excitation systems by changing the terminal voltage input V_C to PF or VAR. On the contrary, the controller function should be modeled considering how they modify the reference signal V_{REF} of AVR, and consequently, the terminal voltage V_T to keep the VAR or PF near to a set value over a specific time span. Some of the controllers have a time delay added to allow the machine to provide

voltage support until the time exceeds. This can be an advantage for synchronous generators, which can support the voltage during the larger synchronous motor being started. Overall, this thesis contains only VAR/PF controller modeling, not regulators, and this section contains modeling of VAR/PF controller based on a combination of VAR and PF controller type 2 and 1 in IEEE Std 421.5-2016 [14] and information from HYMARAG 10 user manual [22]. [14]

4.6.1 Power Factor Normalizer

PF controller fundamentally takes control of actions based on the generator operating region. The generator operating region can be either an overexcited or underexcited region. While the power factor is principally calculated using Eq. (4.14). [14]

$$PF = \frac{P_T}{\sqrt{P_T^2 + Q_T^2}} \tag{4.14}$$

where

PF	:	The power factor of the synchronous generator	$[-]$
P_T	:	The active power output of the generator	$[pu]$
Q_T	:	The reactive power output of the generator	$[pu]$

Despite this, the equation above cannot be used to identify whether the power factor is in an overexcited or underexcited region. Therefore, the power factor needs to be defined in order to recognize whether the machine operates overexcited or underexcited region. Figure 4.36 (a) illustrates a relationship between power factor and varying field current, considering a fixed active power output of the generator. The plot shows that the power factor is equal to 1 when the reactive power is zero. Otherwise, the power factor reduces when the reactive power increases in both operation regions. There are two different field current setpoints in the overexcited and underexcited region, which could result in the same power factor as indicated with the line “X” in Figure 4.36 (a). Hence, the power factor needs to be defined so that each field current setpoint has a unique power factor value and should result in a continuous function for increasing field current. Figure 4.36 (b) depicts a defined normalized power factor as a continuous function from -1 to 1, which would be desirable for modeling and control purposes.[14]

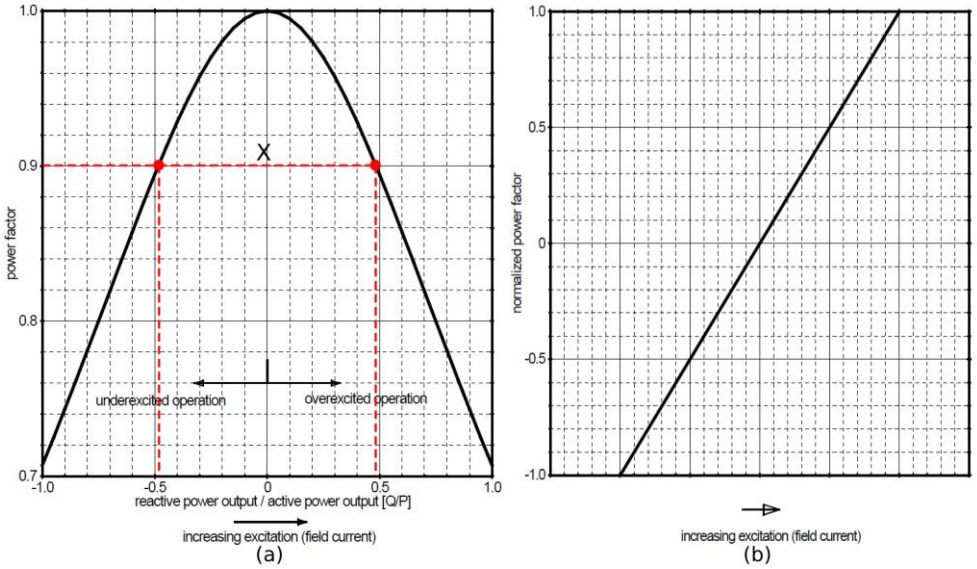

Figure 4.36: (a) Power factor of a generator for varying excitation levels (line X indicated same power factor for two field current values) (b) Normalized power factor from -1 to +1. [14]

The normalized power factor is shown in Figure 4.36 (b) can be modeled as shown in Figure 4.37. Initially, the power factor is calculated using Eq. (4.14), then modified to be negative for underexcited operation and positive for overexcited operation. Finally, the modified power factor to be a continuous function that goes from negative to positive power factor as field current from underexcited to overexcited region. This power factor normalizer has been used to normalize the PF input PF_{norm}, and for PF setpoint input $PF_{REFnrom}$ in this thesis, the Modelica code is presented in Appendix Q and R, respectively.[14]

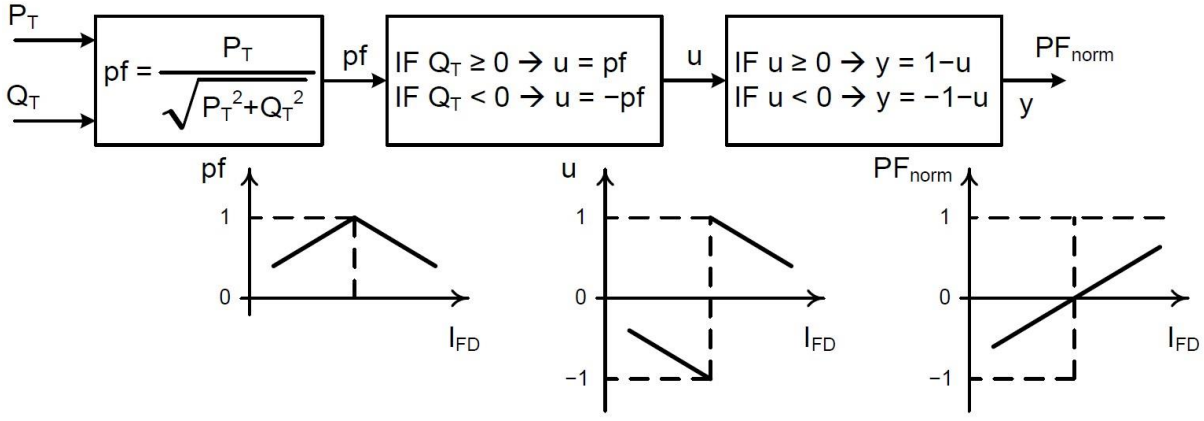

Figure 4.37: Model for normalized power factor from -1 to +1. [14]

4.6.2 Modeling of VAR/PF Controller

VAR/PF controller is a summing point type controller, which interacts with AVR as an addition to the voltage reference V_{REF}. This controller consists of two controllers, the VAR controller, and the PF controller, but only one of the controllers can be active at a time. Both controllers have a separate PID controller, which can be adequately tuned to control the generator's reactive power or power factor output to reach the desired setpoints smoothly. Figure 4.38 portrays a block diagram of the VAR/PF controller.[14]

Both controllers have a control logic that controls each controller's output, displayed in Figure 4.38. Controllers become inactive if the magnitude of the generator terminal current I_T drops below the limit V_{ITmin}, or generator terminal voltage V_T goes above threshold V_{VTmax} or below V_{VTmin}. If any excitation limiters OELs (FCOEL or SCOEL), UELs (SCUEL or FCUEL), or SCL becomes active, the VAR/PF controller becomes inactive. Further, these controllers also contain deadbands and delay times. When the reactive power error exceeds the deadband range between VAR_{DBW} and $-VAR_{DBW}$ for a time greater than VAR_{Td}, the VAR controller's output modifies the V_{REF} of the AVR and causes the generator to increase or decrease the reactive power output. Similarly, when the power factor error exceeds the deadband range between PF_{DBW} and $-PF_{DBW}$ for a time greater than PF_{Td}, the output of the PF controller modifies the V_{REF} of the AVR and causes the generator to vary the reactive power output to obtain the desire power factor. As well, the circuit breaker should be closed in order to activate the controllers.[14]

Additionally, both controllers have a setpoint ramp that ramps up the speed of the setpoint change according to the defined ramping speed, VAR_{spramp} and PF_{spramp}. And, there is a setpoint limiter for each controller to limit the setpoints within $VAR_{spmax} - VAR_{spmin}$ and $PF_{spmax} - PF_{spmin}$ for VAR and PF controllers, respectively. [14]

The power factor controller uses normalized power factor as mentioned in Section 4.6.1 for PF input and PF setpoint. But, the setpoints in the PF controller are given as an angle which is $(\cos^{-1}(PF))$.[14]

There are added switches at each controller's output to enable or disable their output, where a Boolean signal applies to switch the switches' position.

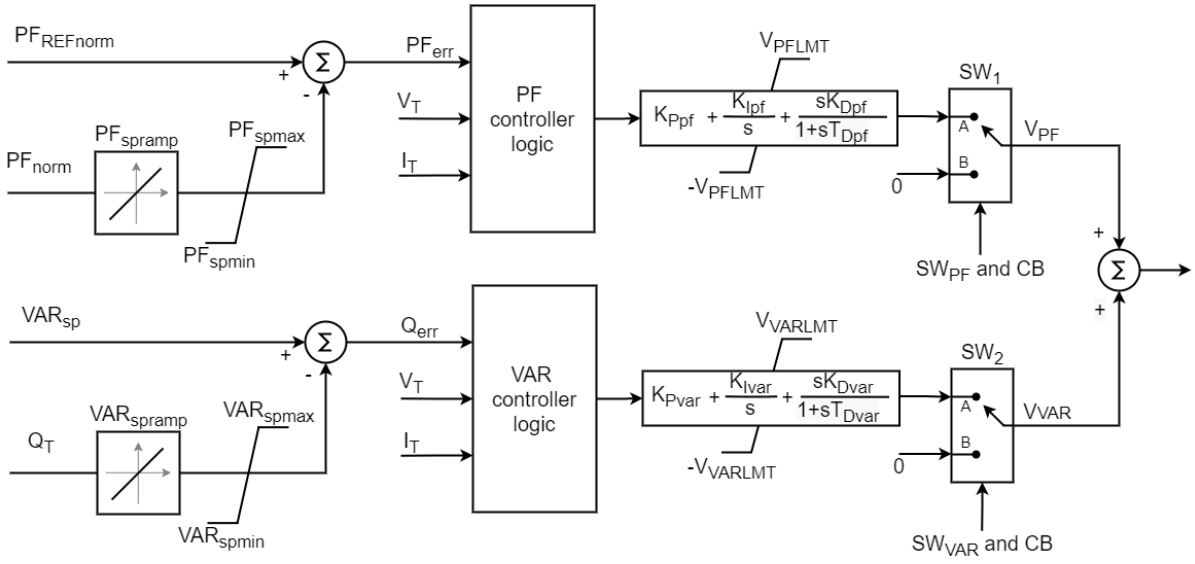

Figure 4.38: Block diagram of the VAR/PF controller [14] (modified)

Figure 4.39 shows modeled VAR/PF controller in Modelica, and options to choose the type of controller are implemented with a drop-down list which is pointed out in Figure 4.40 as (I). The dashed lines indicate the conditional connections that are coded to alter between the constant setpoint or the variable setpoint by choosing checkboxes $Enable_{PF_{vsp}}$ and $Enable_{VAR_{vsp}}$, which is indicated with (II) and (III) in the Figure 4.40, respectively. Also, by

checking these checkboxes, the variable setpoint for PF controller and VAR controller enabled. The Modelica cope only with the radians, while the constant and variable setpoint is the degree; therefore, a block called “from_deg” is used to convert from degree to radians. Consequently, the $PF_{REFnorm}$ block slightly differs from the power factor normalizer, as mentioned in Section 4.6.1. There are added logical blocks as AND, NOR, and NOT gates to ensure that the controller’s output becomes zero if the status signal from OELs, UELs, and SCL becomes “true”, or if the CB, SW_{PF}, and SW_{VAR} signals become “false”, or Boolean variable PF_{active} and VAR_{active} become “false”. Where the Boolean variable PF_{active} or VAR_{active} becomes “true” if PF controller or VAR controller is activated by the user.

Appendix K, the VAR/PF controller parameters are presented, where the parameters are obtained from the IEEE Std 421.5-2016 [14] and commissioning report [34] from the Hogstad power station. The rest of the parameters are determined during the tuning of the controller. Please note that the VAR controller’s parameters are given in percentage in the commissioning report [34], but they are converted to per unit to apply to the model. Lastly, the Modelica script for VAR or PF controller logic is presented in Appendix S.

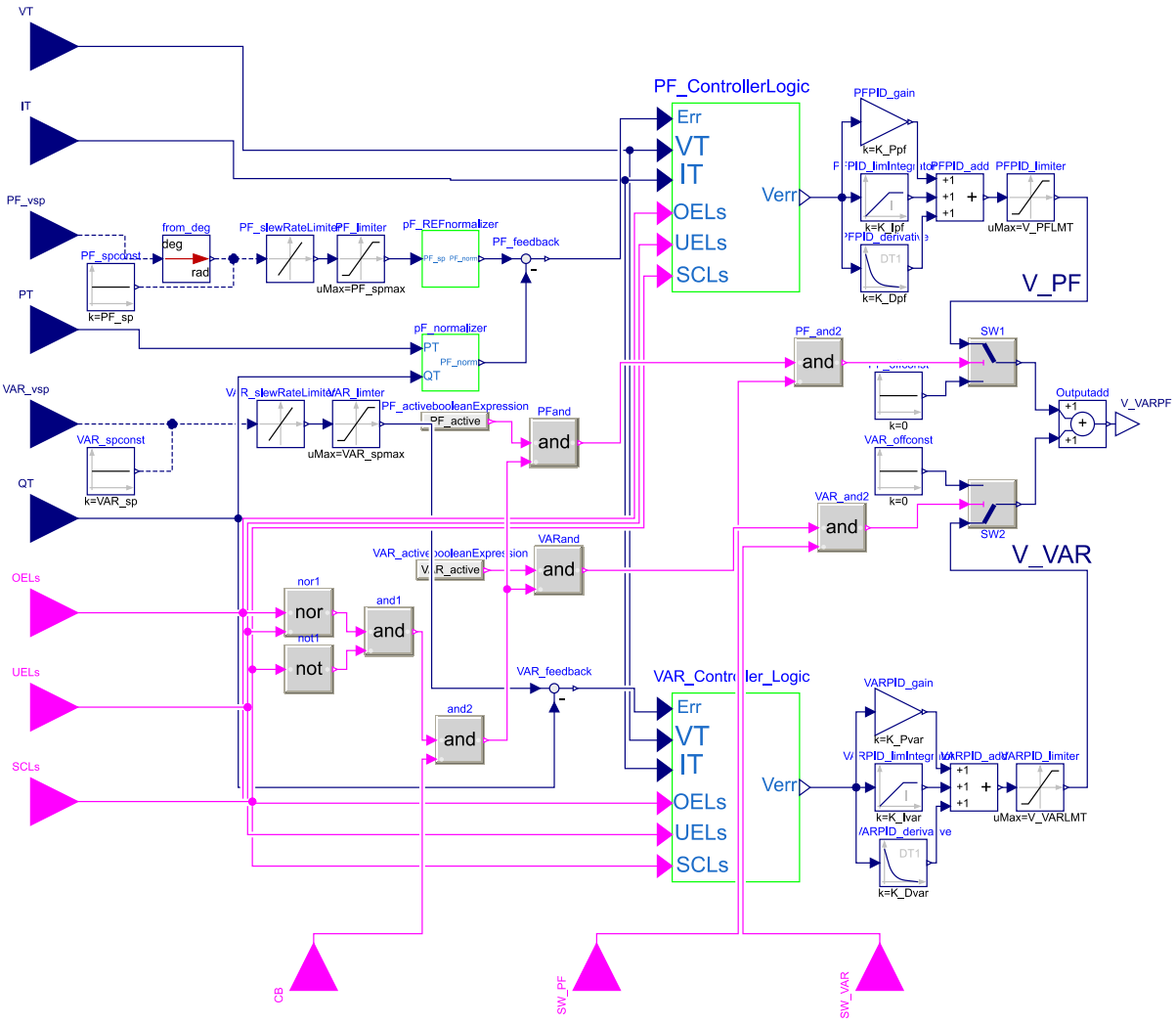

Figure 4.39: Implementation of VAR/PF controller in Modelica

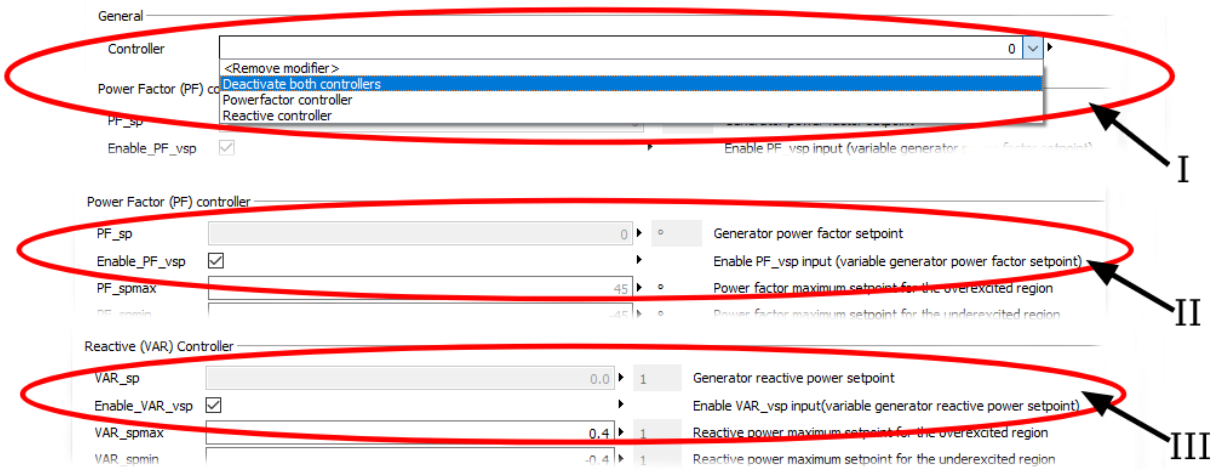

Figure 4.40: Implemented the dropdown list and checkboxes in Modelica for VAR/PF controller. 1: Drop-down list for controller type choice, 2: Checkbox for enabling PF variable setpoint input, 3: Checkbox for enabling VAR variable setpoint input

4.7 Excitation Control System

Shown in Figure 4.41 is the final implementation of the excitation control system. In this model, all the controllers and protective limiters are connected with the AVR or excitation system type *ST7C*. And the output of this model will be the field voltage, which shall be connected to the generator. Moreover, the inputs V_F and V_{FB} are set to constant zero due to a lack of outputs from the *ST7C* model, and for the inputs, V_{OEL3} and V_{UEL3}, a constant of 100 and -100 applied in order to eliminate the inputs. Besides, the input "VOTHSG", where the PSS's or discontinuous excitation control function output should be connected, is also set to zero to eliminate the input. There are some logical blocks such as OR gates, greater-than, and less-than blocks to determine whether the FCOEL, SCUEL, SCL, SCOEL, or FCUEL is active or not to enable the VAR/PF controller. The dashed lines illustrate the conditional connections between the blocks that alternate connection between the constant setpoints to variable setpoints. Finally, Figure 4.42 depicts the tabs that were implemented in the final excitation control system to parametrize the inherent controllers and limiters.

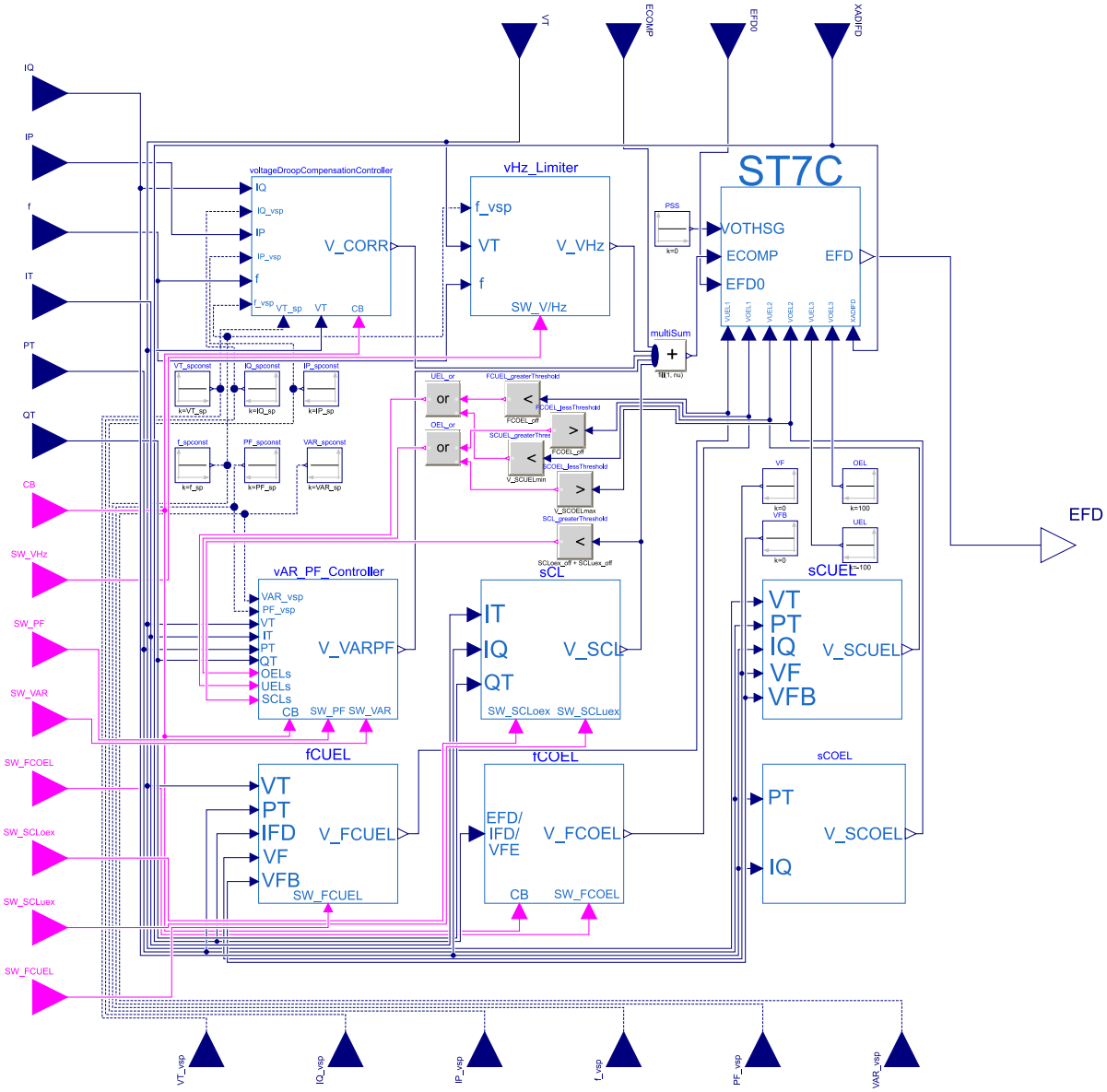

Figure 4.41: Final implementation of excitation control system

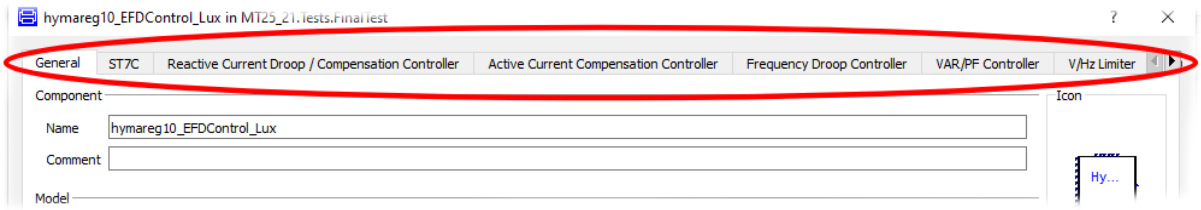

Figure 4.42: Tabs for parameters of controllers and limiters of excitation control system

5 Simulation Results

The models presented in chapter 4 will be simulated, and the results will be presented in order to study the performance of each model. Simultaneously, the presented results will be compared with the actual data from the Hogstad power plant as well.

Furthermore, the parameters of the common components in the test setup, such as GENSAL generator, transmission line, and excitation system type *ST7C*, are acquired from Appendix B, Table 4.2, and Appendix C. In addition, the system power base and frequency for all the components are set to 10 MVA and 50 Hz, accordingly. Also, the generator is initialized, as presented in Table 5.1, during the various simulations. Since the initial active power P_0 and the reactive power Q_0 will be varied for different simulation tests, the values are not presented in Table 5.1.

Table 5.1: Initialization of GENSAL generator for simulation

Parameters	Description	Values	Units
P_0	Initial active power	-	MW
Q_0	Initial reactive power	-	$Mvar$
v_0	Initial voltage magnitude	1	pu
$angle_0$	Initial voltage angle	0	°
ω_0	Initial speed deviation from nominal	0	pu

5.1 Excitation System

The simulation test setup for examining the excitation system type *ST7C* is displayed in Figure 5.1. The test adjusts the excitation system's setpoint from 0.95 pu to 1.0 pu corresponding, 95 to 100 %, and from 100 to 95 % as well. Due to the lack of ability to directly vary the reference of the excitation system, the input of compensated voltage ECOMP is varied to influence the reference. Despite this, the terminal voltage counteracted for the changes in the ECOMP, meaning if the input to the ECOMP rises 5 %, the terminal voltage decreased 5 %. As shown in Figure 5.1, some arrangements are made to visually see that the terminal voltage rises when the setpoint increases and declines when the setpoint decreases. Thus, it might help during the comparison of the simulation results with the real measurement from the Hogstad power plant. Besides, the generator's initial voltage magnitude v_0 is set to 0.95 pu during the step-up response test while 1 pu during the step-down response test. The initial active P_0 and reactive power Q_0 of the generator are set to zero during both simulations.

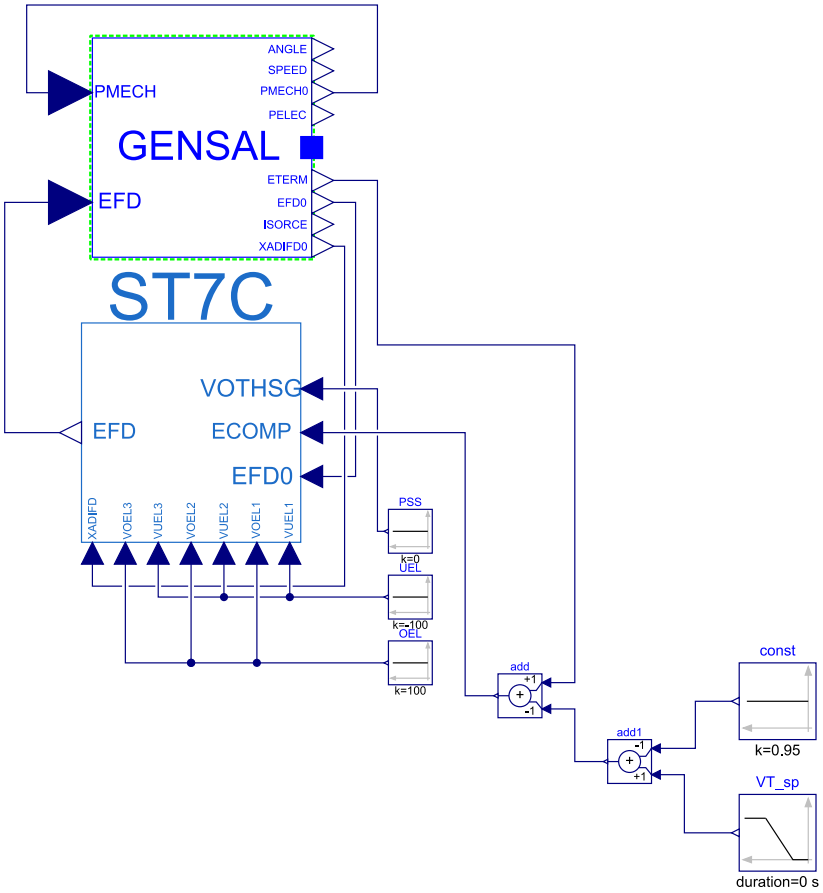

Figure 5.1: Test setup for examining the performance of excitation system type *ST7C*

Figure 5.2 shows the step-up and step-down response of the generator terminal voltage, which is plot "A" and "B", respectively. Likewise, Figure 5.3 illustrates the actual measurement data of step-up and step-down response of the 10 MVA generator in the Hogstad power plant. Please note that during the simulations and actual generator commissioning, the setpoints are changed at 1 s, but the scale of abscissa is different for Figure 5.2 and Figure 5.3.

Comparing the results shows that the model has a slow response, meaning the settling time (time to reach steady-state with ±5 % of ΔV_{Tsp} deviation) of the real plant is about 2 –2.5 s while simulations show roughly 30 – 40 s. Also, the model takes 5 s to reach 90 % of the setpoint change ΔV_{Tsp}, while the actual plant takes roughly 0.75 s. According to NVF 2020 [23], the generator with less than 30 MW nominal power without PSS should reach 90 % of the ΔV_{Tsp} within 1.0 s, while the settling time should be less than 2.5 s. Moreover, according to NVF 2020 [23], the maximum overshoot should be less than 15 % of ΔV_{Tsp}. But the simulation results depict that the model has an overshoot of 35 %, while the actual plant has almost no overshoot.

Be aware that during the commissioning, after 5 s, some other changes in the plant led to a fluctuation in the voltage, seen in Figure 5.3 that is not considered in this case.

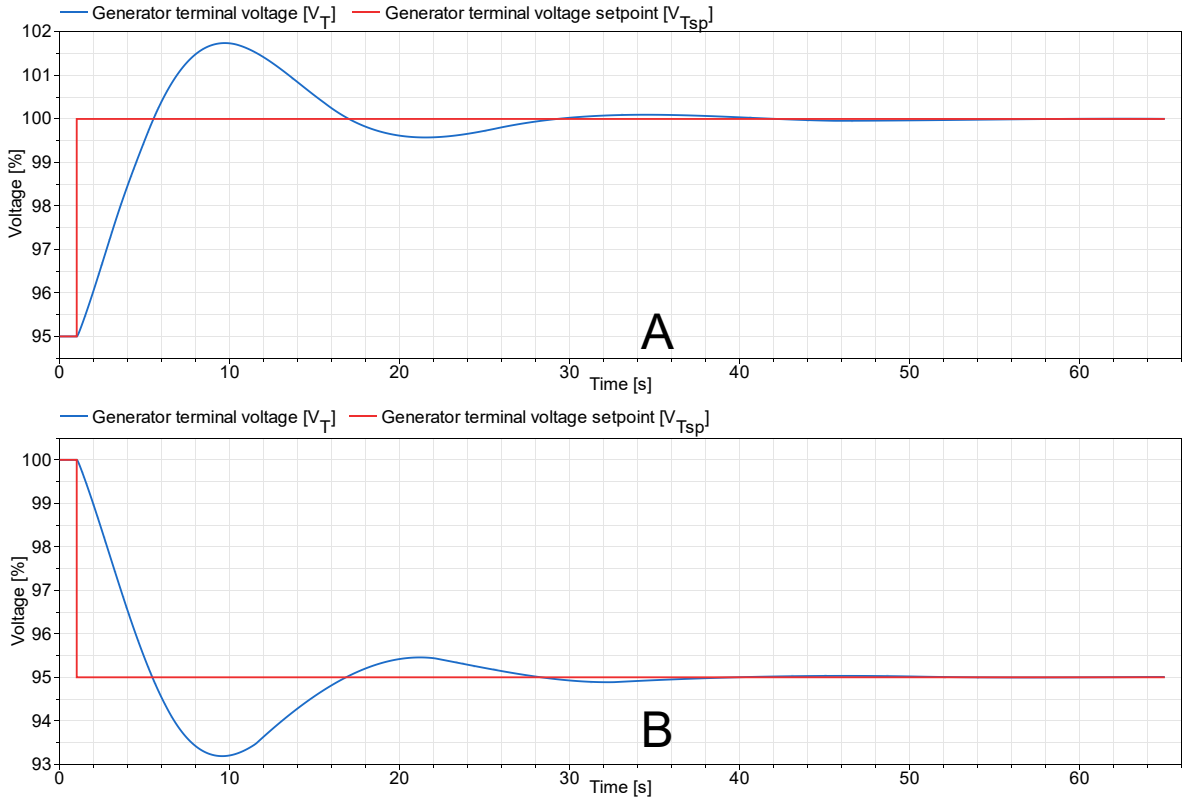

Figure 5.2: Step response of the GENSAL generator with real and estimated parameters. A: Step-up response for +5 % change in V_{Tsp}, B: Step-down response for -5 % change in V_{Tsp}

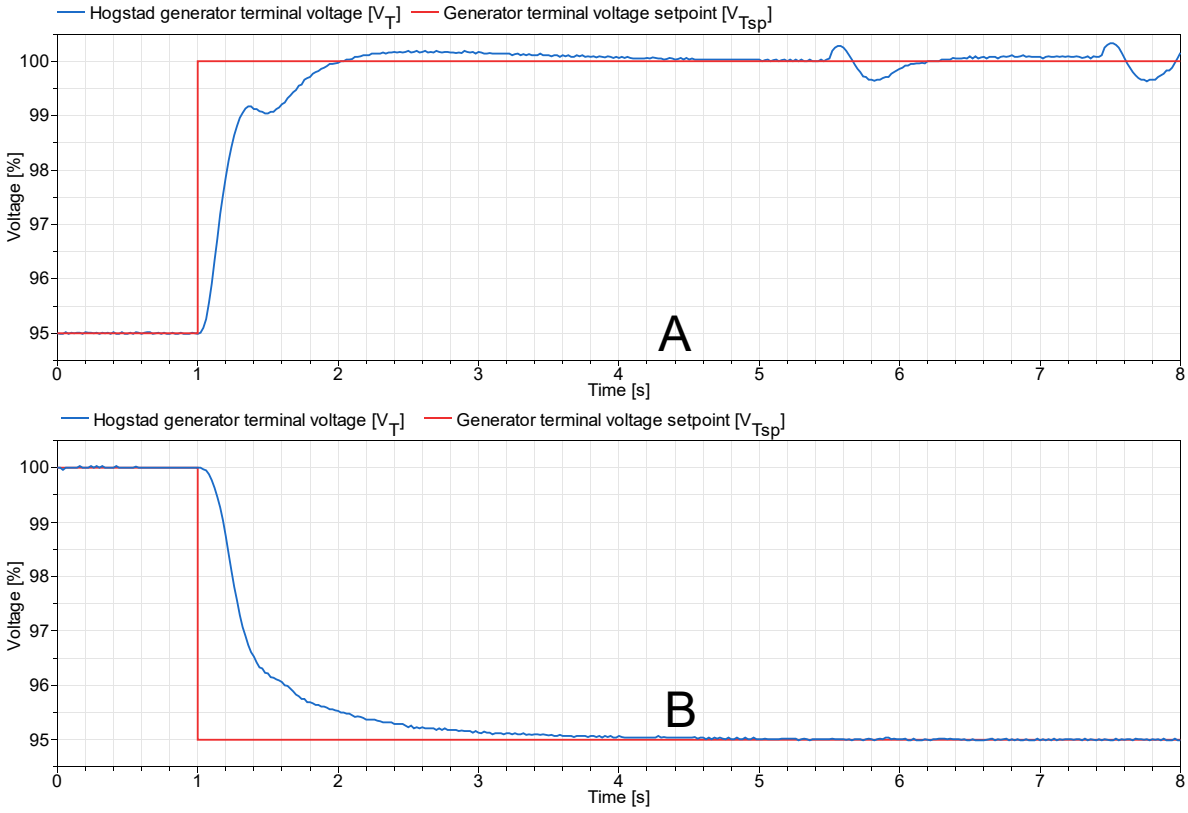

Figure 5.3: Step response measurement data of the real 10 MVA generator in the Hogstad power station. A: Step-up response for +5 % change in V_{Tsp}, B: Step-down response for -5 % change in V_{Tsp}.

5.2 Limiters

This section presents the simulation results of field current overexcitation limiter (FCOEL), stator current underexcitation limiter (SCUEL), stator current limiter (SCL), stator current overexcitation limiter (SCOEL), field current underexcitation limiter (FCUEL), and lastly, volts-per-hertz (V/Hz) limiter.

5.2.1 Field Current Overexcitation Limiter (FCOEL)

The test setup for FCOEL is depicted in Figure 5.4, and parameter values of the FCOEL are obtained from Appendix D. The test is performed by enabling the limiter output at 1100 s and open the circuit breaker at 2500 s. The initial active power P_0 and reactive power Q_0 of the generator are set to 8 MW and 6 $Mvar$, accordingly.

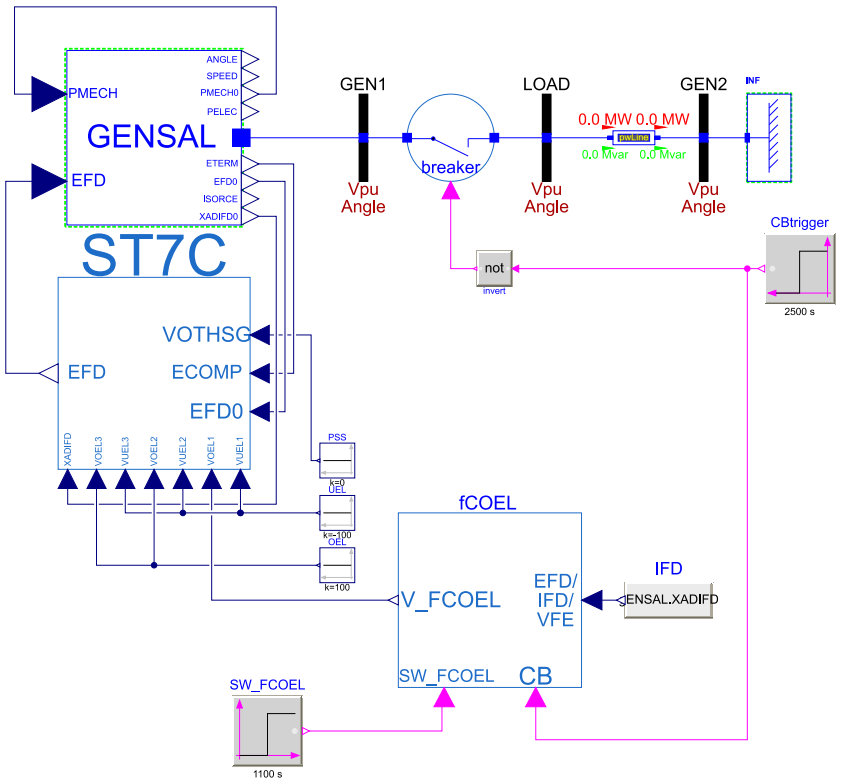

Figure 5.4: Test setup for field current overexcitation limiter (FCOEL) model

The test results of the field current overexcitation limiter are presented in Figure 5.5. After the startup, the generator field current I_{FD} is stabilized to 2.15 pu, but the output of the FCOEL V_{FCOEL} is continuously at 100. When the limiter output is enabled, the field current is limited to $I_{lim} = 1.95\ pu$, and consequently, the V_{FCOEL} reduces. Further, when the circuit breaker opens, the field current is limited to $I_{NL} = 1.07\ pu$, as desired.

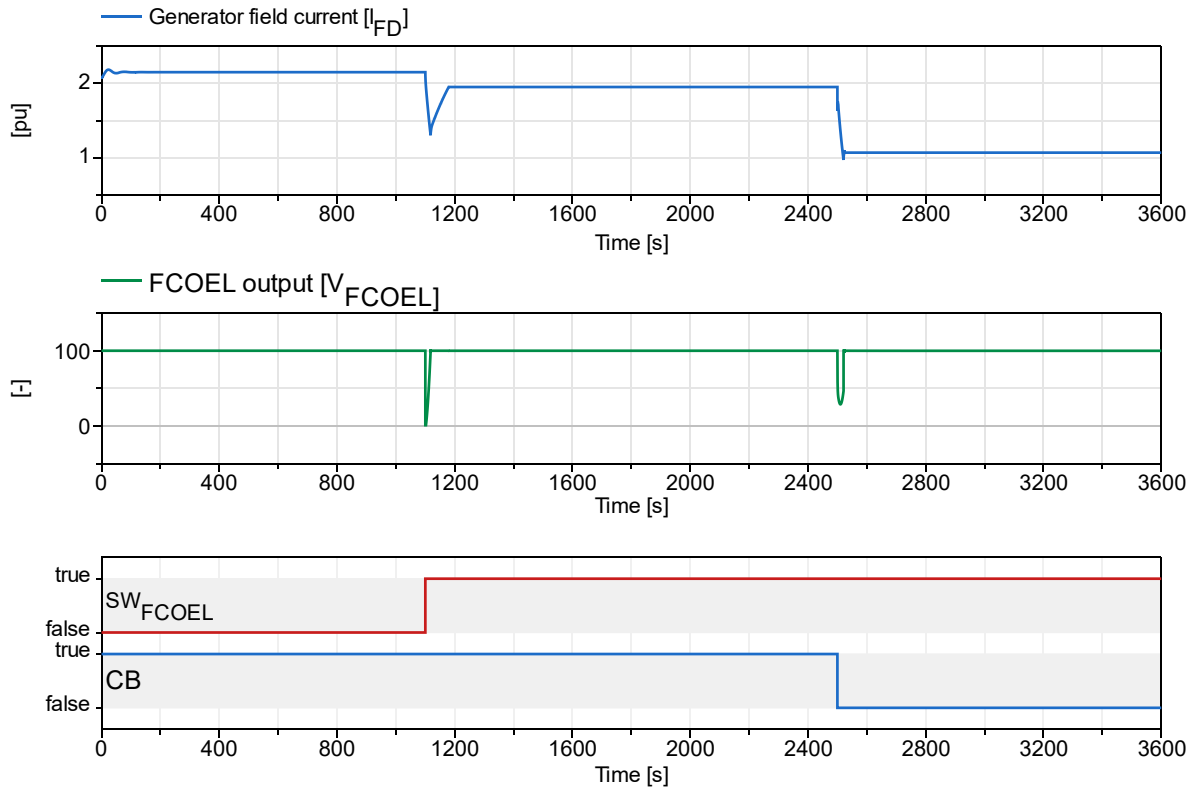

Figure 5.5: Performance of the field current overexcitation limiter (FCOEL)

5.2.2 Stator Current Underexcitation Limiter (SCUEL)

The test setup to simulate the SCUEL model is shown in Figure 5.6, where a switch is manually added to the output of the SCUEL in order to control the output of the limiter. The switch's position is set to change at 1800 s to enable the output of the SCUEL, and the parameter values of the SCUEL are obtained from Appendix E. The initial active power P_0 and reactive power Q_0 of the generator are set to 7.5 MW and -4 $Mvar$, respectively, during the SCUEL simulation test. Besides, the inputs V_F and V_{FB}, are set to zero due to a lack of outputs from the *ST7C* model.

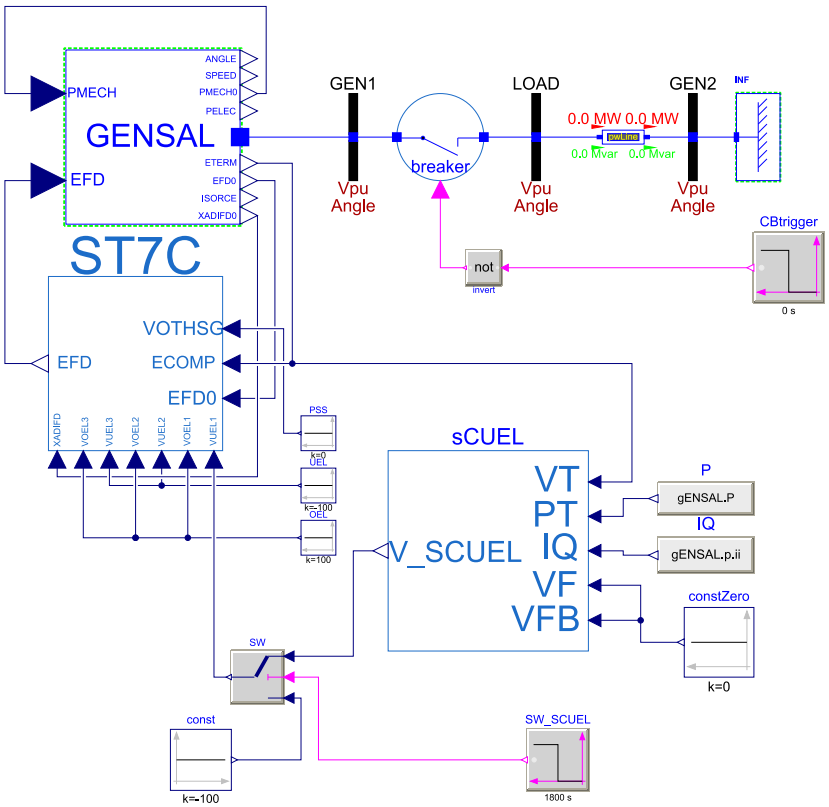

Figure 5.6: Test setup for stator current underexcitation limiter (SCUEL) model

Initially, the limiter output is not connected to the AVR, and the reactive current I_Q is in a steady-state around -0.36 pu, while the underexcitation I_Q limit is set to -0.25 pu at 0.75 pu active power P_T. As a result, the limiter tries to increase the field current by increasing the output of the limiter towards the maximum limit (see Figure 5.7). When the limiter output is connected to the AVR at 1800 s, the limiter gradually decreases the output. Hence the reactive current increases, and it ends up at -0.25 pu, as expected. The output of the limiter is decreased and stabilized to a signal value of -99.98.

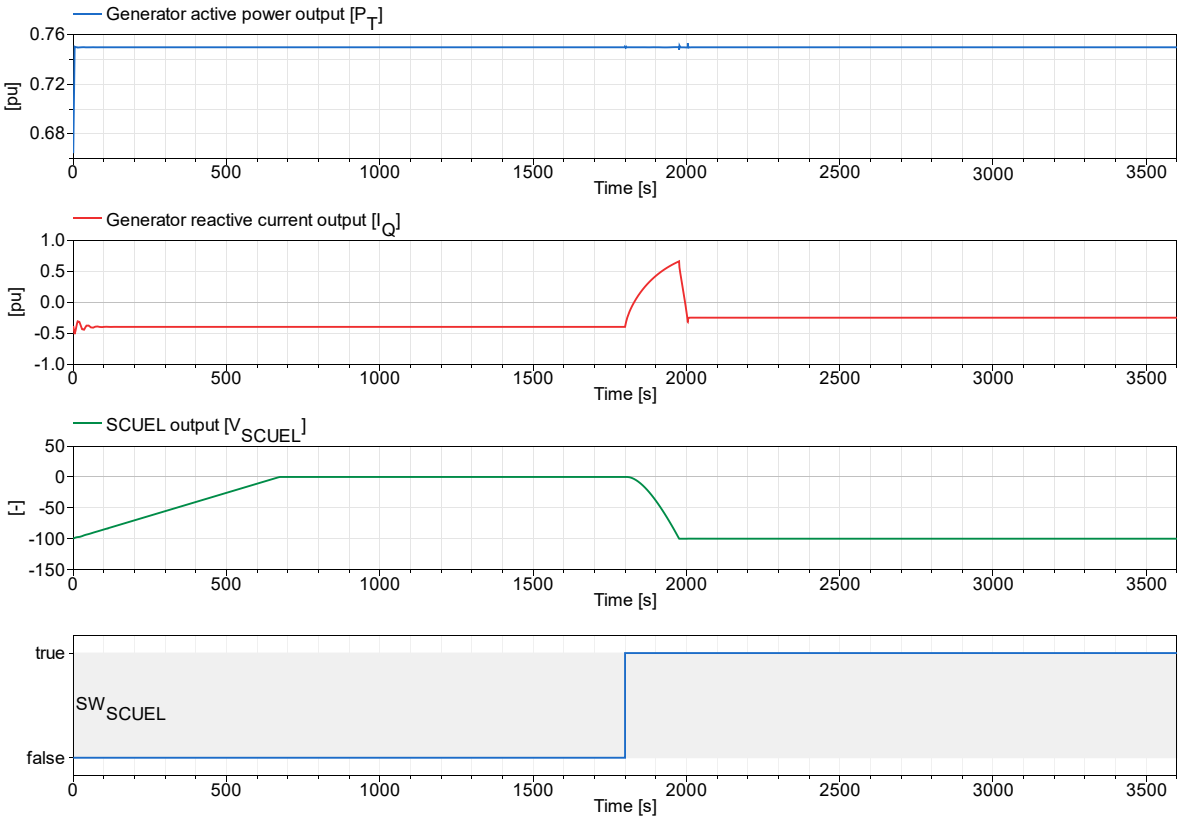

Figure 5.7: Performance of stator current underexcitation limiter (SCUEL)

5.2.3 Stator Current Limiter (SCL)

The SCL model's test setup is shown in Figure 5.8, and the simulation test for the SCL is performed under two operational regions, inside the overexcited and underexcited regions. And both regions have separate PID controllers to operate under each region. As mentioned in Section 4.4.3, SCL also consists of two types of controllers, reactive current and reactive power controllers. And each controller is also examined under each operational region. The output of the overexcited and underexcited regions is controlled by the Boolean input signals SW_{OEX} and SW_{UEX}, respectively, and these are set to "true" at 800 and 1800 s. The parameters of SCL are given in Appendix F. In order to obtain generator terminal current I_T above the pickup level I_{SCLlim} during the overexcited region, the initial active power P_0 and reactive power Q_0 of the generator are set to 8 MW and 8 $Mvar$, accordingly. Whereas during the underexcited region test, only the initial reactive power Q_0 of the generator is changed to -8 $Mvar$. In addition, the reactance of the transmission line X is set to zero during the simulations.

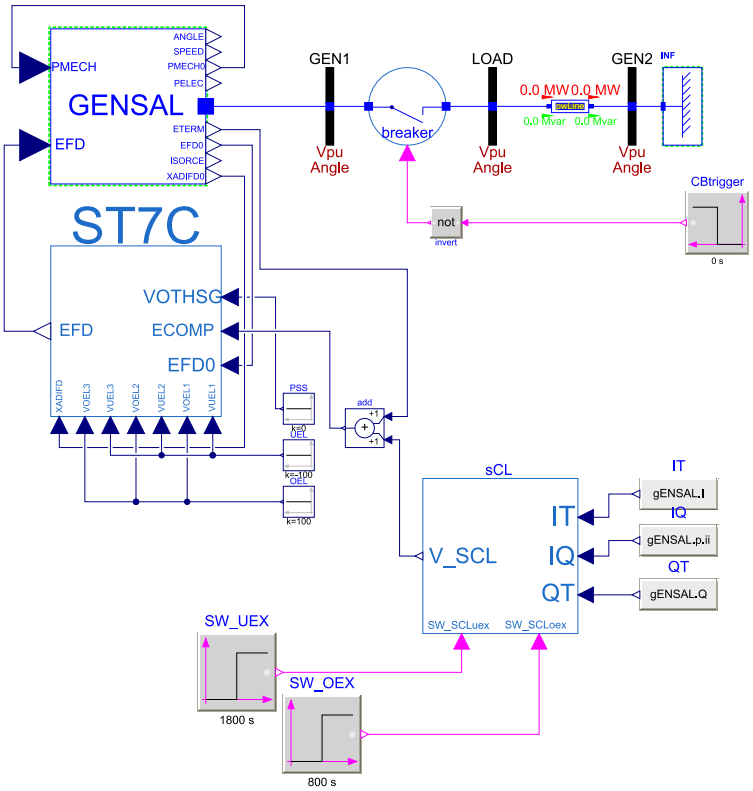

Figure 5.8: Test setup for stator current limiter (SCL) model

Figure 5.9 shows the performance of SCL during the overexcited region, where the solid lines illustrate reactive power controller performance while the dashed lines illustrate reactive current controller performance. Both controllers are simulated with similar parameters, except that each controller's proportional and integral gain are tuned separately to secure proper stator current limitations. Note that, during the reactive power controller simulation test, the PID controller is tuned with proportional gain K_{Poex} and integral gain K_{Ioex}, $0.0025\,pu$, and $0.0025/1.50\,pu/s$, respectively, which is quite different from the value of the parameter in Appendix F. The overexcited region's output is enabled at 800 s, whereas the underexcitation region's output is enabled at 1800 s. The stator current limiter output V_{SCL} is reduced immediately after the overexcitation output is enabled and causes the field voltage to be reduced. As a consequence, the reactive power or current output of the generator reduces, thereby the generator terminal current I_T to reduced from 1.11 pu towards the threshold value of 1.05 pu, as anticipated. However, enabling the output of the underexcitation region does not cause any reasonable changes. Furthermore, there is a notable difference between the performance of the reactive power and the current controller. As the results show that the reactive power controller reduces the terminal current smoothly; thereby, the overshoot that occurs during the reactive current control is eliminated.

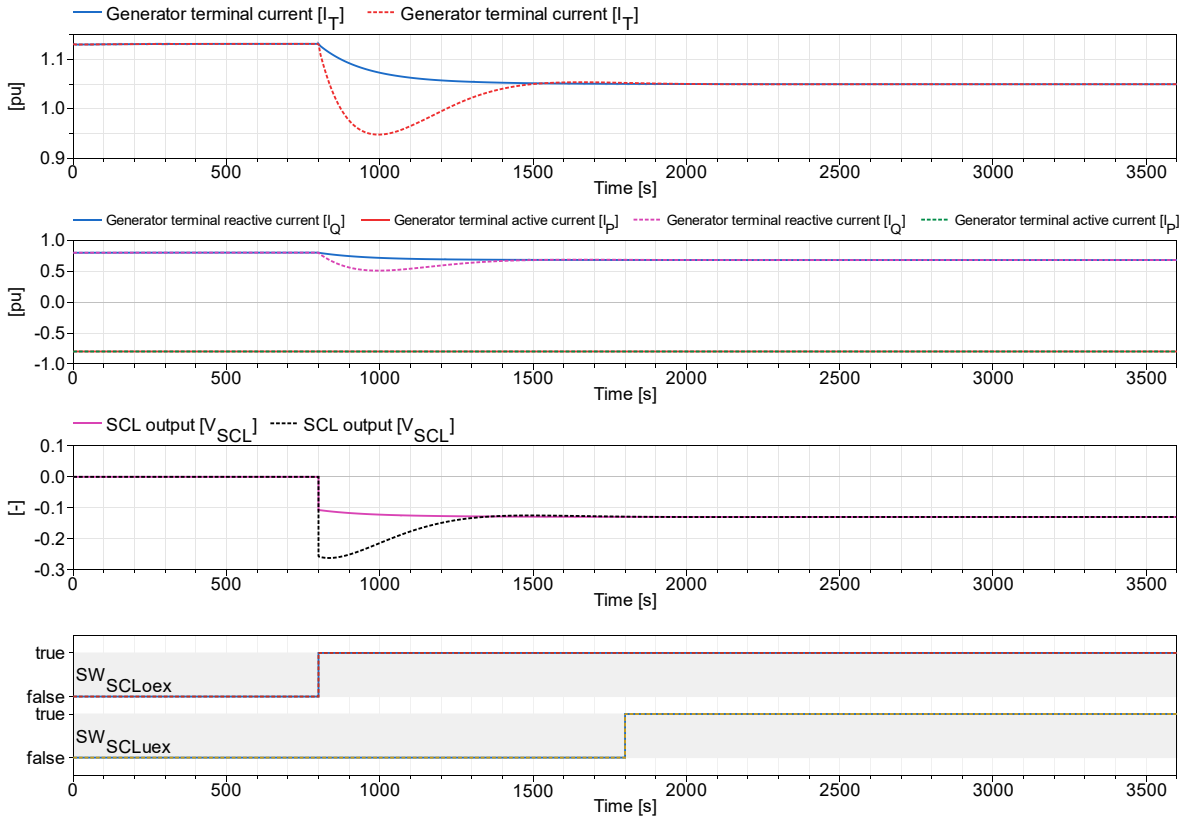

Figure 5.9: Performance of reactive current controller in SCL during the overexcited region. Solid lines: Reactive power controller simulation results, Dashed lines: Reactive current controller simulation results.

The simulation results of the reactive power controller in SCL during the underexcited condition are illustrated in Figure 5.10. The test is performed similarly to the overexcitation simulations when the Boolean signal SW_{UEX} turns "true" at 1800 s, the output V_{SCL} is increased, and causes the reactive power to increase into the overexcitation region. Hence, the SCL overexcitation part takes control of the reactive power and reduces until the terminal current reaches within I_{SCLlim}, as desire. There are some oscillations when the reactive power starts to increase into the overexcitation region as well as when the reactive power is reduced into the underexcitation region. The simulation results of the reactive current controller of SCL during the underexcited condition are not presented due to the random oscillations.

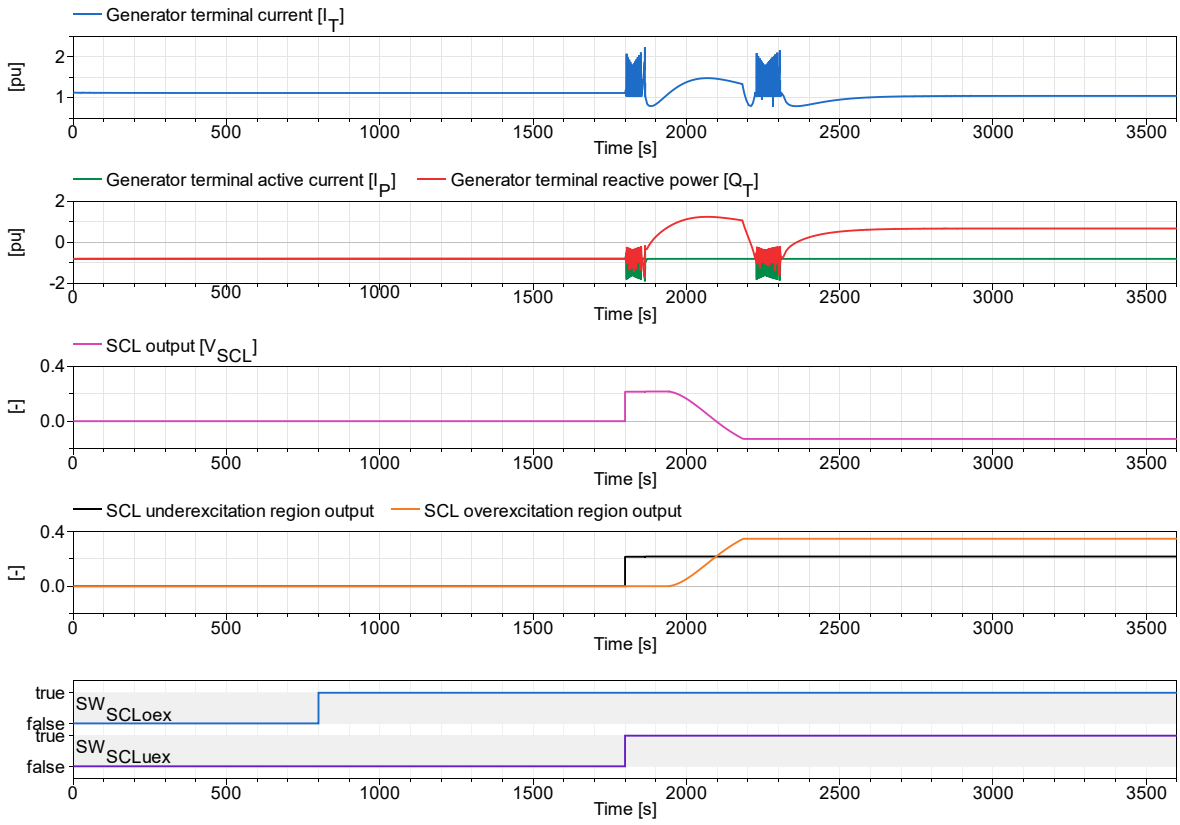

Figure 5.10: Performance of reactive power controller in SCL during the underexcited region

5.2.4 Stator Current Overexcitation Limiter (SCOEL)

The test setup for the stator current overexcitation limiter (SCOEL) is shown in Figure 5.11 with a manually configured switch at the output. The switch changes the position at 1800 s to enable the SCOEL's output to reduce the stator current. As well, the parameters of SCOEL are given in Appendix G. Moreover, P_0 and Q_0 of the GENSAL generator is set to 5 MW and 7 $Mvar$,accordingly.

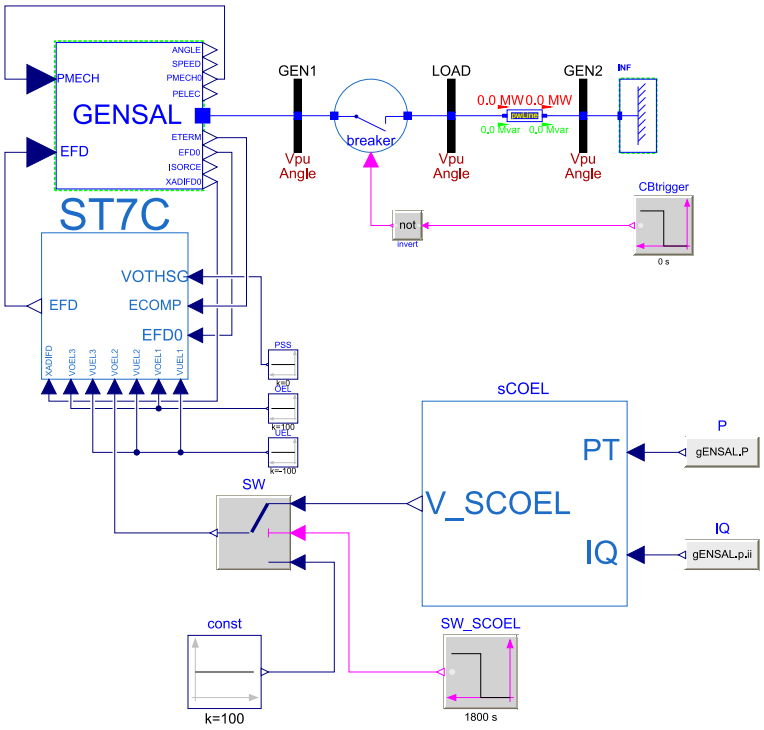

Figure 5.11: Test setup for stator current overexcitation limiter (SCOEL) model

As shown in Figure 5.12, the reactive current I_Q is reached a steady state at roughly 0.59 pu before the limiter output activates. When the limiter is activated, the I_Q is reduced to 0.4 pu according to the active power output, which is at 0.5 pu. Since the output of the limiter can not make any changes in the AVR before 1800 s, the output of the limiter continually reduces until the minimum output limit $V_{SCOELmin}$, which is zero. But after 1800 s, the control signal increases to roughly 1.9, and simultaneously the stator current is reduced to 0.4 pu, as expected.

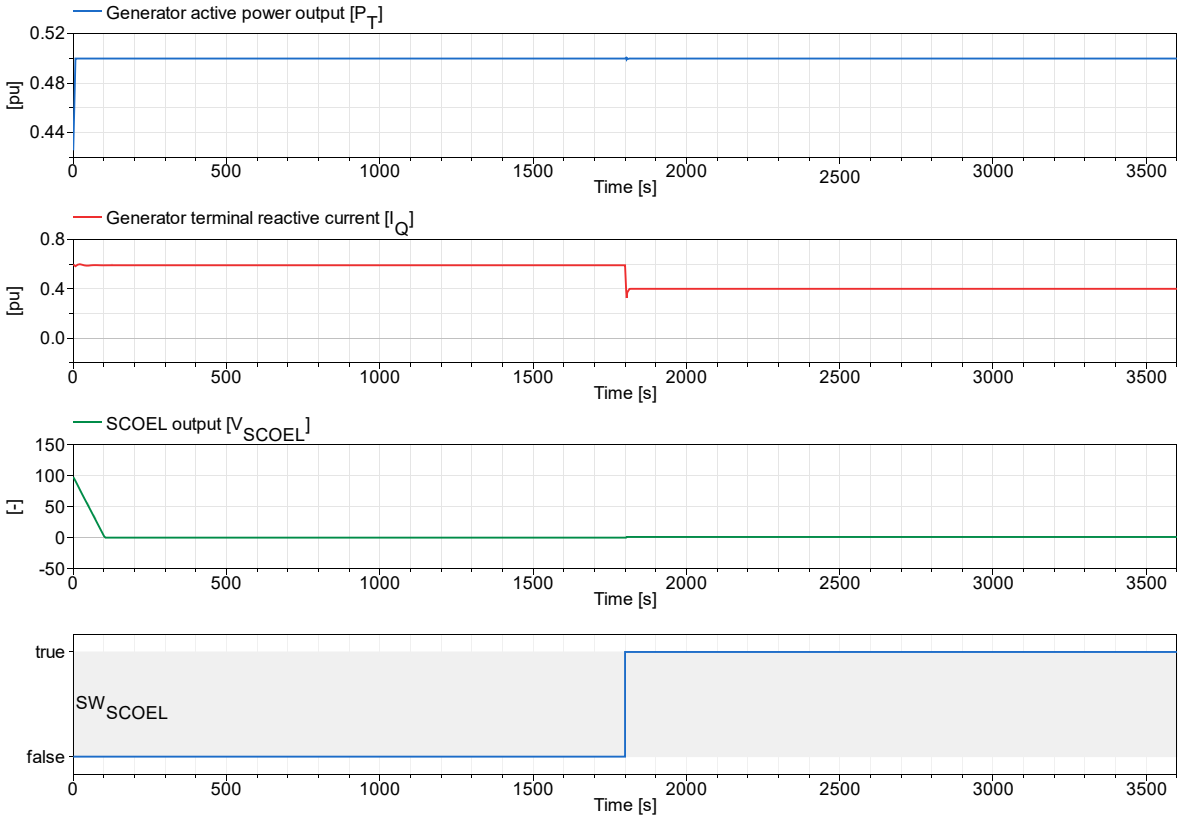

Figure 5.12: Performance of stator current overexcitation limiter (SCOEL) performance

5.2.5 Field Current Underexcitation Limiter (FCUEL)

Figure 5.13 portrays the test setup of field current underexcitation limiter (FCUEL), where the parameters of FCUEL are given in Appendix H. The initial active power and reactive power Q_0 of the generator are set to $P_0 = 5\,MW$ and $Q_0 = -5\,Mvar$, and the FCUEL output is activated at 1800 s. As mentioned in Section 5.2.2, the inputs V_F and V_{FB} are not being used in this thesis, thereby, these are set to constant zero.

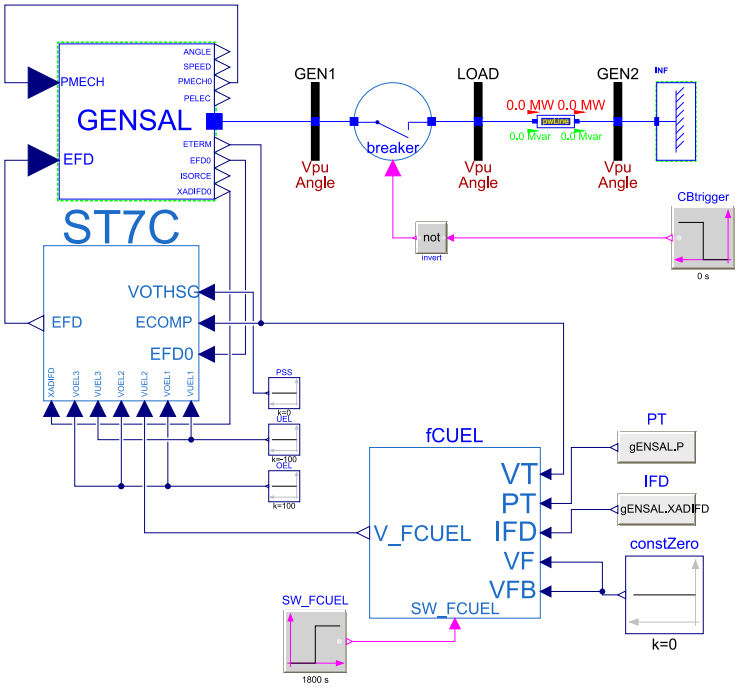

Figure 5.13: Test setup for field current underexcitation limiter (FCUEL) model

The FCUEL is preset with five minimum field current threshold values concerning active power load. According to that, the limiter should be held the field current I_{FD} to 0.78 pu at 0.5 pu active power load P_T. As shown in Figure 5.14, the field current was about 0.71 pu at the initial state (when FCUEL is inactive), and the output signal of the FCUEL is 0.0. Whereas, when the output of the FCUEL is active, the field current is increased to 0.78 pu as well as FCUEL's control signal is stabilized at about 1.0, which is reasonable. As a consequence, there is a notable change in the active power output at 1800 s, as seen in Figure 5.14. However, it can be realized that the change is minor by observing the ordinate.

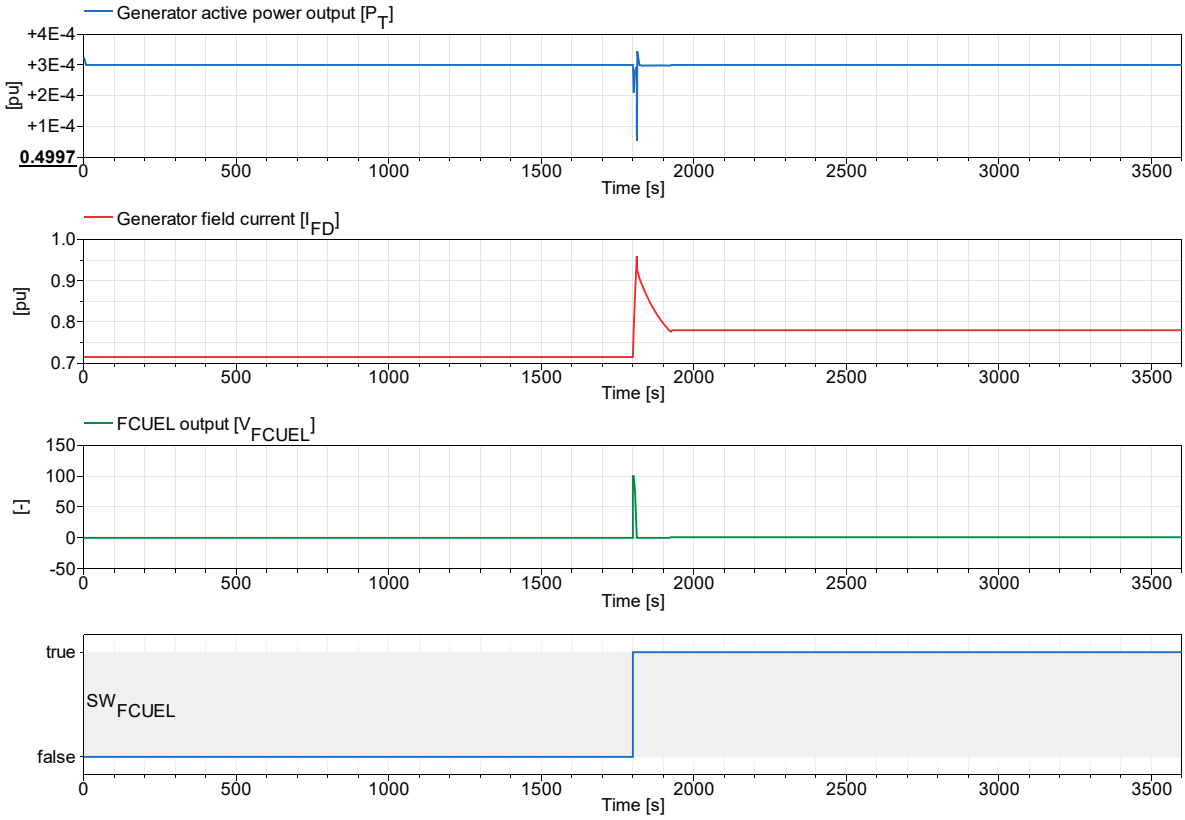

Figure 5.14: Performance of field current underexcitation limiter (FCUEL)

5.2.6 Volts-per-Hertz (V/Hz) Limiter

The test setup of the V/Hz limiter is displayed in Figure 5.15, which has a ramp logic that represents actual frequency and a Boolean signal input that controls the output of the limiter. At 800 s, the Boolean signal turns “true”, so the output of the V/Hz limiter gets enabled, and then at 1800 s, the ramp logic reduces the frequency from nominal frequency 50 Hz to 45 Hz. The V/Hz limiter is parametrized according to Appendix I, and the generator is initialized with parameters $P_0 = 8\ MW$ and $Q_0 = 5\ Mvar$.

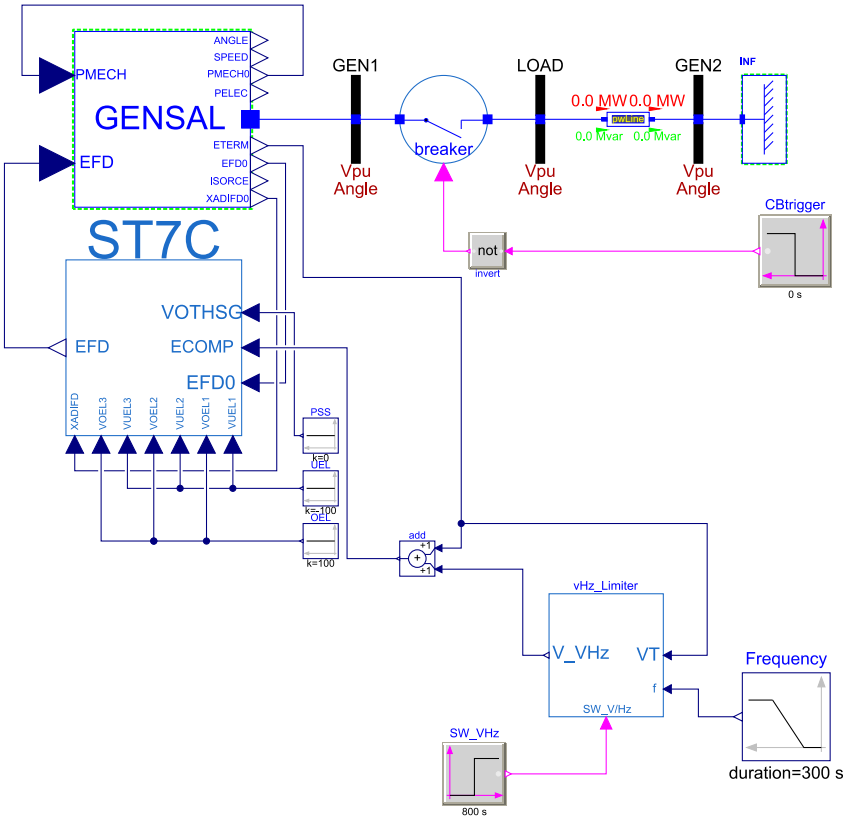

Figure 5.15: Test setup for volts-per-hertz limiter model

Figure 5.16 illustrates the performance of the V/Hz limiter, where the terminal voltage in the steady-state at 1.086 pu before the setpoint changes. When the frequency reduces, the deviation between voltage and frequency will increase above the defined limit. Thus, the limiter's output signal starts to increase. As a consequence, the voltage starts to decrease nicely and stabilized at 0.99 pu as expected.

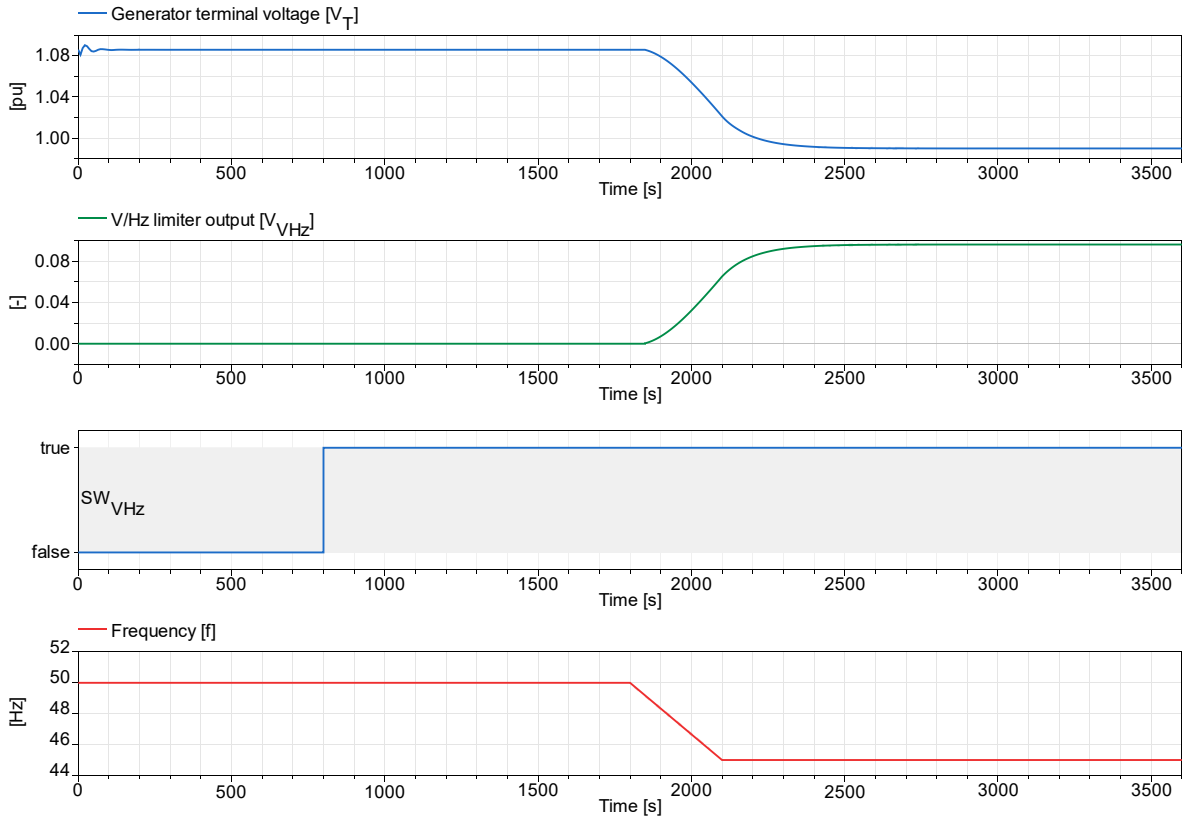

Figure 5.16: Performance of volts-per-hertz limiter

5.3 Voltage Droop/Compensation Controller

A test setup of the voltage droop/compensation controller is portrayed in Figure 5.17. During the test, voltage setpoint V_{Tsp}, reactive current setpoint I_{Qsp}, active current setpoint I_{Psp}, and frequency setpoint f_{sp} are varied to examine the controller. Parameters of the voltage droop/compensation controller are obtained from Appendix J. The simulation is performed individually for each controller by changing the controller's latter setpoints at 1200 s and the voltage setpoint at 2200 s. Also, during all the simulations tests, the initial active power P_0 and reactive power Q_0 of the generator are set to 2 MW and 1 $Mvar$, respectively.

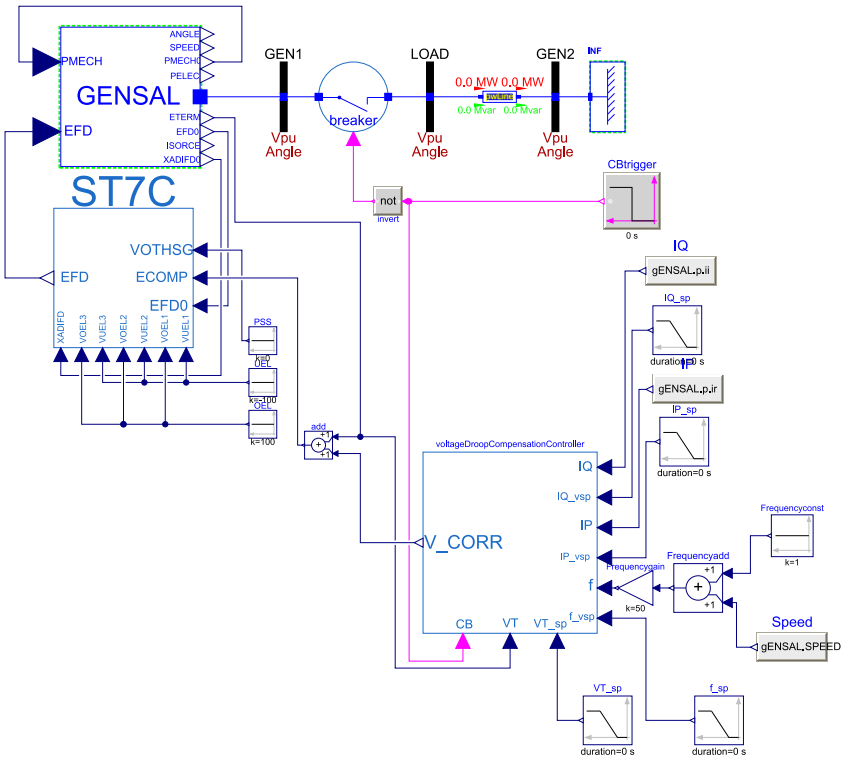

Figure 5.17: Test setup for voltage droop/compensation controller model

5.3.1 Reactive Current Droop and Compensation Controller

There are performed two tests with this controller, first with the droop function and the second with the compensation function. The generator reactive current setpoint I_{Qsp} is changed from zero to 0.5 pu at 1200 s, and the voltage setpoint V_{Tsp} is changed from 1 to 1.05 pu at 2200 s. Initially, the controller starts to influence the AVR to reduce the terminal voltage equal to the predefined voltage setpoint, as shown in Figure 5.18. Please note that when the AVR influences, the field voltage applied to the generator will be affected. Consequently, the reactive power or current output is affected to obtain the desired terminal voltage. Hence, the terminal voltage is stabilized at 1 pu before the I_{Qsp} changes. When the I_{Qsp} changes, the reactive current increases, hence the voltage increases. The stabilized voltage ends up at 1.00748 pu, which is similar to the calculated value. Simultaneously, when the V_{Tsp} increases, there is a significant change in terminal voltage due to an increase in the reactive current. And the deviation between the calculated value and the simulated value is found to be about $1.97 \cdot 10^{-6}$, which is reasonable. Note that the steady-state terminal voltage after a setpoint change can be calculated using Eq. (4.11) to verify the results.

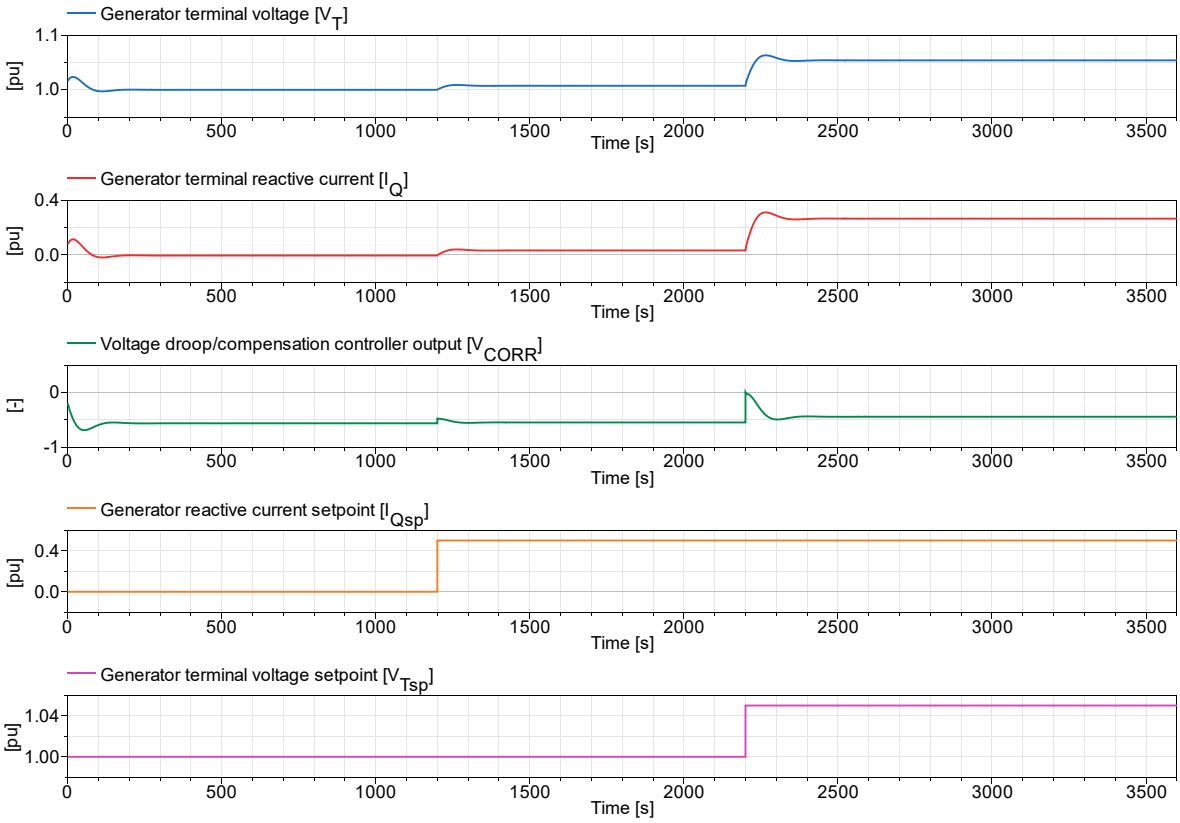

Figure 5.18: Performance of voltage droop/compensation controller when the reactive current droop function is activated.

Since the initial terminal voltage is higher than the preset setpoint, the controller reduces the terminal voltage, as shown in Figure 5.19. And the voltage is finally stabilized at 0.999913 pu before any setpoint changes, which is corresponds to manually calculated terminal voltage using Eq. (4.11). After the increase in the I_{Qsp} at 1800 s, the reactive current and the terminal voltage are decreased to roughly -0.0489 pu and 0.991216 pu, respectively. Whereas change in the V_{Tsp} is causing the voltage to rise again to 1.04533 pu, as expected.

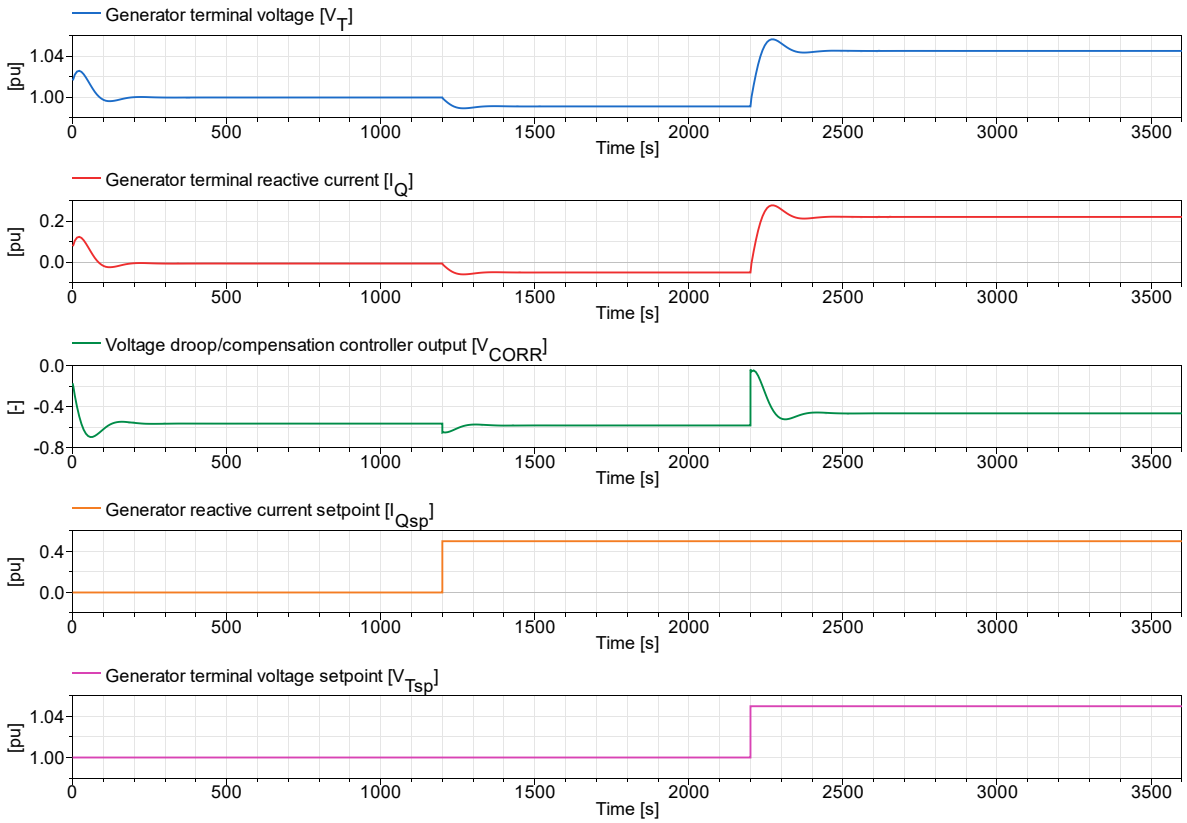

Figure 5.19: Performance of voltage droop/compensation controller when the reactive current compensation function is activated.

5.3.2 Active Current Compensation Controller

The results from the active current compensation controller simulation are presented in Figure 5.20. Where the generator active current setpoint I_{Psp} is changed from 0 to -0.5 pu at 1200 s, and the voltage setpoint V_{Tsp} is changed from 1 to 1.05 pu at 2200 s. At the initial stage, when setpoint at zero, the generator active current output I_P at -0.1996 pu, thus the controller not reacts for the I_P. Rather, it will consider the setpoint as an actual active current output, and it compensates for it because the controller does not operate for any I_P below the setpoint. Thus, the terminal voltage is reduced to 1 pu by regulating the generator's reactive power or current. Later, the setpoint reduces to -0.5 pu, then the controller starts to compensate for the actual active current output. Hence, the I_P is higher than the setpoint, the terminal voltage decreased and stabilized at 0.9952 pu, as expected. As well, when the voltage setpoint increased, as a result, the terminal voltage increased to 1.04496 pu, which is equal to the manually calculated value, where the manually calculated value is acquired by using the Eq. (4.12).

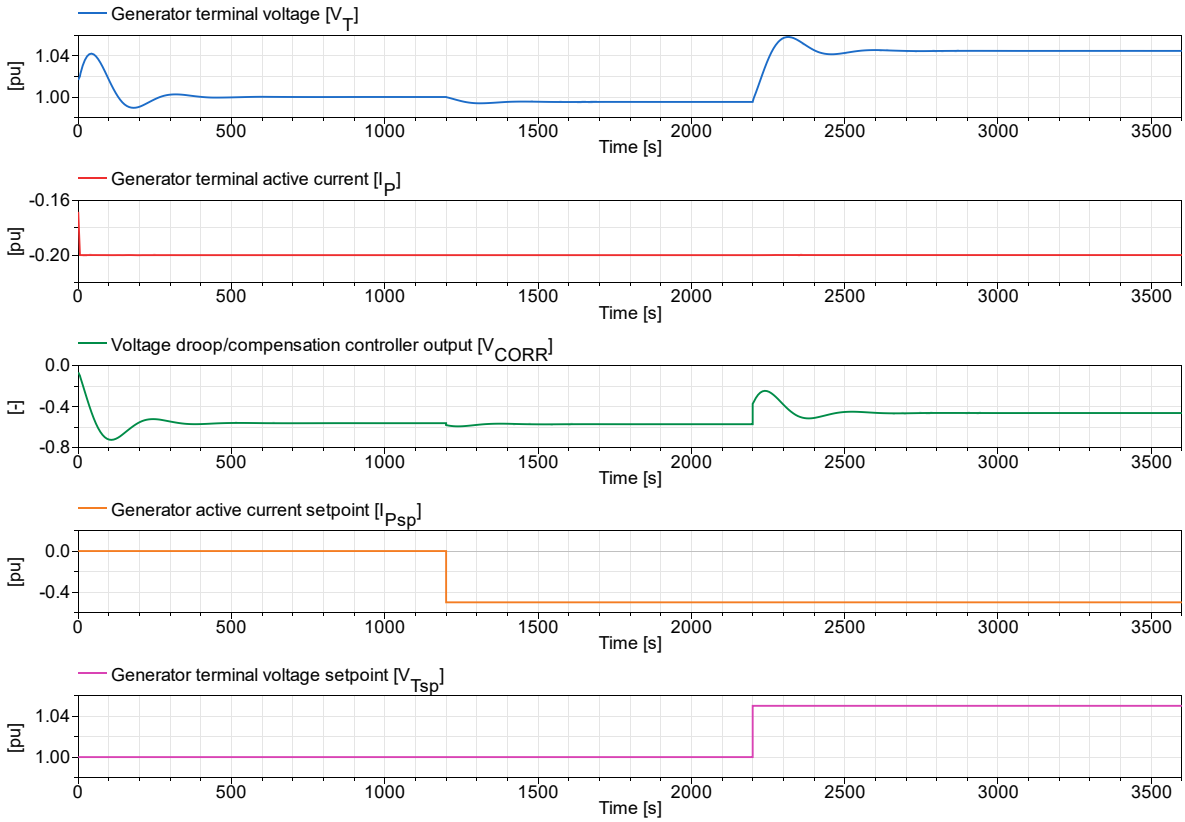

Figure 5.20: Performance of voltage droop/compensation controller when the active current compensation function is activated.

5.3.3 Frequency Droop Controller

Figure 5.21 illustrates the simulation results of the voltage droop/compensation controller using the frequency droop function. Since in the beginning, the nominal frequency and the frequency setpoint is at 50 Hz, and terminal voltage is higher than the V_{Tsp}, the controller, as usual, tries to reduce the voltage to 1 pu. Afterward, when the frequency setpoint is reduced to 48 Hz, consequently the voltage is increased to 1.001 pu as expected. And, when the voltage setpoint V_{Tsp} is increased to 1.05 pu at 2200 s, the terminal voltage arises again and stabilizes at roughly 1.05 pu as desired.

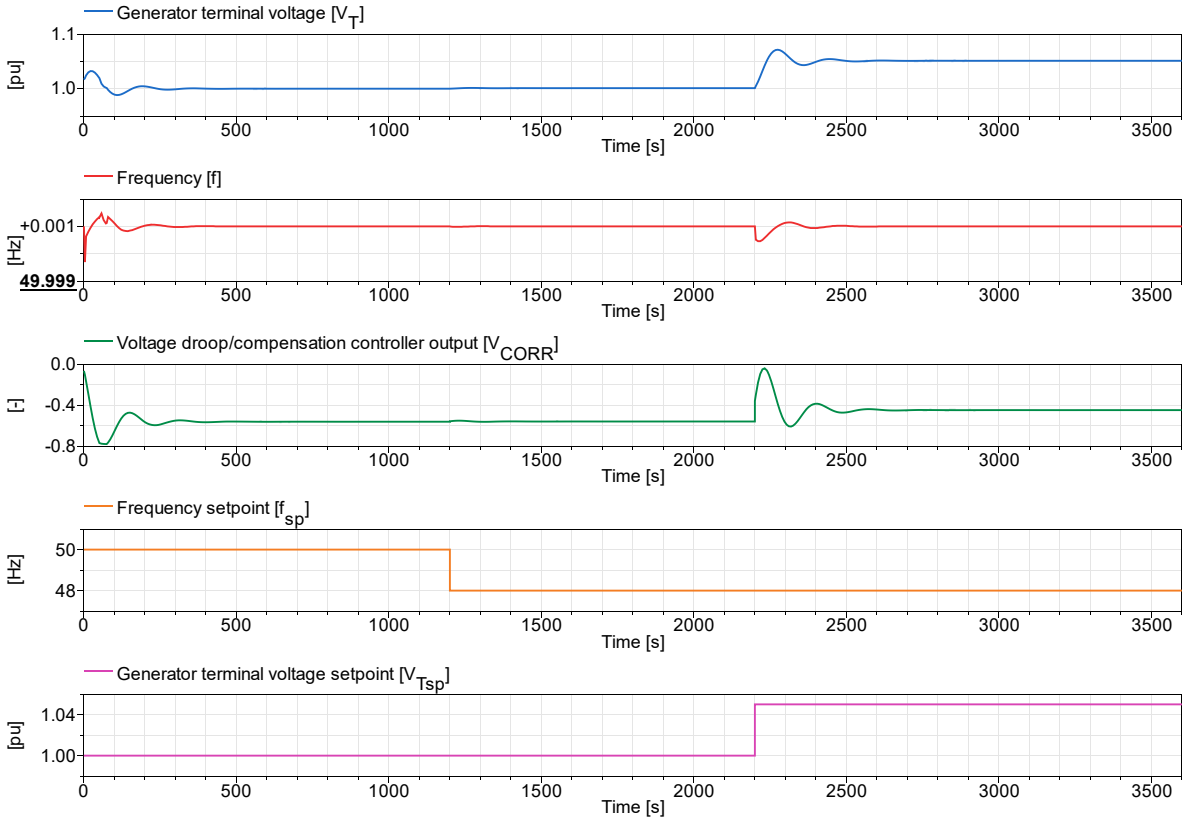

Figure 5.21: Performance of voltage droop/compensation controller when the frequency droop function is activated.

5.4 Reactive Power (VAR) or Power Factor (PF) Controller

The simulation setup for VAR/PF controller model is shown in Figure 5.22. During the simulation, the controller activates at 800 s, later at 2200 s, the power factor setpoint PF_{sp} and reactive power setpoint VAR_{sp} changes. The controller activates by shifting the Boolean signal from the block $SW_{OELUELSCL}$ to "false", to pretend that the OELs or UELs, or SCLs are deactivated. Moreover, the simulation is performed one at a time, first with the PF controller then the VAR controller. Parameters for the VAR/PF controllers are acquired from Appendix K and the initial active power P_0 and reactive power Q_0 of the generator are set to 5 MW and 6 $Mvar$, accordingly. However, in order to clearly visualize the VAR/PF controller's performance, the PF minimum and maximum terminal voltage limit, PF_{VTmin} and PF_{VTmax} and VAR minimum and maximum terminal voltage limit, VAR_{VTmin} and VAR_{VTmax} are set to 0 and 2 pu, respectively, so the terminal voltage can vary between 0 – 2 pu .

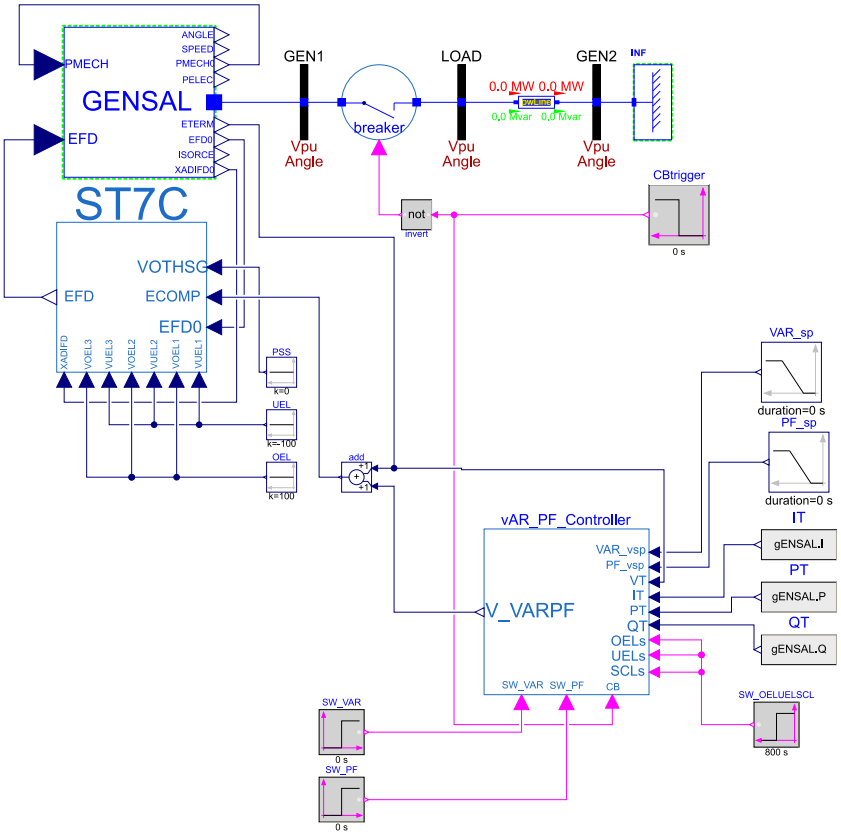

Figure 5.22: Test setup for reactive power/power factor (VAR/PF) controller model

5.4.1 Power Factor Controller

When the PF controller activates, the output of the controller reached the maximum output suddenly. Consequently, there is a slight variation in the active and reactive power output for a particular time. Afterward, the active power P_T is reached back to the original value, and the reactive power Q_T is increased in order to obtain the setpoint power factor (see Figure 5.23). As there is no straightforward way to determine or observe whether the system power factor is changed as expected. Therefore, a plot called "PF error" is shown in Figure 5.23. The PF error plot illustrates the deviation between the system power factor and the power factor setpoint. As depicted in the plot PF error, the error reaches zero right after the controller's output enables.

Further, when the setpoint changes from 32 degrees to 42 degrees, it corresponds to the power factor approximately from 0.85 to 0.74. Consequently, the generator's reactive power output is reduced, as predicted. And the reactive power is stabilized at around 1.88 pu; simultaneously, the error also reached nearly zero.

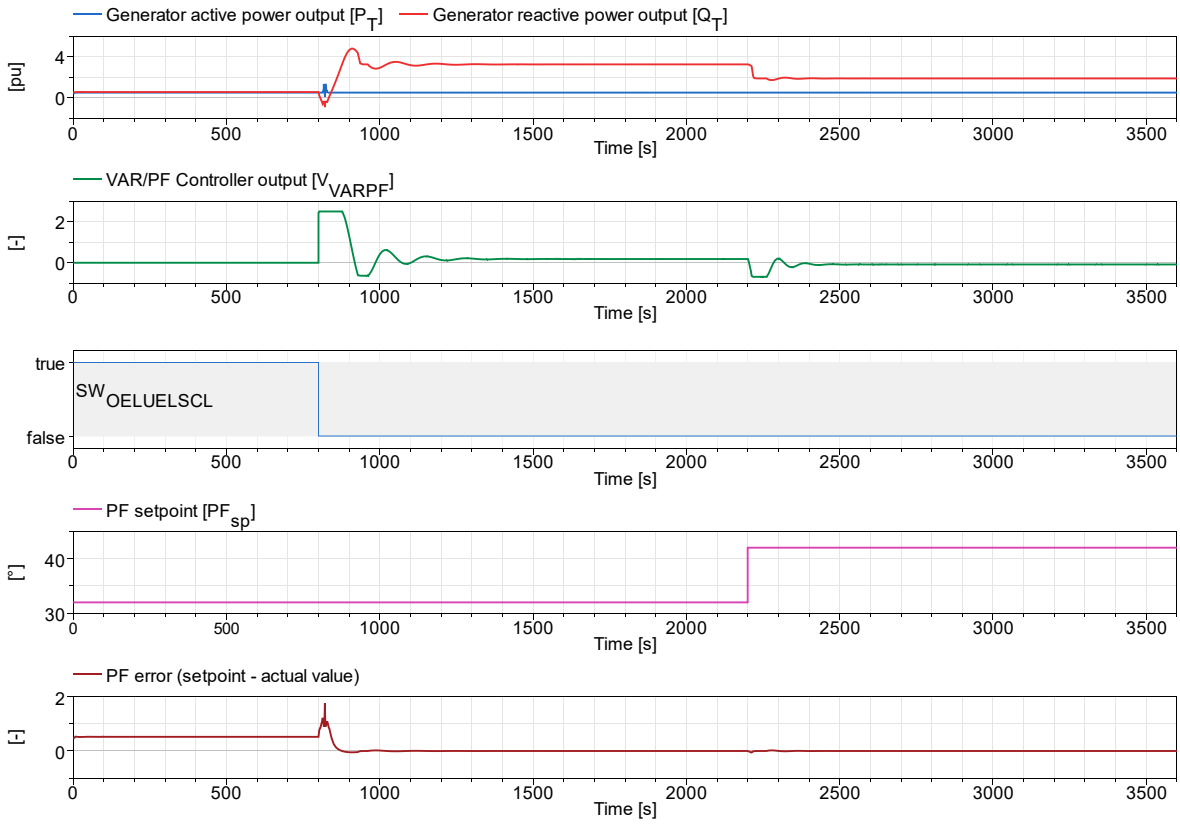

Figure 5.23: Performance of VAR/PF controller when the power factor control function is activated.

5.4.2 Reactive Power Controller

Initially, the reactive power setpoint is set to -0.4 pu, while the actual generator reactive power output was more or less at 0.46 pu as shown in Figure 5.24. When the reactive controller is activated, the reactive power pulls down smoothly to the setpoint, as desire. Likewise, when the setpoint is changed to 0.4 pu, the controller increases the field voltage to increase the reactive power. There are some micro oscillations in the control signal during the stabilizing, which is not well visible in the plot.

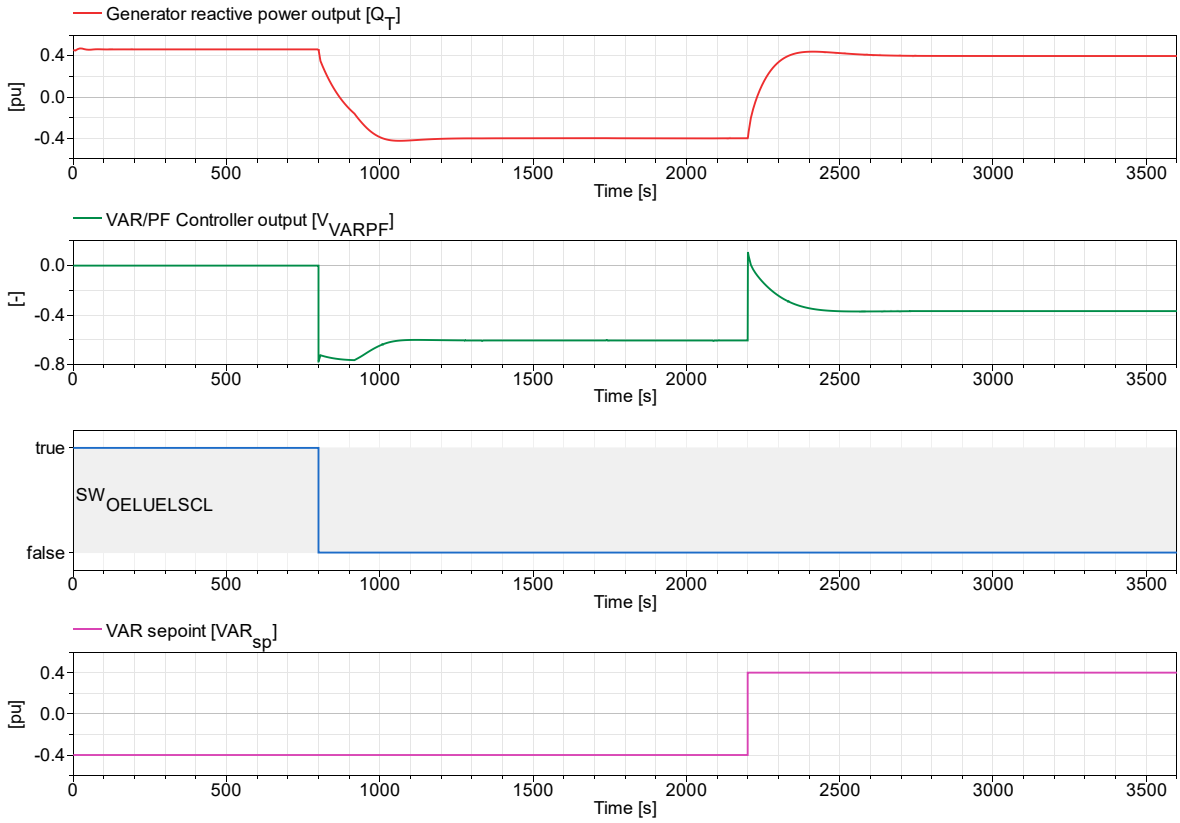

Figure 5.24: Performance of VAR/PF controller when the reactive power control function is activated.

6 Discussion

This thesis aims to make a digital twin of the excitation control system in the hydropower controller HYMAREG 10. The excitation control system is modeled mainly based on HYMAREG 10's user manual [22] and the information and the instructions from the manufacturer and the supervisor. According to their advice, protective limiters and VAR/PF controller are fundamentally modeled based on IEEE Std 421.5-2016 [14] with additional functionalities implemented in the HYMAREG 10. However, due to modeling purposes and complexities, the models have been modified a bit. The excitation system, type *ST7C*, is obtained from the OpenIPSL library, and the V/Hz limiter is modeled based on Kundur [13]. During this thesis, the Hogstad power plant's commissioning test data was provided by Hymatek Controls AS. Also, they provided scaling factors to convert the actual HYMAREG 10 AVR parameters from the Hogstad commissioning report to the *ST7C* model parameters to represent the actual controller.

6.1 Generator

The generator's data was given by the Skagerak Kraft AS. However, to parametrize the GENSAL generator model to represent the real generator in the Hogstad power plant, the parameters given were not enough. Therefore, some estimations are made to determine all the parameters for the generator model as described in Section 4.1.1. Despite this, the generator produced random oscillations during the simulation. This is turned to be because of the estimated significant armature resistance R_a. Thus, the R_a is set to zero in order to eliminate the unwanted oscillations.

6.2 Test Grid

Since this thesis's primary focus is to model the excitation control system, the test setup modeling is kept simple as possible to analyze the modeled excitation control system's performance. However, it should be properly modeled in the future for better examination of the model's performance.

6.3 Excitation System

A function called manual modus is implemented in the HYMAREG 10 that takes over the control when the AVR fails. Since this thesis focus on automatic control of field voltage or field current, the function is chosen not to be modeled.

The AVR in the actual HYMAREG 10 has some additional functionality, such as disconnecting the field flash, rectifiers firing angle limiter, fast synchronization, ramp-up or down to the specific voltage after synchronization, and the AVR follows grid voltage during the idle mode are not implemented in the model due to modeling complexity and time restriction.

By comparing the voltage step response results of the model and the real excitation system shown in Figure 5.2 and Figure 5.3, the model has a very slow response and a considerable overshoot compared to the real data. Since the parameters and the scaling factors of excitation systems are given by the manufacturer, the likelihood of the inaccurate performance of the excitation system is considered low. But the possible issue could be uncertainties in the

estimation of the generator's parameter. Thus, it has been considered that the simulation results of the models are relatively slower than the actual controller's and the limiter's behavior.

6.4 Limiters

According to IEEE Std 421.5-2016 [14], the lead-lag function in FCOEL, SCUEL, SCOEL, and FCUEL disables by setting their time constants to zero. However, it causes errors during the simulations. Thus, those time constants are set to constant epsilon to be able to simulate. Despite this, the simulations failed randomly. This problem is solved by adding the switches to bypass the control signal from the PID controller to the output.

A PID controller is implemented in all the limiters, even if it is not stated in IEEE Std 421.5-2016 [14], in order to provide the user access to tune the controller's output properly.

Fundamentally in HYMAREG 10, the SCUEL, SCOEL, and FCUEL using stator active current to determine the reactive current or field current limits. But the models in this thesis use active power instead of current since the active power is equivalent to the current and is in a positive value, which is a reasonable assumption. Besides, the actual controller's parameters are given in percentage, but it is chosen not to implement in the models to avoid confusion during the modeling and parameterization.

According to IEEE Std 421.5-2016 [14], one of the FCOEL inputs could be generator field voltage E_{FD} as described in Section 4.4.1, but during the simulations, using the E_{FD} as an input cause simulation error. The reason could be that in the FCOEL model, the signal I_{act} obtained from the input and connected to the output, causing algebraic loop. But the simulation error may be eliminated by adding a delay in the signal I_{act} or at the input.

In the SCOEL model, voltage-dependent characteristic, adjustable gain reduction K_{adj}, and inputs V_T, V_F and V_{FB} are removed compared to the model *UEL2C* to keep the model as simple as possible and assure that underexcitation limiters characteristics are not included. Similarly, the calculation of K_{adj} is removed in the FCUEL model compared to the reference *UEL2C* because using field current instead of reactive current may lead to a wrong calculation of the gain.

The inputs V_F and V_{FB} in the SCUEL and FCUEL models are not used during the simulation due to the lack of corresponding outputs in the excitation system *ST7C* model. But, to examine the behavior of these models, an *ST7C* model needs to be adapted to add the V_F and V_{FB} outputs. Also, the voltage bias logic and equation blocks F_1 and F_2 in the SCUEL and FCUEL model are disabled during the simulation because it has been considered that the effect of the voltage terminal is not necessary to compare the HYMAREG 10 functionalities.

The V/Hz limiter model is fundamentally modeled based on Kundur [13], as described in Section 4.4.6. However, simulation results showed that the model's behavior was not desirable. Hence, the lead-lag function of the limiter was replaced by the PID controller, and the gain blocks were removed to get a similar theoretical behavior as HYMAREG 10 controller. The V/Hz limiter in the HYMAREG 10 has a control function that cuts the field voltage when the frequency drops below half of the nominal frequency. But it is not a feasible operation during the simulation because when the field voltage to the generator cuts off instantaneously, it will lead to simulation error.

The overall behavior of all the models was reasonable, but in order to compare the simulation results with the measurement data, there are not enough tests have been performed during the

commissioning. Therefore, only the voltage step response is recreated in this thesis, and the rest of the excitation control models are mainly tested to verify their performance.

Be aware that the proportional and integral gains of the FCOEL and FCUEL are quite high. The reason is not clear yet. However, the model works as desire.

There are some oscillations when the reactive power starts to increase into the overexcitation region as well as when the reactive power is reduced into the underexcitation region (see Figure 5.10). The reason could be that the test grid is not adequately modeled in order to tackle the high current underexcitation operation. The simulation results of the reactive current controller of SCL during the underexcited condition are not presented in Section 5.2.3 due to the random oscillations for the same reason. The SCL model should be further analyzed in the future with a proper grid model to avoid unwanted oscillations. Further, by reflecting on the SCL's simulation results, the power controller may be the desired controller since it has the advantage of time delay and deadband, also work smoothly. However, better and smooth control of the reactive current controller could be achieved by better tuning of the PID controller.

For the overvoltage scenario, no simulation test of the V/Hz limiter has been performed. It was considered that the model behaves almost identical to the results as presented in Figure 5.16 in Section 5.2.6. For the future, the simulation test for the overvoltage scenario can be performed to verify the assumptions.

Most of the limiter and controller models have a switch at the output to disable the control function. These switches are used to enable the output during the simulation, which results in a sudden change in the control signal. This sudden increase in the control signal also impacted, for example, field current, active power, or reactive power output. The main reason might be explained that the PID controller pushed the maximum control signal to the output, and the output signal does not make any changes in the system. Therefore, when the switches enable the outputs, the maximum control signal is applied instantaneously. One possible way to fix this problem is by adding a self-reset function for the PID controller to reset when the output is re-enabled.

6.5 Voltage Droop/Compensation Controller

In the real HYMAREG 10 excitation controller, the voltage droop/compensation control function is inherent in AVR that influences the reference. Since the AVR is inherent in the excitation system *ST7C* model, this controller is modeled separately with a separate PID controller for each control function.

The overall behavior of the model was reasonable to compare to the theoretical behavior. However, to compare the simulation results with the measurement data, no voltage droop/compensation controller tests were performed during the commissioning, and it should be tested to verify the model performance.

The controller models have a switch at the output to disable the control function. And these switches may cause a sudden increase in the control signal, consequently, overshoot in terminal voltage output. It can be eliminated by adding a self-reset function for the PID controller to reset when the output is re-enabled.

6.6 Reactive Power (VAR) or Power Factor (PF) Controller

The VAR/PF controller in the actual HYMAREG 10 controller can be set to different modus, such as disabled, intermittent operation, continuous operation, and always ON. However, the modeled VAR/PF controller in the thesis contains essential functions from the latter modus, but changing the different modus is not modeled due to time restrictions.

And this controller fundamentally has a PI controller according to IEEE Std 421.5-2016 [14], but the model is implemented with a PID controller to provide the user access to tune the controller's output properly.

The reactive power controller parameters are given in percentage, but it is chosen not to implement in the models to avoid confusion during the modeling and parameterization.

The switches SW_{VAR} and SW_{PF} enables the output during the simulation, which may cause a sudden change in the control signal that leads to some influence in, i.e., active power or current. However, it can be eliminated by adding a self-reset function for the PID controller to reset when the output is re-enabled.

The performance of the VAR/PF controller model during the simulations was reasonable, comparing the theoretical behavior. However, different tests with the real HYMAREG 10's VAR/PF controller should be performed to verify the model performance. Note that some minor oscillations in the control signal during the stabilizing period are tough to observe in Figure 5.23 and Figure 5.24. The reason could be explained that the test grid does not perform as desire.

7 Conclusions and Future Work

7.1 Conclusions

During this study, the excitation control system of the real-life hydropower controller, HYMAREG 10, is mainly object-oriented modeled in Modelica modeling language using Dymola software. The control system models are fundamentally modeled based on functionalities of the HYMAREG 10 [22]with the reference to IEEE Std 421.5-2016 [14].

The excitation control system in the HYMAREG 10 consist of an automatic voltage regulator (AVR), field current overexcitation limiter (FCOEL), stator current underexcitation limiter (SCUEL), stator current limiter (SCL), stator current overexcitation limiter (SCOEL), field current underexcitation limiter (FCUEL), volts-per-hertz (V/Hz) limiter, voltage droop/compensation controller, and reactive power (VAR) or power factor (PF) controller. All these controllers and the limiters were modeled separately from scratch, except the AVR, obtained from the external library OpenIPSL. Later, these models were fitted together into the finished model. The models mentioned above were simulated separately and then compared to these controller's and limiter's theoretical behavior, while the AVR was compared with the actual data from commissioning from the Hogstad power station.

In conclusion, all the models performed as desired but still need proper tuning and further development to enhance the performance. As well, there are a few functionalities that are missing compared to the actual controller. In the future, real power plant data with essential tests of the controllers and the limiters are necessary in order to verify the model's behavior.

7.2 Future Work

From the modeling point of view, the V/Hz limiter should be modeled with the field voltage cutoff function when the nominal frequency drops below a certain value. Also, the AVR and VAR/PF controller with the different operating modus should be implemented in the future. Besides, additional functionalities such as field flash disconnector, rectifiers firing angle limiter, fast synchronizer, the specific voltage after synchronization, voltage monitoring during the idle mode should be modeled for proper representation of the HYMAREG 10. Further, the excitation control system should be combined with other control functions such as a water-level controller to obtain a complete hydropower controller. More importantly, a more complex grid model is crucial to properly simulate and examine the performance of the excitation control system model.

From the simulation point of view, the generator needs to be accurately parameterized with respect to the real generator to obtain similar behavior as a real generator. Lastly, in the real power plant with HYMAREG installed, as Hogstad power plant should perform some tests on the controllers and the limiters to recreate similar tests during the simulation to compare the simulations results with the real power plant behavior in order to verify the models.

Bibliography

[1] Jonatan Hellborg, K. Bhusal, and T. Tollefsen, 'Modelling of a hydro power control unit in Modelica', University of South-Eastern Norway, Nov. 2020.

[2] Statkraft AS, 'Hydropower | Statkraft'. https://www.statkraft.com/what-we-do/hydropower/ (accessed Mar. 18, 2021).

[3] Noregs vassdrags- og energidirektorat (NVE), 'Vannkraft - NVE'. https://www.nve.no/energiforsyning/kraftproduksjon/vannkraft (accessed Mar. 19, 2021).

[4] Noregs vassdrags- og energidirektorat (NVE), 'Små vannkraftverk - NVE'. https://www.nve.no/konsesjonssaker/konsesjonsbehandling-av-vannkraft/sma-vannkraftverk (accessed Mar. 19, 2021).

[5] M. Rotilio, C. Marchionni, and P. De Berardinis, 'The Small-Scale Hydropower Plants in Sites of Environmental Value: An Italian Case Study', *Sustainability*, vol. 9, no. 12, p. 2211, Nov. 2017, doi: 10.3390/su9122211.

[6] Khaled Aleikish, Okbe Kifle Habte, and Hector Camilo Zambrano Hernandez, 'Modelling of a small hydropower system in Modelica', University of South-Eastern Norway, Nov. 2019.

[7] Hector Camilo Zambrano Hernandez, 'Dynamic Modelling of the Sølia Hydropower System Using Modelica', p. 83.

[8] Hymatek Controls AS, 'Hymatek Controls'. https://www.hymatek.no/ (accessed Mar. 21, 2021).

[9] Hymatek Controls AS, 'HYMAREG 10'. http://www.hymatek.no/produkter/hymareg/ (accessed Mar. 21, 2021).

[10] Skagerak Kraft AS, 'Hogstad'. https://www.skagerakkraft.no/hogstad/category1352.html (accessed Apr. 11, 2021).

[11] S. J. Chapman, *Electric machinery fundamentals*, 5th ed. New York: McGraw-Hill, 2012.

[12] EIA-Technology for volt and current, 'Synchronous generator interview questions with answer', *EIA-Technology for Volt & Current*, Feb. 02, 2018. https://sksinghei.blogspot.com/2018/02/synchronous-generator-interview.html (accessed Jan. 12, 2021).

[13] P. Kundur, N. J. Balu, and M. G. Lauby, *Power system stability and control*. New York: McGraw-Hill, 1994.

[14] IEEE Power and Energy Society, 'IEEE Recommended Practice for Excitation System Models for Power System Stability Studies', *IEEE Std 4215^{TM}-2016 Revis. IEEE Std 4215-2005*, p. 207, Aug. 2016, doi: 10.1109/IEEESTD.2016.7553421.

[15] Pterra Consulting, 'Approaches to Complying with NERC Standard PRC-019-2 on the "Coordination of Generating Unit or Plant Capabilities, Voltage Regulating Controls, and Protection"', Jan. 30, 2017. https://www.pterraph.com/nerc-compliance/approaches-

to-complying-with-nerc-standard-prc-019-2-on-the-coordination-of-generating-unit-or-plant-capabilities-voltage-regulating-controls-and-protection/ (accessed Jan. 11, 2021).

[16] Science Guru, 'Elements of excitation system', *Physics (PHY)*. https://www.scienceguru.co.in/subject.aspx?id=2&code=7EE5A&unitid=22&topicid=104 (accessed Jan. 12, 2021).

[17] REIVAX, 'What is an Excitation System? - Reivax North America', *REIVAX*. https://www.reivax.com/us/what-is-an-excitation-system/ (accessed Jan. 13, 2021).

[18] S. Tsegaye and K. A. Fante, 'Analysis of Synchronous Machine Excitation Systems: Comparative Study', *Int. J. Energy Power Eng.*, vol. 10, no. 12, p. 5, 2016.

[19] Gayathri K, 'Classification of Excitation System | Power Plants', *Engineering Notes India*, Dec. 07, 2017. https://www.engineeringenotes.com/power-plants-2/equipment/classification-of-excitation-system-power-plants/29729 (accessed Jan. 13, 2021).

[20] T. Wildi, *Electrical machines, drives, and power systems*, 5. ed., International ed. Upper Saddle River, NJ: Pearson Education, 2002.

[21] ElProCus, 'Excitation System: Types, Elements, Advantages & Disdvantages', *ElProCus - Electronic Projects for Engineering Students*, Feb. 22, 2020. https://www.elprocus.com/what-is-an-excitation-system-types-and-its-elements/ (accessed Jan. 13, 2021).

[22] Hymatek Contols AS, 'Aggregatregulator HYMAREG 10 Brukermanual', Jan. 2007.

[23] Statnett SF, 'Nasjonal Veileder for Funksjonskrav i kraftsystemet', 19/01229-50. [Online]. Available: https://www.statnett.no/contentassets/6898d191962944518333e8343dfd7b33/19-01229-50-2-nasjonal-veileder-for-funksjonskrav-nvf-2020---vedlegg-til-retningslinjer-fos--14---oversendt-rme-for-godkjenning.pdf.

[24] Modelica Association, 'Language Specification', Version 3.5, Feb. 2021. [Online]. Available: https://specification.modelica.org/.

[25] Modelica Association, 'Modelica Libraries — Modelica Association'. https://www.modelica.org/libraries (accessed Apr. 19, 2021).

[26] Modelica Association, 'Modelica Language — Modelica Association'. https://www.modelica.org/modelicalanguage (accessed Feb. 28, 2021).

[27] Dymola, 'Multi-Engineering Modeling and Simulation - Dymola product line'. https://www.3ds.com/products-services/catia/products/dymola/key-advantages/ (accessed Feb. 28, 2021).

[28] L. Vanfretti, T. Rabuzin, M. Baudette, and M. Murad, 'iTesla Power Systems Library (iPSL): A Modelica library for phasor time-domain simulations', *SoftwareX*, vol. 5, pp. 84–88, 2016, doi: 10.1016/j.softx.2016.05.001.

[29] ABB Energi AS, 'Technical data'. Skagerak Kraft AS, 1993.

[30] ABB Energi AS, 'Test report', Hogstad Kraftstasjon, 9.1, Oct. 1993.

[31] Skagerak Energi AS, ‘Besøkskraftverk - Skagerak Energi’. https://www.skagerakenergi.no/besokskraftverk/category1563.html (accessed Mar. 17, 2021).

[32] PSS®E, ‘Model Library - PSS®E 33.12.1’, p. 729.

[33] F. A. Haugen, *Automatic Control*. Porsgrunn, 2019.

[34] Hymatek Controls AS, ‘Idriftsettelsesrapport, Aggregatregulator HOGSTAD KRAFTSTASJON, aggregat 1’, ARN2019-026.

[35] P. Schavemaker and L. Van der Sluis, *Electrical power system essentials*. Chichester, England ; Hoboken, NJ: Wiley, 2008.

Appendices

Appendix A: Master's Thesis Description

Appendix B: Summary of Estimated Parameters for 10 (Confidential)

Appendix C: Excitation *System* (*ST7C* Model) Parameters (Confidential)

Appendix D: Field Current Overexcitation Limiter (FCOEL) Parameters (Confidential)

Appendix E: Stator Current Underexcitation Limiter (SCUEL) Parameters (Confidential)

Appendix F: Stator Current Limiter (SCL) Parameters (Confidential)

Appendix G: Stator Current Overexcitation Limiter (SCOEL) Parameters (Confidential)

Appendix H: Field Current Underexcitation Limiter (FCUEL) Parameters (Confidential)

Appendix I: V/Hz Limiter Parameters (Confidential)

Appendix J: Voltage Droop/Compensation Controller Parameters (Confidential)

Appendix K: Reactive Power (VAR) or Power Factor (PF) Controller Parameters (Confidential)

Appendix L: FCOEL Activation Logic Code

Appendix M: FCOEL Ramp Rate Logic Code

Appendix N: FCOEL Timer Logic Code

Appendix O: SCL Delayed Reactive Power Logic

Appendix P: SCOEL Activation Logic Code

Appendix Q: PF Normalizer Code

Appendix R: PF Setpoint Normalizer Code

Appendix S: PF/VAR Controller Logic Code

Appendix A: Master's Thesis Description

University of South-Eastern Norway

Faculty of Technology, Natural Sciences and Maritime Sciences, Campus Porsgrunn

FMH606 Master's Thesis

Title:
Extending the automatic voltage regulation of hydropower turbine controller in Modelica

USN supervisor: Dietmar Winkler

External partner: HYMATEK controls, Asgeir Åsnes (asgeir.aasnes@hymatek.no)

Task background:

Hymatek Controls AS is a part of the Rainpower group (www.rainpower.no). It is a specialist company that employs over 30 dedicated workers and is committed to maintain Norwegian expertise with the fields of turbine governing and excitation.

During the autumn semester of 2020 the Master Project group MP-07-20 worked on a Modelica based implementation of the HYMAREG® 10 controller. The focus then was on the turbine governor with water level control and synchronisation sequence.

Task description:

As part of the Master's Thesis the previously implemented hydropower controller is to be extended with voltage regulation parts. As template of the unit the existing HYMAREG® 10 controller should be used.

Tasks:

1. Investigate the functionality of a typical hydro power control unit for small hydro power systems especially wrt voltage regulation.
2. Make yourself familiar with the excitation options as offered by the HYMAREG 10
3. Create a typical power system model in Modelica using the OpenIPSL(openipsl.org) in order to serve as a test bench for the voltage regulation functionality of the hydropower controller.
4. Model, implement and simulate a hydro power control unit with the following functionalities of the automatic voltage regulation:
    a. Current regulation and limitation
    b. Active and reactive power control (droop and compensation)
    c. V/f limitation
    d. Power factor control (if time allows)
5. Test the model for different operation scenarios and test against empirical data provided by the external partner.
6. Document the models.
7. Optionally look into the possibility to run the model via Python using OMPython in order to integrate with a Python based user interface.

Student category: EPE

The task is suitable for online students (not present at the campus): Yes

Practical arrangements: Access to needed software and licenses is given.

Supervision:
As a general rule, the student is entitled to 15-20 hours of supervision. This includes necessary time for the supervisor to prepare for supervision meetings (reading material to be discussed, etc).

Signatures:

Supervisor (date and signature):

2021-01-26 D. Dietz

Student (write clearly in all capitalized letters):

LUXSHAN MANORANJAN

Student (date and signature):

26.01.2021

Appendix B: Summary of Estimated Parameters for 10 MVA Machine

Parameters	Description	Values	Units
M_b	Machine base power	-	MVA
T'_{d0}	d-axis transient open-circuit time constant	-	s
T''_{d0}	d-axis sub-transient open-circuit time constant	-	s
T''_{q0}	q-axis sub-transient open-circuit time constant	-	s
H	Inertia constant	-	s
D	Speed damping	-	$-$
X_d	d-axis reactance	-	pu
X_q	q-axis reactance	-	pu
X'_d	d-axis transient reactance	-	pu
X''_d	d-axis sub-transient reactance	-	pu
X''_q	q-axis sub-transient reactance	-	pu
X_l	Leakage reactance	-	pu
$S_{1.0}$	Saturation factor at 1.0 pu	-	pu
$S_{1.2}$	Saturation factor at 1.2 pu	-	pu
R_a	Armature resistance	-	pu

Appendix C: Excitation System (ST7C Model) Parameters

Parameters	Description	Values	Units
T_R	Regulator input filter time constant	-	s
T_G	Lead time constant of voltage input	-	s
T_F	Lag time constant of voltage input	-	s
V_{max}	Voltage reference maximum limit	-	pu
V_{min}	Voltage reference minimum limit	-	pu
K_{PA}	Voltage regulator gain (it must be greater than zero)	-	pu
V_{RMAX}	Voltage regulator output maximum limit	-	pu
V_{RMIN}	Voltage regulator output minimum limit	-	pu
K_H	Feedback gain for high voltage gate	-	pu
K_L	Feedback gain for low voltage gate	-	pu
T_C	Lead time constant of voltage regulator	-	s
T_B	Lag time constant of voltage regulator	-	s
K_{IA}	Gain of the first order feedback block (it must be greater than 0)	-	pu
T_{IA}	Time constant of the first order feedback block (it must be greater than 0)	-	s
T_A	Thyristor bridge firing control equivalent time constant (it must be greater than 0)	-	s

Appendix D: Field Current Overexcitation Limiter (FCOEL) Parameters

Parameters	Description	Values	Units
$I_{resetFCOEL}$	FCOEL reset-reference, if FCOEL is inactive	-	pu
$T_{enFCOEL}$	FCOEL activation delay time	-	s
$T_{offFCOEL}$	FCOEL reset delay time	-	s
$I_{THoffFCOEL}$	FCOEL reset threshold	-	pu
K_{SCALE}	FCOEL input scaling factor	-	pu
T_{Rfcoel}	FCOEL input signal filter time constant	-	s
K_{act}	FCOEL actual value scaling factor	-	pu
I_{TFpu}	FCOEL reference for inverse time calculations	-	pu
I_{NL}	FCOEL no-load field current limit	-	pu
I_{inst}	FCOEL instantaneous field current limit	-	pu
I_{lim}	FCOEL thermal field current limit	-	pu
T_{Afcoel}	FCOEL reference filter time constant	-	s
c_1	FCOEL exponent for calculation of IERRinv1	-	pu
K_1	FCOEL gain for calculation of IERRinv1	-	pu/pu
c_2	FCOEL exponent for calculation of IERRinv2	-	pu
K_2	FCOEL gain for calculation of IERRinv2	-	pu/pu
V_{INVmax}	FCOEL maximum inverse time output	-	pu
V_{INVmin}	FCOEL minimum inverse time output	-	pu
$Fixed\_ru$	FCOEL fixed delay time output	-	pu
$Fixed\_rd$	FCOEL fixed cooling-down time output	-	pu

T_{FCL}	FCOEL time reference	-	pu
T_{max}	FCOEL timer maximum level	-	pu
T_{min}	FCOEL timer minimum level	-	pu
K_{FB}	FCOEL timer feedback gain	-	pu
K_{rd}	FCOEL reference ramp-down rate	-	pu/s
K_{ru}	FCOEL reference ramp-up rate	-	pu/s
K_{ZRU}	FCOEL thermal reference release threshold	-	pu
$FCOEL_{off}$	Desired output value when the FCOEL is turned off	-	–
$RampRateType$	Type of ramp rate	-	–
K_{Pfcoel}	FCOEL PID controller proportional gain	-	pu
K_{Ifcoel}	FCOEL PID controller integral gain	-	pu/s
K_{Dfcoel}	FCOEL PID controller differential gain	-	pu
T_{Dfcoel}	FCOEL PID controller differential time constant	-	s
$V_{FCOELmax}$	FCOEL PID controller maximum output limit	-	pu
$V_{FCOELmin}$	FCOEL PID controller minimum output limit	-	pu
$LeadLag_{fcoel}$	Check this box to use the lead-lag function	-	–
T_{FCOEL1}	FCOEL numerator (lead) time constant (first block)	-	s
T_{FCOEL2}	FCOEL denominator (lead) time constant (first block)	-	s
T_{FCOEL3}	FCOEL numerator (lead) time constant (second block)	-	s
T_{FCOEL4}	FCOEL denominator (lead) time constant (second block)	-	s

$V_{FCOELmax1}$	Maximum FCOEL lead-lag 1 output limit	-	pu
$V_{FCOELmin1}$	Minimum FCOEL lead-lag 1 output limit	-	pu
$V_{FCOELmax2}$	Maximum FCOEL lead-lag 2 output limit	-	pu
$V_{FCOELmin2}$	Maximum FCOEL lead-lag 2 output limit	-	pu

Appendix E: Stator Current Underexcitation Limiter (SCUEL) Parameters

Parameters	Description	Values	Units
T_{Pscuel}	SCUEL active power filter time constant	-	s
T_{Vscuel}	SCUEL voltage filter time constant	-	s
$T_{IQscuel}$	SCUEL reactive current filter time constant	-	s
$V_{biasSCUEL}$	SCUEL voltage bias	-	pu
K_{1scuel}	Voltage exponent for active power input to SCUEL table (0, 1, or 2)	-	–
K_{2scuel}	Voltage exponent for reactive current input to SCUEL table (0, 1, or 2)	-	–
K_{Fscuel}	SCUEL excitation system stabilizer gain	-	pu
$T_{IQrefSCUEL}$	SCUEL reactive current reference time constant	-	s
$T_{adjSCUEL}$	SCUEL adjustable gain reduction time constant	-	s
$K_{FBscuel}$	V_{FB} signal input gain	-	pu
$T_{FBscuel}$	V_{FB} signal input filter time constant	-	s
K_{Pscuel}	SCUEL PID controller proportional gain	-	pu
K_{Iscuel}	SCUEL PID controller integral gain	-	pu/s
K_{Dscuel}	SCUEL PID controller differential gain	-	pu
T_{Dscuel}	SCUEL PID controller differential time constant	-	s
$V_{SCUELmax}$	SCUEL PID controller maximum output limit	-	pu
$V_{SCUELmin}$	SCUEL PID controller minimum output limit	-	pu
$LeadLag_{scuel}$	Check this box to use the lead-lag function	-	–

T_{SCUEL1}	SCUEL numerator (lead) time constant (first block)	-	s
T_{SCUEL2}	SCUEL denominator (lag) time constant (first block)	-	s
T_{SCUEL3}	SCUEL numerator (lead) time constant (second block)	-	s
T_{SCUEL4}	SCUEL denominator (lag) time constant (second block)	-	s
$V_{SCUELmax1}$	Maximum SCUEL lead-lag 1 output limit	-	pu
$V_{SCUELmin1}$	Minimum SCUEL lead-lag 1 output limit	-	pu
$V_{SCUELmax2}$	Maximum SCUEL lead-lag 2 output limit	-	pu
$V_{SCUELmin2}$	Maximum SCUEL lead-lag 2 output limit	-	pu
P_{1scuel}	Active power (first point)	-	pu
$I_{Q1scuel}$	Reactive current (first point)	-	pu
P_{2scuel}	Active power (second point)	-	pu
$I_{Q2scuel}$	Reactive current (second point)	-	pu
P_{3scuel}	Active power (third point)	-	pu
$I_{Q3scuel}$	Reactive current (third point)	-	pu
P_{4scuel}	Active power (fourth point)	-	pu
$I_{Q4scuel}$	Reactive current (fourth point)	-	pu
P_{5scuel}	Active power (fifth point)	-	pu
$I_{Q5scuel}$	Reactive current (fifth point)	-	pu
$K_{adjSCUEL}$	Check this box to enable the adjustable gain reduction	-	$-$
$K_{fixSCUEL}$	SCUEL fixed gain reduction factor	-	pu
X_q	q-axis synchronous reactance	-	pu

Appendix F: Stator Current Limiter (SCL) Parameters

Parameters	Description	Values	Units
I_{SCLlim}	SCL terminal current pick up level	-	pu
T_{IT}	Terminal current transducer equivalent time constant	-	s
K	SCL timing characteristic factor	-	pu
T_{QSCL}	Reactive current transducer equivalent time constant	-	s
I_{Qmin}	Deadband for reactive current	-	pu
V_{SCLdb}	Deadband for reactive power or power factor	-	pu
T_{INV}	Inverse time delay after pickup	-	s
T_{DSCL}	Fixed-time delay after pickup	-	s
$ControllerType$	SCL controller type	-	$-$
$TimeDelayType$	SCL time delay type	-	$-$
K_{Poex}	SCL PID controller proportional gain (overexcited range)	-	pu
K_{Ioex}	SCL PID controller integral gain (overexcited range)	-	pu
K_{Doex}	SCL PID controller differential gain (overexcited range)	-	pu
T_{Doex}	SCL PID controller differential time constant (overexcited range)	-	s
K_{Puex}	SCL PID controller proportional gain (underexcited range)	-	pu

K_{Iuex}	SCL PID controller integral gain (underexcited range)	-	pu
K_{Duex}	SCL PID controller differential gain (underexcited range)	-	pu
T_{Duex}	SCL PID controller differential time constant (underexcited range)	-	s
V_{SCLmax}	SCL PID controller maximum output limit	-	pu
V_{SCLmin}	SCL PID controller minimum output limit	-	pu
$SCLoex_{off}$	Desired output value when the overexcitation region in SCL is turned off	-	$-$
$SCLuex_{off}$	Desired output value when the underexcitation region in SCL is turned off	-	$-$

Appendix G: Stator Current Overexcitation Limiter (SCOEL) Parameters

Parameters	Description	Values	Units
T_{Pscoel}	SCOEL active power filter time constant	-	s
$T_{IQscoel}$	SCOEL reactive current filter time constant	-	s
$I_{resetSCOEL}$	SCOEL reset-reference, if SCOEL is inactive	-	pu
$T_{enSCOEL}$	SCOEL activation delay time	-	s
$T_{offSCOEL}$	SCOEL reset delay time	-	s
$I_{THoffSCOEL}$	SCOEL reset threshold value	-	pu
$K_{fixSCOEL}$	SCOEL fixed gain reduction factor	-	pu
K_{Pscoel}	SCOEL PID controller proportional gain	-	pu
K_{Iscoel}	SCOEL PID controller integral gain	-	pu/s
K_{Dscoel}	SCOEL PID controller differential gain	-	pu
T_{Dscoel}	SCOEL PID controller differential time constant	-	s
$V_{SCOELmax}$	SCOEL PID controller maximum output limit	-	pu
$V_{SCOELmin}$	SCOEL PID controller minimum output limit	-	pu
$LeadLag_{scoel}$	Check this box to use the lead-lag function	-	–
T_{SCOEL1}	SCOEL numerator (lead) time constant (first block)	-	s
T_{SCOEL2}	SCOEL denominator (lag) time constant (first block)	-	s
T_{SCOEL3}	SCOEL numerator (lead) time constant (second block)	-	s
T_{SCOEL4}	SCOEL denominator (lag) time constant (second block)	-	s
$V_{SCOELmax1}$	Maximum SCOEL lead-lag 1 output limit	-	pu
$V_{SCOELmin1}$	Minimum SCOEL lead-lag 1 output limit	-	pu
$V_{SCOELmax2}$	Maximum SCOEL lead-lag 2 output limit	-	pu
$V_{SCOELmin2}$	Maximum SCOEL lead-lag 2 output limit	-	pu

P_{1scoel}	Active power (first point)	-	pu
$I_{Q1scoel}$	Reactive current (first point)	-	pu
P_{2scoel}	Active power (second point)	-	pu
$I_{Q2scoel}$	Reactive current (second point)	-	pu
P_{3scoel}	Active power (third point)	-	pu
$I_{Q3scoel}$	Reactive current (third point)	-	pu
P_{4scoel}	Active power (fourth point)	-	pu
$I_{Q4scoel}$	Reactive current (fourth point)	-	pu
P_{5scoel}	Active power (fifth point)	-	pu
$I_{Q5scoel}$	Reactive current (fifth point)	-	pu

Appendix H: Field Current Underexcitation Limiter (FCUEL) Parameters

Parameters	Description	Values	Units
T_{Pfcuel}	FCUEL active power filter time constant	-	s
T_{Vfcuel}	FCUEL voltage filter time constant	-	s
$T_{IFDfcuel}$	FCUEL reactive current filter time constant	-	s
$V_{biasFCUEL}$	FCUEL voltage bias	-	pu
K_{1fcuel}	Voltage exponent for active power input to FCUEL table (0, 1, or 2)	-	$-$
K_{2fcuel}	Voltage exponent for field current input to FCUEL table (0, 1, or 2)	-	$-$
K_{Ffcuel}	FCUEL excitation system stabilizer gain	-	pu
$T_{IFDrefFCUEL}$	FCUEL reactive current reference time constant	-	s
$K_{fixFCUEL}$	SCUEL fixed gain reduction factor	-	pu
$K_{FBfcuel}$	V_{FB} signal input gain	-	pu
$T_{FBfcuel}$	V_{FB} signal input filter time constant	-	s
I_{FDmin}	Absolutely minimum field current should be less or equal than $I_{FD1fcuel}$	-	pu
$FCUEL_{off}$	Desired output value when the FCUEL is turned off	-	$-$
K_{Pfcuel}	FCUEL PID controller proportional gain	-	pu
K_{Ifcuel}	FCUEL PID controller integral gain	-	pu/s
K_{Dfcuel}	FCUEL PID controller differential gain	-	pu
T_{Dfcuel}	FCUEL PID controller differential time constant	-	s

$V_{FCUELmax}$	FCUEL PID controller maximum output limit	-	pu
$V_{FCUELmin}$	FCUEL PID controller minimum output limit	-	pu
$LeadLag_{fcuel}$	Check this box to use the lead-lag function	-	–
T_{FCUEL1}	FCUEL numerator (lead) time constant (first block)	-	s
T_{FCUEL2}	FCUEL denominator (lag) time constant (first block)	-	s
T_{FCUEL3}	FCUEL numerator (lead) time constant (second block)	-	s
T_{FCUEL4}	FCUEL denominator (lag) time constant (second block)	-	s
$V_{FCUELmax1}$	Maximum FCUEL lead-lag 1 output limit	-	pu
$V_{FCUELmin1}$	Minimum FCUEL lead-lag 1 output limit	-	pu
$V_{FCUELmax2}$	Maximum FCUEL lead-lag 2 output limit	-	pu
$V_{FCUELmin2}$	Maximum FCUEL lead-lag 2 output limit	-	pu
P_{1fcuel}	Active power (first point)	-	pu
$I_{FD1fcuel}$	Field current (first point)	-	pu
P_{2fcuel}	Active power (second point)	-	pu
$I_{FD2fcuel}$	Field current (second point)	-	pu
P_{3fcuel}	Active power (third point)	-	pu
$I_{FD3fcuel}$	Field current (third point)	-	pu
P_{4fcuel}	Active power (fourth point)	-	pu
$I_{FD4fcuel}$	Field current (fourth point)	-	pu
P_{5fcuel}	Active power (fifth point)	-	pu
$I_{FD5fcuel}$	Field current (fifth point)	-	pu

Appendix I: V/Hz Limiter Parameters

Parameters	Description	Values	Units
f_{sp}	Frequency setpoint	-	Hz
$Enable_{f\ vsp}$	Enable f_{vsp} input (variable frequency setpoint)	-	$-$
T_d	Time delay	-	s
V_{ZLM}	Limiting value	-	%
K_{PVHz}	V/Hz limiter PID controller proportional gain	-	pu
K_{IVHz}	V/Hz limiter PID controller integral gain	-	pu/s
K_{DVHz}	V/Hz limiter PID controller differential gain	-	pu
T_{DVHz}	V/Hz limiter PID controller differential time constant	-	s
V_{VHzmax}	V/Hz limiter PID controller maximum output limit	-	pu
V_{VHzmin}	V/Hz limiter PID controller minimum output limit	-	pu

Appendix J: Voltage Droop/Compensation Controller Parameters

Parameters	Description	Values	Units
V_{Tsp}	Generator terminal voltage setpoint	-	pu
$Enable_{V_{Tvsp}}$	Enable V_{Tvsp} input (variable generator terminal voltage setpoint)	-	–
$I_{Qcontoller}$	Check this box to activate the reactive current droop/compensation controller	-	–
I_{Qn}	Nominal generator terminal reactive current	-	pu
I_{Qsp}	Generator terminal reactive current setpoint	-	pu
$Enable_{I_{Qvsp}}$	Enable I_{Qvsp} input (variable generator terminal reactive current setpoint)	-	–
R_{IQ}	Droop (regulation) in [%] Use "-" for droop or "+" for compensation	-	%
K_{PIQ}	Reactive current droop/compensation PID controller proportional gain	-	pu
K_{IIQ}	Reactive current droop/compensation PID controller integral gain	-	pu
K_{DIQ}	Reactive current droop/compensation PID controller differential gain	-	pu
T_{DIQ}	Reactive current droop/compensation PID controller differential time constant	-	s
V_{IQmax}	Reactive current droop/compensation PID controller maximum output limit	-	pu
V_{IQmin}	Reactive current droop/compensation PID controller minimum output limit	-	pu

$I_{Pcontroller}$	Check this box to activate the active current compensation controller	-	–
I_{Pn}	Nominal generator terminal active current	-	pu
I_{Psp}	Generator terminal active current setpoint	-	pu
$Enable_{I_{Pvsp}}$	Enable I_{Pvsp} input (variable generator terminal active current setpoint)	-	–
R_{IP}	Droop (regulation) in [%]	-	%
K_{PIP}	Active current compensation PID controller proportional gain	-	pu
K_{IIP}	Active current compensation PID controller integral gain	-	pu
K_{DIP}	Active current compensation PID controller differential gain	-	pu
T_{DIP}	Active current compensation PID controller differential time constant	-	s
V_{IPmax}	Active current compensation PID controller maximum output limit	-	pu
V_{IPmin}	Active current compensation PID controller minimum output limit	-	pu
$f_{controller}$	Check this box to activate the frequency droop controller	-	–
f_n	Nominal frequency	-	Hz
f_{sp}	Frequency setpoint	-	Hz
$Enable_{f_{vsp}}$	Enable f_{vsp} input (variable frequency setpoint)	-	–
R_f	Droop (regulation) in [%]	-	%
$f_{maxlimit}$	Maximum frequency limit for voltage support	-	Hz

$f_{minlimit}$	Minimum frequency limit for voltage support	-	Hz
K_{Pf}	Frequency droop PID controller proportional gain	-	pu
K_{If}	Frequency droop PID controller integral gain	-	pu
K_{Df}	Frequency droop PID controller differential gain	-	pu
T_{Df}	Frequency droop PID controller differential time constant	-	s
V_{fmax}	Frequency droop PID controller maximum output limit	-	pu
V_{fmin}	Frequency droop PID controller minimum output limit	-	pu

Appendix K: Reactive Power (VAR) or Power Factor (PF) Controller Parameters

Parameters	Description	Values	Units
Controller	Choose the controller type	-	–
PF_{sp}	Generator power factor setpoint	-	°
$Enable_{PF_{vsp}}$	Enable PF_{vsp} input (variable generator power factor setpoint)	-	–
PF_{spmax}	Power factor maximum setpoint for the overexcited region	-	°
PF_{spmin}	Power factor maximum setpoint for the underexcited region	-	°
PF_{spramp}	Power factor controller setpoint ramping speed	-	$°/s$
PF_{DBW}	Power factor controller deadband magnitude	-	°
PF_{Td}	PF controller delay time	-	s
V_{PFLMT}	PF controller output limit	-	pu
K_{Ppf}	PF controller PID controller proportional gain	-	pu
K_{Ipf}	PF controller PID controller integral gain	-	pu
K_{Dpf}	PF controller PID controller differential gain	-	pu
T_{Dpf}	PF controller PID controller differential gain time constant	-	s
PF_{ITmin}	PF controller minimum terminal current limit	-	pu
PF_{VTmin}	PF controller minimum terminal voltage limit	-	pu
PF_{VTmax}	PF controller maximum terminal voltage limit	-	pu
VAR_{sp}	Generator reactive power setpoint	-	pu

$Enable_{VAR_{vsp}}$	Enable VAR_{vsp} generator reactive power variable setpoint	-	–
VAR_{spmax}	Reactive power maximum setpoint for the overexcited region	-	pu
VAR_{spmin}	Reactive power maximum setpoint for the underexcited region	-	pu
VAR_{spramp}	VAR controller setpoint ramping speed	-	pu/s
VAR_{DBW}	VAR controller deadband magnitude	-	pu
VAR_{Td}	VAR controller delay time	-	s
V_{VARLMT}	VAR controller output limit	-	pu
K_{Pvar}	VAR controller PID controller proportional gain	-	pu
K_{Ivar}	VAR controller PID controller integral gain	-	pu/s
K_{Dvar}	VAR controller PID controller differential gain	-	pu
T_{Dvar}	VAR controller PID controller differential time constant	-	pu
VAR_{ITmin}	VAR controller minimum terminal current limit	-	pu
VAR_{VTmin}	VAR controller minimum terminal voltage limit	-	pu
VAR_{VTmax}	VAR controller maximum terminal voltage limit	-	pu

Appendix L: FCOEL Activation Logic Code

```
model FCOEL_ActivationLogic "Activates and resets FCOEL with time delays"

  parameter Modelica.SIunits.Time T_en=0.2 "FCOEL activation delay time";
  parameter Modelica.SIunits.Time T_off=5.0 "FCOEL reset delay time";
  parameter Modelica.SIunits.PerUnit I_THoff=0.05 "FCOEL reset threshold value";
  parameter Modelica.SIunits.PerUnit I_reset=100.0
    "FCOEL reset-reference, if FCOEL is inactive";
  parameter Modelica.SIunits.PerUnit I_inst=6.0
    "FCOEL instantaneous field current limit";
  Modelica.Blocks.Interfaces.RealInput Terr
    "Error signal between fixed parameter(T_FCL) and timer output (T_lim)"
    ;
  Modelica.Blocks.Interfaces.RealOutput Ibias
    "FCOEL activation logic output"
    ;
  Modelica.Blocks.Interfaces.RealInput Iact "Actual feedback"
    ;
  Modelica.Blocks.Interfaces.RealInput Iref
    "Determined FCOEL reference value" ;

protected
  discrete Modelica.SIunits.Time entryTime1 "Time instant when condition became true";
  discrete Modelica.SIunits.Time entryTime2 "Time instant when condition became true";
  Modelica.SIunits.Time t1(start = 0.0) "Time counter 1";
  Modelica.SIunits.Time t2(start = 0.0) "Time counter 2";
  Modelica.SIunits.PerUnit L_I_bias(start = I_reset) "Last I_bias value";
initial equation
 pre(entryTime1) = 0;
 pre(entryTime2) = 0;
equation
  when (Iact >= Iref) then
    entryTime1 = time;
  end when;
  when ((Iref - Iact) >= I_THoff) then
    entryTime2 = time;
  end when;

  t1 =if Iact >= Iref then time - entryTime1 else 0.0;
  t2 =if ((Iref - Iact) >= I_THoff) then time - entryTime2 else 0.0;

  if (Terr <= 0) or (t1>=T_en) or (T_en ==0) then
    Ibias = 0 "enable";
    L_I_bias = 0;

  elseif (Iref >= I_inst) and (t2 >= T_off) then
    Ibias = I_reset "reset";
    L_I_bias = I_reset;
  else
    Ibias = L_I_bias;
    L_I_bias =Ibias;
  end if;

  
end FCOEL_ActivationLogic;
```

Appendix M: FCOEL Ramp Rate Logic Code

```
model FCOEL_RampRateLogic
  "Uses error signal to determine if the FCOEL reference field current  should be ramped up or down"
  parameter Modelica.SIunits.PerUnit K_ZRU=0.99
    "FCOEL thermal reference release threshold";

  parameter Modelica.SIunits.PerUnit T_FCL=10.0 "FCOEL timer reference ";

  parameter Modelica.SIunits.PerUnit K_ru=1000.0 "FCOEL reference ramp-up rate ";

  parameter Modelica.SIunits.PerUnit K_rd=-1000.0
    "FCOEL reference ramp-down rate";

  Modelica.Blocks.Interfaces.RealInput Terr
    "Error signal between fixed parameter(T_FCL) and timer output (T_lim)"
    ;
  Modelica.Blocks.Interfaces.RealOutput Z "FCOEL ramp rate  logic output"
    ;
  Modelica.Blocks.Interfaces.RealInput IERRinv1
    "Inverse-time characteristic 1" ;
  Modelica.Blocks.Interfaces.BooleanInput SW1
    "Fixed ramp rates or a ramprate function of the field current error"
    ;
protected
  Real C(start = 0.0);
  Real D(start = 0.0);
equation
  if SW1 == false then
    C = K_ru;
    D = K_rd;
  else
    C =IERRinv1;
    D =IERRinv1;
  end if;
  if Terr >= (K_ZRU*T_FCL) then  //ramp I_ref up
    Z = C;
  elseif Terr <= 0 then           //ramp I_ref down
    Z = D;
  else
    Z = 0;
  end if;

end FCOEL_RampRateLogic;
```

Appendix N: FCOEL Timer Logic Code

```
model FCOEL_TimerLogic "Choosing the time characteristic for FCOEL"
  Modelica.Blocks.Interfaces.RealInput Ipu "Actual field current"
    ;
  Modelica.Blocks.Interfaces.RealOutput W "FCOEL timer logic output"
    ;
  Modelica.Blocks.Interfaces.RealInput IERRinv2
    "Inverse-time characteristic 2" ;

  parameter Modelica.SIunits.PerUnit Fixed_ru=0.0 "FCOEL fixed delay time output";

  parameter Modelica.SIunits.PerUnit Fixed_rd=-0.001
    "FCOEL fixed cooling-down time output";

  parameter Modelica.SIunits.PerUnit I_TFpu=3.0
    "FCOEL reference for inverse time calculations";
equation
  if (I_TFpu - Ipu) >= 0 then
    W =Fixed_ru + IERRinv2;
  else
    W =Fixed_rd + IERRinv2;
  end if;

end FCOEL_TimerLogic;
```

Appendix O: SCL Delayed Reactive Power Logic

```
model SCL_DelayedReactivePowerLogic
 "Use reactive power to determine the deadband and error to control the SCL"
 parameter Modelica.SIunits.Time T_DSCL=10.0 "Fixed-time delay after pickup";
 parameter Modelica.SIunits.PerUnit V_SCLdb=0.1
   "Dead-band for reactive power or power factor";
 Modelica.Blocks.Interfaces.RealInput ISCLerr "SCL current error signal"
   ;
 Modelica.Blocks.Interfaces.RealOutput Ioex2
   "Output to overexcitation side SW_1"
   ;
 Modelica.Blocks.Interfaces.RealInput ISCLinv
   "SCL inverse current error"
   ;
 Modelica.Blocks.Interfaces.RealInput QT
    "Generator reactive power output"
   ;
 Modelica.Blocks.Interfaces.BooleanInput SW2
   "Fixed-time delay or inverse time delay selector"  ;
 Modelica.Blocks.Interfaces.RealOutput Iuex2
   "Output to underexcitation side SW_1"
   ;
protected
 discrete Modelica.SIunits.Time entryTime "Time instant when condition became true";
 Modelica.SIunits.Time t(start = 0.0) "Time counter";
initial equation
pre(entryTime) = 0;
equation
 when (ISCLerr > 0) then
   entryTime = time;
 end when;
 t =if (ISCLerr > 0) then time - entryTime else 0.0;
 if ((SW2 == false) and (t >= T_DSCL)) or ((SW2 == true) and (ISCLinv >
     0)) then
   if QT >= V_SCLdb then
     Ioex2 = ISCLerr;
     Iuex2 = 0;
   elseif QT <= -V_SCLdb then
     Ioex2 = 0;
     Iuex2 = ISCLerr;
   else
     Ioex2 = 0;
     Iuex2 = 0;
   end if;
 else
   Ioex2 = 0;
   Iuex2 = 0;
 end if;
 
end SCL_DelayedReactivePowerLogic;
```

Appendix P: SCOEL Activation Logic Code

```
model SCOEL_ActivationLogic "Activates and resets the SCOEL"

  parameter Modelica.SIunits.Time T_en=0.2 "SCOEL activation delay time";
  parameter Modelica.SIunits.Time T_off=5.0 "SCOEL reset delay time";
  parameter Modelica.SIunits.PerUnit I_THoff=0.05 "SCOEL reset threshold value";
  parameter Modelica.SIunits.PerUnit I_reset=100.0
    "SCOEL reset-reference, if SCOEL is inactive";
  Modelica.Blocks.Interfaces.RealInput Err
    "Error signal between IQref and IQ"
    ∂ ;
  Modelica.Blocks.Interfaces.RealOutput Ibias
    "SCOEL activation logic output"
    ∂ ;
  Modelica.Blocks.Interfaces.RealInput IQ_F
    "Filtered generator reactive current output"
    ∂ ;
  Modelica.Blocks.Interfaces.RealInput IQref
    "Determined IQ reference value" ∂ ;

protected
  discrete Modelica.SIunits.Time entryTime1 "Time instant when condition became true";
  discrete Modelica.SIunits.Time entryTime2 "Time instant when condition became true";
  Modelica.SIunits.Time t1(start = 0.0) "Time counter 1";
  Modelica.SIunits.Time t2(start = 0.0) "Time counter 2";
  Modelica.SIunits.PerUnit L_I_bias(start = I_reset) "Last I_bias value";
initial equation
 pre(entryTime1) = 0;
 pre(entryTime2) = 0;
equation
  when (IQ_F >= IQref) then
    entryTime1 = time;
  end when;
  when ((IQref - IQ_F) >= I_THoff) then
    entryTime2 = time;
  end when;

  t1 =if IQ_F >= IQref then time - entryTime1 else 0.0;
  t2 =if ((IQref - IQ_F) >= I_THoff) then time - entryTime2 else 0.0;

  if (Err <= 0) and (t1 >= T_en) or (T_en == 0) then
    Ibias = 0 "enable";
    L_I_bias = 0;

  elseif (IQref <= IQ_F) and (t2 >= T_off) then
    Ibias = I_reset "reset";
    L_I_bias = I_reset;
  else
    Ibias = L_I_bias;
    L_I_bias =Ibias;
  end if;

  ∂
end SCOEL_ActivationLogic;
```

Appendix Q: PF Normalizer Code

```
model PF_normalizer
  "Normalizing the powerfactor to obtain a continuous function for VAR/PF controller/regulator"
  Modelica.Blocks.Interfaces.RealInput P_T
    "Active power output of the generator"
    ;
  Modelica.Blocks.Interfaces.RealInput Q_T
    "Reactive power output of the generator"
    ;
  Modelica.Blocks.Interfaces.RealOutput PF_norm "Normalized power factor"
    ;
protected
    Real PF(start = 0);
    Real u(start= 0);
equation
  PF = P_T/sqrt((P_T^2)+(Q_T^2));
  if Q_T >= 0 then
    u = PF;
  else
    u = -PF;
  end if;
  if u >= 0 then
    PF_norm = 1-u;
  else
    PF_norm = -1-u;
  end if;

end PF_normalizer;
```

Appendix R: PF Setpoint Normalizer Code

```
model PF_REFnormalizer
  "Normalizing the powerfactor to obtain a continuous function for VAR/PF controller/regulator"
  Modelica.Blocks.Interfaces.RealInput PF_sp "Power Factor setpoint"
    ;
  Modelica.Blocks.Interfaces.RealOutput PF_norm "Normalized power factor"
    ;

equation

  if PF_sp >= 0 then
    PF_norm =cos(PF_sp);
  else
    PF_norm =-cos(PF_sp);
  end if;

end PF_REFnormalizer;
```

Appendix S: PF/VAR Controller Logic Code

```
model PFVAR_ControllerLogic
  "Control logic that determine the output of the PF_controllerfor VAR/PF controller/regulator"
  Modelica.Blocks.Interfaces.RealInput Err "Error signal"
                                                ;
  Modelica.Blocks.Interfaces.RealInput VT "Generator terminal voltage"
                                          ;
  Modelica.Blocks.Interfaces.RealInput IT "Generator terminal current "
                                          ;
  Modelica.Blocks.Interfaces.BooleanInput OELs "OELs status"
    ;
  Modelica.Blocks.Interfaces.RealOutput Verr
    "Output of the PF controller logic"  ;
  Modelica.Blocks.Interfaces.BooleanInput UELs "UELs status"
    ;
  Modelica.Blocks.Interfaces.BooleanInput SCLs "SCLs status"
    ;
  parameter Modelica.SIunits.PerUnit V_ITmin=0.1
    "Controller minimum terminal current limit";
  parameter Modelica.SIunits.PerUnit V_VTmin=0.95
    "Controller minimum terminal voltage limit";
  parameter Modelica.SIunits.PerUnit V_VTmax=1.05
    "Controller maximum terminal voltage limit";
  parameter Modelica.SIunits.DimensionlessRatio V_DBW=0.1
    "Controller deadband magnitude";
  parameter Modelica.SIunits.Time T_d=0.5
    "Controller delay time";
protected
  discrete Modelica.SIunits.Time entryTime1 "Time instant when condition became true";
  Modelica.SIunits.Time t1(start = 0.0) "Time counter 1";
initial equation
 pre(entryTime1) = 0;
equation
  when (Err >= V_DBW) or (Err <= -V_DBW) then
    entryTime1 = time;
  end when;
  t1 =if (Err >= V_DBW) or (Err <= -V_DBW) then time - entryTime1 else 0.0;
  if OELs == false and UELs == false and SCLs == false then
    if (IT >= V_ITmin)  and (VT >= V_VTmin) and (VT <=
        V_VTmax) then
          if (Err >= V_DBW) and (t1 >= T_d) then
        Verr = Err;
          elseif (Err <= -V_DBW) and (t1 >= T_d) then
        Verr = Err;
          else
        Verr = 0;
          end if;
        else
      Verr = 0;
        end if;
    else
    Verr = 0;
  end if;
  
end PFVAR_ControllerLogic;
```